Mechanochemistry for sustainable, efficient dehydrogenation/hydrogenation

Blaine G. Fiss[1], Austin J. Richard[1], Tomislav Friščić[1*], Audrey Moores[1,2*]

1. Centre in Green Chemistry and Catalysis, Department of Chemistry, McGill University, 801 Sherbrooke Street West, Montréal, Québec H3A 0B8, Canada

2. Department of Materials Engineering, McGill University, 3610 University Street, Montréal, Québec H3A 0C5, Canada

Keywords: Ball-milling, solvent-free, organic synthesis, catalysis, green chemistry

tomislav.friscic@mcgill.ca

audrey.moores@mcgill.ca

Abstract

Hydrogenation reactions are one of the pillars of the chemical industry, with applications from bulk chemicals to pharmaceuticals manufacturing. The ability to selectively add hydrogen across double and/or triple bonds is key in the chemist's toolbox, and the enabling component in the development of sustainable processes. Traditional solution-based approaches to hydrogenation reactions are tainted by significant consumption of energy and production of solvent waste. This review highlights the development and applications of recently emerged solvent-free approaches to conduct the hydrogenation of organic molecules using mechanochemistry, *i.e.* chemical transformations induced or sustained by mechanical force. In particular, we will show how mechanochemical techniques such as ball-milling enable catalytic or stoichiometric metal-mediated hydrogenation reactions that are simple, fast, and are conducted under significantly milder conditions compared to traditional solution routes. Importantly, we highlight the current challenges and opportunities in this field, while also identifying exciting cases in which mechanochemical hydrogenation strategies lead to new, unique targets and reactivity

1. Introduction

Hydrogenation reactions have long been a staple of the chemical industry, ranging from the bulk chemical manufacturing to the pharmaceutical and agrochemical sectors.[1] The scope of bond types that can be transformed through hydrogenation reactions include carbon-carbon, carbon-oxygen, carbon-nitrogen and nitrogen-oxygen bonds, allowing access to a variety of products, often in a stereo- or regio-controlled fashion. Along with π-bonded motifs, such as carbonyl moieties, as well as carbon-carbon double (C=C) and triple (C≡C) bonds often seen in organic chemistry, sustainable approaches to hydrogenation have also made advances towards the conversion of small molecule feedstocks, such as carbon monoxide (CO) and carbon dioxide (CO_2)

into value-added products. Since the early development of catalytic processes based on solid platinum and palladium as catalysts, highlighted in the seminal work of Sabatier in 1897,[2, 3] significant strides have been made towards the development of more reactive, selective and recyclable catalysts in the form of organometallic complexes and nanoparticles (NPs).[4-7] Such development has at the same time included a shift towards the use of more sustainable, less toxic, and Earth-abundant metals as active catalyst components.[8, 9]

The development of cleaner and more sustainable catalytic processes is not focused only on creation of new, more efficient catalysts, but also seeks to ameliorate or completely eliminate the overall negative environmental impacts of many traditional synthetic procedures. Among these negative impacts, particular attention has been given to reducing the production of waste, either due to excess solvent[10] or to the loss of energy associated with reactor heating. This has made way for the development of synthetic methodologies which are both solvent-free, and have a low energy demand. Particularly successful among these emergent approaches to cleaner, solvent-free chemistry are mechanochemical techniques, in which chemical and/or materials transformations are induced and/or sustained by mechanical agitation in the form of grinding, milling or other types of shear and extrusion, with or without the need for milling media.[11-28]

Mechanochemical transformations have a long history, with one of the earliest reports coming from Theophrastus of Eresus, who described a methodology for mechanochemical production of mercury metal by manual grinding of cinnabarite (mercury(II) sulfide) using a mortar and pestle made from copper or bronze.[29] While inorganic materials, such as ores and minerals, have been processed through mechanical grinding since Antiquity, the underlying chemical transformations have not been systematically investigated until the late 19th century, when Faraday described the mechanically-induced transformations of metal salts (1820),[30, 31] and

Carey Lea demonstrated that mechanical treatment of silver and mercury halides leads to different outcomes compared to treatment by heat or pressure.[32] This work, together with pioneering investigations by Wöhler in mechanically-inducted transformations of organic solids,[33] provides the foundation for the development of solid-state, solvent-free chemistry by mechanical grinding.

Mechanochemical reactions can be conducted using diverse equipment, ranging from simple and readily accessible mortar and pestle, to much more sophisticated and automated equipment, such as shaker mills, planetary mills, extruders or devices operating through (ultra)sonic irradiation (Figure 1).

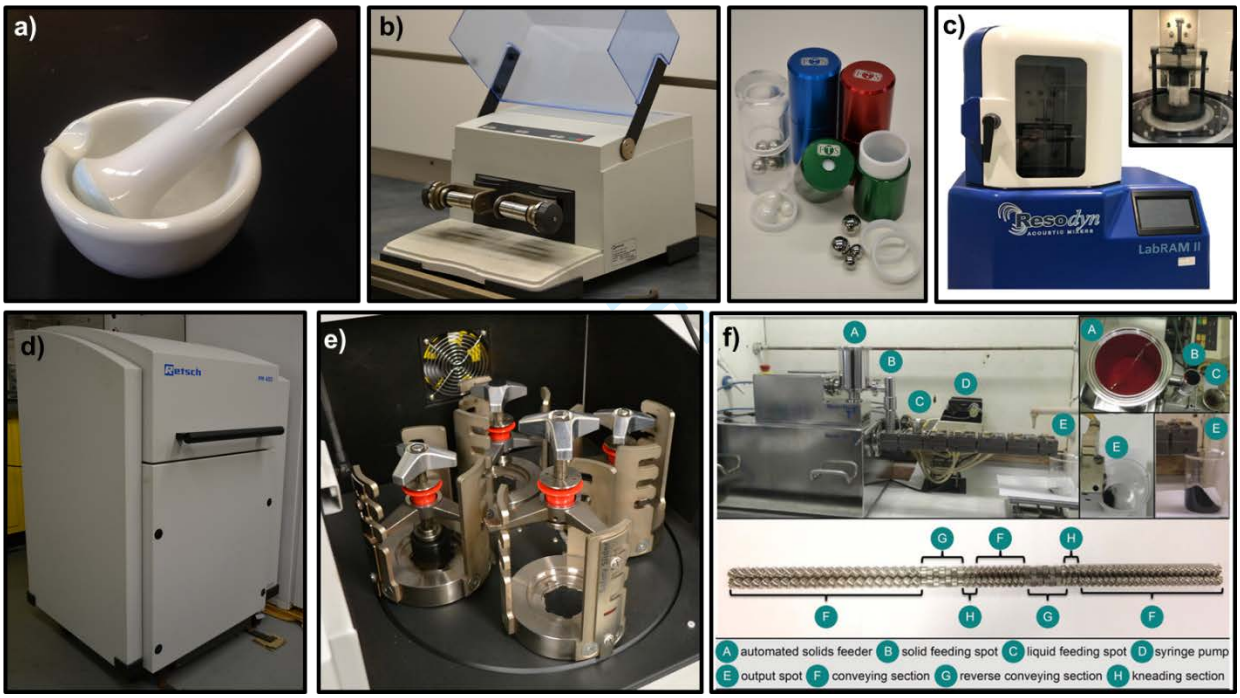

Fig 1. Equipment for mechanochemical reactions a) mortar and pestle b) vibrational mill and small-scale milling jars and balls c) resonant acoustic mixer (RAM) exterior and in operation (insert) d) planetary mill external and e) internal f) twin-screw extruder (TSE)[34] allowing for continuous processing

Mechanochemical reactions can be performed using neat substrates, or in the presence of a small amount of a liquid additive, stoichiometrically comparable to or even lower than the amount of reacting substrate, in a process known as liquid-assisted grinding (LAG). The amount of liquid

additive in LAG and related methods (*e.g.* ion- and liquid-assisted grinding, ILAG[35] or ionic liquid-assisted grinding, IL-AG[36]) is measured using the parameter η, which is the ratio of liquid additive volume to the mass of solid reactants, expressed in μL/mg.[37] The exact mechanisms through which the liquid additive promotes reactivity in LAG are not yet known, but are generally considered to be based on surface activation and improvement of molecular mobility. The ability to improve, optimize and direct the course of a mechanochemical process by varying the choice or amount of liquid additive has provided unprecedented generality to chemical reactions by milling, providing tolerance to molecular size, shape and functionality in solvent-free synthesis. At the same time, the unique mechanically-agitated environment of neat or LAG reactions has enabled access to molecular targets, materials and chemical transformations that are difficult or perhaps even considered impossible in conventional solution processes.[38] In the area of materials science, mechanochemistry has proven paramount in making readily accessible a range of materials, including novel metal-organic frameworks,[39-41] cocrystals,[42, 43] polymers, enabling the efficient functionalization of inorganic and organic substrates,[44-48] as well as the solvent-free, room-temperature synthesis and functionalization of discrete metal NPs.[49-51]

Over the past two decades, the applications of mechanochemistry to organic synthesis have been rapidly expanding, and it is now well established that the mechanochemical reaction environment sustains and promotes a wide range of transformations, including organocatalytic, enzyme- and metal-catalyzed reactions, and can often lead to selectivities that are very different from those encountered in solution. While the scope of mechanochemistry in organic synthesis has been extensively reviewed within the last decade,[18, 24, 52] this review focuses specifically on the emergent applications of ball-milling for conducting the reactions of hydrogenation and/or dehydrogenation which are critical for the development of cleaner, more sustainable chemical

manufacturing. For that reason, we will particularly highlight the recent applications of mechanochemistry to key transformations, such as the reduction of carbon monoxide (CO) and carbon dioxide (CO_2).

2. Typical reductants and catalyst design

2.1 Reductant choice

Hydrogen gas is the most atom-economic reagent for hydrogenation reaction and, therefore, a staple of chemical industry.[53] While hydrogen gas is readily deployed in laboratory and industrial scale applications, its use in mechanochemical processes has been limited by the lack of equipment designed to handle gaseous reagents. The development of such equipment is an area of rising importance, as described in the recent review of gas-based mechanochemical milling reactions by Bolm and Hernández.[54] An alternative to gaseous H_2 as a reactant in milling reactions is the use of simpler and safer to handle solid or liquid reagents that can be used as *in situ* sources of hydrogen. The generation of hydrogen gas *in situ* has recently been investigated using both water,[55, 56] as well as ethers and short alkanes as sources of H_2.[57] In 2015, the Sajiki group showed how the mechanochemical treatment of water in a planetary mill, using milling vessels (jars) and milling media (balls) made of SUS304 stainless steel could lead to production of H_2 gas *via* galvanic splitting of water due to the pairing of chromium and nickel in the milling assembly.[55] This work demonstrated quantitative conversion of H_2O into H_2 (Table 1), which was subsequently collected and quantified using gas chromatography and pressure measurement.

Table 1. Galvanic generation of H_2 gas by milling of water in a Ni- and Cr-containing stainless steel assembly[55]

						Gas proportions (%)[a]		
Entry	**Reaction vessel**	**H_2O (μL)**	**Number of balls**	**Additive**	**Collected gas volume (mL)**	**N_2**	**H_2**	**O_2**
1	SUS304 (80 mL)	270, 15 mmol	100[b]	None	120	44	51	1.5
2	SUS304 (80 mL)	270, 15 mmol	100	None	100	35	50	1.3
3	ZrO_2 (20 mL)	68, 3.8 mmol	25[b]	None	23	78	0.3	20
4	ZrO_2 (20 mL)	68, 3.8 mmol	25	None	40	62	33	3.8
5	ZrO_2 (20 mL)	68, 3.8 mmol	25	Ni (1.88 mmol, 0.5 equiv.)	20	89	2.2	8.0
6	ZrO_2 (20 mL)	68, 3.8 mmol	25	Fe (1.88 mmol, 0.5 equiv.)	20	86	>0.1	13
7	ZrO_2 (20 mL)	68, 3.8 mmol	25	Cr (0.38 mmol, 0.1 equiv.)	35	62	20	13
8	ZrO_2 (20 mL)	68, 3.8 mmol	25	Cr (0.76 mmol, 0.2 equiv.)	45	50	39	8.9
9	ZrO_2 (20 mL)	68, 3.8 mmol	25	Cr (1.88 mmol, 0.5 equiv.)	56	42	47	4.7
10	ZrO_2 (20 mL)	68, 3.8 mmol	25	Cr (3.75 mmol, 1.0 equiv.)	65	40	47	4.3
11	ZrO_2 (20 mL)	68, 3.8 mmol	25	SUS304 58.5 mg (0.21 mmol as Cr)[c]	35	63	29	3.6

[a]Determined by Shimadzu gas chromatograph. [b]SUS304 balls were used. [c]18.89% of Cr was contained in SUS304 purchased from Fritsch Japan Co. Ltd.

A subsequent report expanded the use of SUS304 milling assembly for mechanochemical reduction or deuteration of a range of substrates, by milling in the presence of H_2O or D_2O, respectively.[56] The same approach, based on pairing of chromium and nickel in the stainless steel milling assembly, was also reported to enable the use of alkanes and diethyl ether as liquid sources of hydrogen. In this process, the chromium is thought to lead to galvanic generation of hydrogen gas from simple alkanes or diethyl ether, while the presence of nickel catalyzes subsequent hydrogenation. In 2018, Hernández and coworkers employed *in situ* generation of H_2 *via* the dehydrogenation of ammonia-borane,[58] while the work by Štrukil and coworkers in 2018 described the use of ammonium formate as a solid reductant.[59]

2.2 Mechanochemical catalyst design

Mechanochemists working in methodology and catalyst design have shown successful methods towards making catalytically viable organometallic complexes (Figure 2a), as well as obtaining unique size control of a variety of earth-abundant or noble metal nanoparticles,[15, 60] (Figure 2b) both of which we will highlight in this review. Mechanochemistry, however, also has the unique advantage of employing the materials of the milling assembly, to act as the metal source for chemical transformations (Figure 2c). While we will only highlight a handful of specific examples where the milling assembly plays an active role, other groups have highlighted the advantages of this technique.[61] Herein we have outlined key examples where either catalyst reactivity or selectivity was improved through mechanochemical catalyst synthesis or where employing mechanochemical reduction reactions allowed the reduction of challenging substrates, while reducing bulk solvent waste.

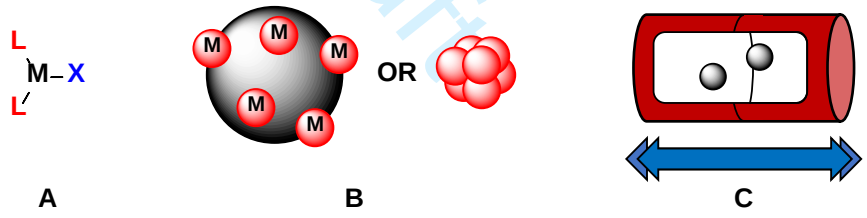

Fig 2. Possible catalysts for mechanochemical reduction reactions. A) molecular species B) nanocatalysts, either supported or free C) the material of the milling assembly itself

2.2.1 Molecular catalysts

Since Sabatier's Nobel Prize winning demonstration of catalytic hydrogenation reactions,[2, 3] the use of organometallic complexes for hydrogenation has been at the forefront of this field. Mechanochemistry has seen a range of utility in fundamental organometallic chemistry, enabling reactivities not previously seen in solution synthesis.[38] However, the mechanochemical application of such complexes towards hydrogenation/dehydrogenation reactions is not very developed . A

seminal example of the successful application of organometallic complexes towards catalytic dehydrogenation and subsequent hydrogenation reactions in mechanochemistry was presented by Hernández et al. of the *in situ* synthesis and use of Wilkinson's catalyst, $[RhCl(PPh_3)_3]$, under ball-milling conditions.[58] Uniquely, the mechanochemical method gave exclusively the orange polymorph of Wilkinson's catalyst, previously known to form when the quantity of solvent used to make the catalyst was reduced.[62, 63] This study demonstrated the overall versatility of ball-milling, demonstrating that the catalyst synthesis, the ammonia-borane dehydrogenation and the catalytic reduction of *trans*-stilbene could all be conducted successfully using a ball mill. Several control reactions were conducted to ensure the release of hydrogen gas through the dehydrogenation of ammonia-borane, which was confirmed both through $^{11}B\{^1H\}$ NMR studies as well as through a modified milling jar that allowed for the capture and volume measurement of the produced hydrogen gas (Figure 3).

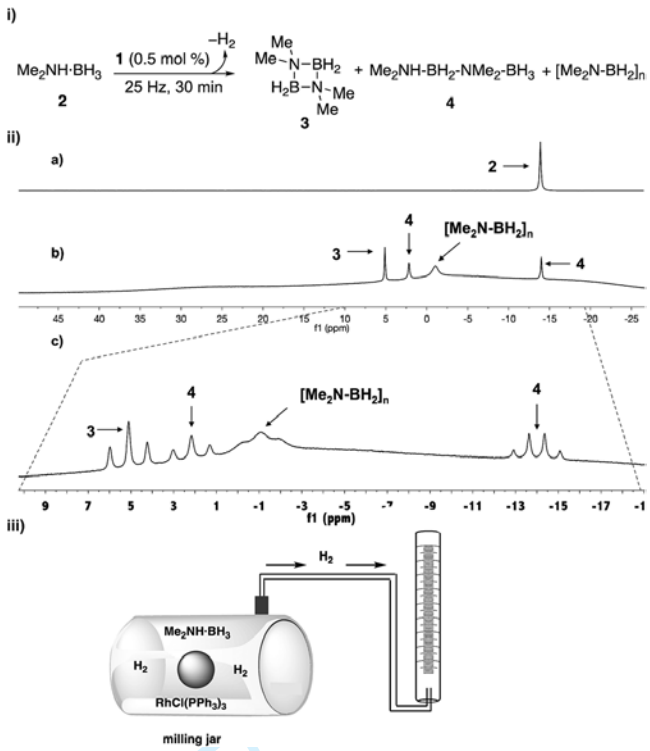

Fig 3. Control experiments showing i) the dehydrogenation of ammonia borane in the presence of Wilkinson's catalyst, as seen from ii) $^{11}B\{^{1}H\}$ NMR a) before and b) after. iii) apparatus to measure hydrogen release[58]

2.2.2 Nanoparticle catalysts

Early works in applied mechanochemical methods to hydrogenation catalysis research focused on comparing mechanical to traditional thermal and solvent based methods. For instance in 1999 by Lomovsky and coworkers synthesised Ni-Al-Mo alloy catalysts pyrometallurgically and mechanically, and studied their application to the hydrogenation of sodium maleate and sodium p-nitrophenolate.[64] They measured better average reaction rates and faster synthesis times for the mechanical version. Particle size reduction was limited and bottomed out at the order of single digit micrometer particle diameters. Due to the top-down approach to synthesis that was taken, ultrasmall sizes less than 10 nm in diameter were simply inaccessible and the particle size dispersity went uncontrolled and non-uniform. Particle characteristics such as these can be typical of mechanical methods where the process is mainly physical, like mechanical alloying of elemental

powders without a chemical change, or where there is either no particle capping agent to nullify aggregation, or no support structure to effectively disperse the particles. Similar works were published in 1993 and in 1994 by the groups of Miani and Cocco respectively, where elemental iron and carbon were ball-milled into nanophase iron carbides,[65] and where mechanically alloyed nickel-zirconium catalysts were ball-milled from their elemental precursors,[66] both as catalysts for the hydrogenation of carbon dioxide and carbon monoxide respectively.

3. Applications towards organic reduction reactions

3.1 Alkenes/Alkynes

3.1.1 Stoichiometric reductant or metal complexes

A methodology for the reduction of alkynes, alkenes, carbonyls, nitro groups and dehalogenation of aryl halides using *in situ* galvanic reduction of water to produce hydrogen was demonstrated by the Sakiji group. The selectivity of the process was limited, most likely due to high reactivity of nickel metal towards hydrogenations.[67] In 2018, the same group demonstrated that diethyl ether, as well as short-chain alkanes in a large excess (20 molar equivalents) could act as liquid sources of hydrogen gas when milled in the same SUS304 stainless-steel milling jars.[57] This work improved reaction yields, giving conversions in the range 29-86% for alkene, as well as full arene hydrogenations within 24 hours (Table 2). With this initial viability to produce stoichiometric amounts of hydrogen gas and the use of the milling vessel and media itself as the metal source to drive this reaction, there were some major setbacks which would need to be improved in future works. Using Entry 2 from Table 2 for example, the η value equates to 13.6 μL mg^{-1}, well within the limit of a traditional solution reaction, as opposed to traditional LAG ranges of 0.1-1 μL mg^{-1}. The galvanic oxidation of the jars in order to drive these reactions also leads to eventual degradation of the reaction vessel, limiting the long-term application of these methods.

Table 2. Substrate scope presented from the in situ generation of H_2 gas, using ethyl ether as a sacrificial source[57]

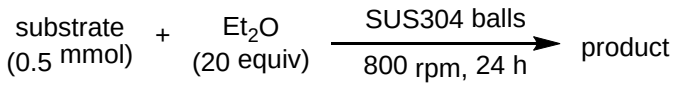

Entry	Substrate	Product	Yield (%)
1	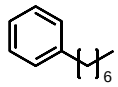	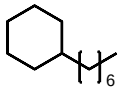	67
2	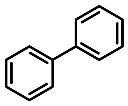	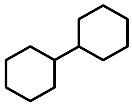	56
3	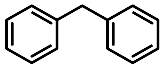	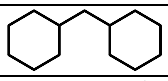	61
4	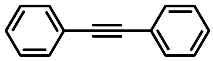	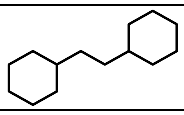	48
5	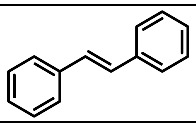	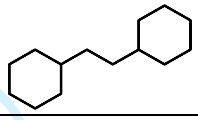	49
6	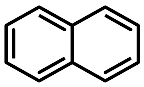	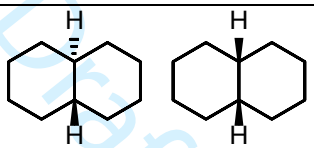	27 (30:70)
7	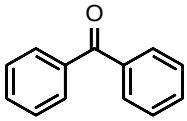	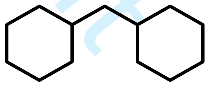	43
8	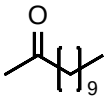	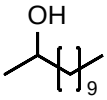	32 (61)[b]
9	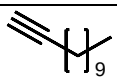	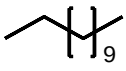	86
10	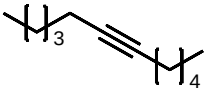	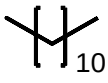	64

[a]The reaction was carried out using a Fritsch Pulverisette 7 Classic Line Ball Mill (PL-7) equipped a 12 mL SUS304 vessel and 50 SUS304 balls (diameter: ca. 5 mm). Et_2O was purchased from commercial sources and used without further purification. [b]Recovery of the substrate.

The work of Hernández et al. in 2018, in which they were able to obtain an orange polymorph of Wilkinson's catalyst as discussed in Section 2.2.1, highlights the fact that both the orange and red polymorphs showed vastly different reactivities towards the mechanochemical hydrogenation of *trans*-stilbene, giving 78% isolated yield after only 90 minutes milling at 25 Hz with the commercial catalyst as opposed to 13% with the catalyst synthesized using the LAG method. The

orange polymorph also showed unique reactivity towards *cis*-stilbene, having comparable yields as well as isomerization to *trans*-stilbene (Figure 4).[58] This highlights the utility of mechanochemical techniques for discovering the reactivity of catalysts in the solid state, not possible by traditional solution-based methods.

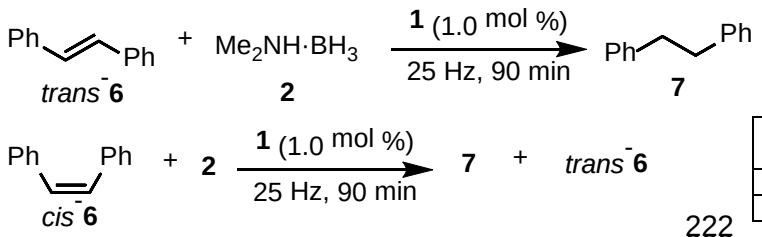

RhCl(PPh$_3$)$_3$	Yield[a]
LAG WC	13%
Red WC	99% (78%)[b]

RhCl(PPh$_3$)$_3$	Yield[a]	
	7	*trans*-**6**
LAG WC	62%	30%
Red WC	77%	23%

[a]Determined by ^{1}H NMR spectroscopy using 1,3,5-trimethoxybenzene as an internal standard. [b]After isolation by column chromatography.

Fig 4. Catalytic reactivity comparing the commercially available Wilkinson's catalyst to the catalyst made by milling (LAG WC) for both *cis* and *trans* stilbene hydrogenation and isomerization[58]

To the best of our knowledge, while mechanochemistry has shown broad and unique applicability in organometallic synthesis, this is the only example in which different polymorphic forms of a discrete metal complex were made mechanochemically and investigated as catalysts towards hydrogenation.

3.1.2 Nanocatalysts

In 2016, the Blair group reported metal-free mechanochemical hydrogenation using defect-laden hexagonal boron nitride (*dh*-BN) as a catalyst for the hydrogenation of olefins with H_2.[68] Boron nitride is not catalytically active until after the defects are introduced into the structure; in order to prepare the catalyst, pristine *h*-BN was milled in a zirconia jar for 30 minutes, yielding nanosheets with defect-rich structure (Figure 5).

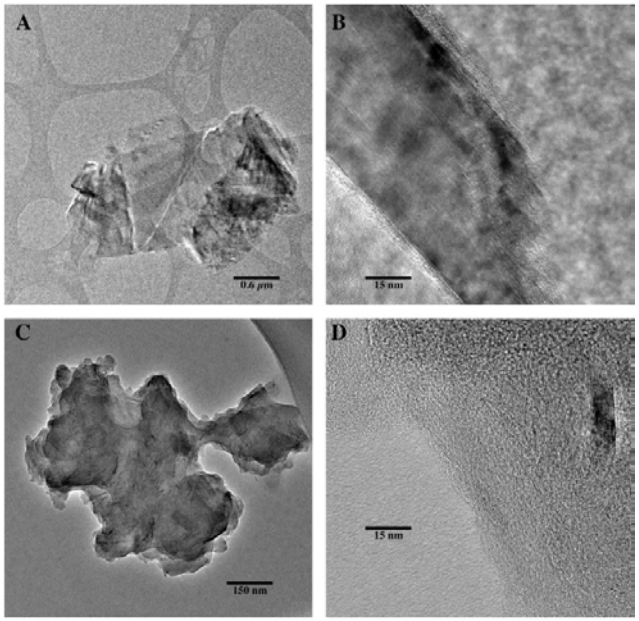

Fig 5. TEM images of as received *h*-BN (A and B) and *dh*-BN (C and D). The as received material is large flakes (A) with well ordered staking of the BN sheets (B). The *dh*-BN is much smaller and thinner flakes (C) with much less order in the c direction. Evidence of delamination and curling of the BN sheet can be seen in (C)[68]

With density functional theory (DFT) calculations as support, and with already existing work on hydrogen sorption energies to *dh*-BN sheets and nanotubes,[58] the authors identified the particular types of defect sites that contributed most to the catalytic activity of the *dh*-BN. If the binding energy of the site is too strong or too weak then the reactivity will be hindered. The nitrogen vacancies (V_N) and sites where boron atoms substituted for nitrogen (B_N) were found to be the most energetically similar to the binding energies of known metal catalysts, indicating their favourability for catalytic olefin hydrogenation. Solid-state NMR (ssNMR) spectroscopy revealed that the concentration of B_N sites is low compared to that of V_N sites, supporting the view that catalytic activity originates from nitrogen vacancies.

Outcomes of mechanochemical catalytic hydrogenation of various olefins are presented in Table 3; hydrogenations took place inside a temperature controlled and air-sealed custom alumina

pebble mill shaped like a double truncated cone. Full conversion could be reached in some cases with temperatures as low as 20°C, in stark contrast to typical industrial hydroprocessing that can require much higher temperatures (300 – 400°C). Conversion values across the ten different substrates were generally good; turnover frequencies (TOFs) and turnover numbers (TONs) were also calculated based on an assumption that the catalysis is deactivated after first use, but in practice the authors were able to recycle the catalyst at least three times with minimal loss of catalytic activity.

Table 3. Mechanochemical hydrogenation Yields, TOFs, and Single-Use TONs of Various Substrates over dh-BN with a Mill Speed of 66 rpm Unless Otherwise Specified [68]

Reactant	Products(s)	Reaction Temp. (°C)	TOF (s^{-1})/TON	Yield/Comments
		20	1.25×10^{-3}/16.10	100%; 114 RPM
		200	4.15×10^{-3}/90.69	100%
		20	2.88×10^{-4}/15.88	100%; 114 RPM
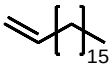	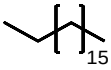	150	4.15×10^{-5}/90.69	35% at 150°C
		220	2.88×10^{-4}/15.88	100% at 220°C[a]
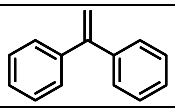	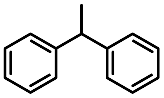	170	1.17×10^{-3}/21.07	97%
	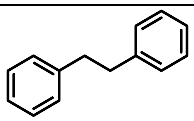	170	1.41×10^{-3}/14.49	100%
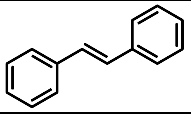	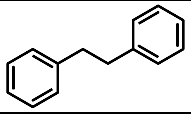	135	1.09×10^{-3}/5.00	99%
			1.15×10^{-3}/13.47	99%
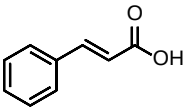	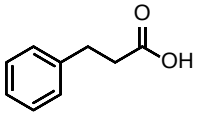	170	1.19×10^{-4}/10.28	55.1% hydrocinnamic acid after catalyst recycle
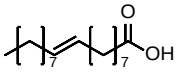	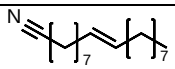	170	5.79×10^{-5}/5.00	58% olyel nitrile
	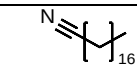			33% steryl nitrile
	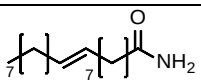			10% oleylamide
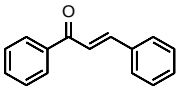	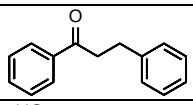	240	1.56×10^{-4}/13.56	90%
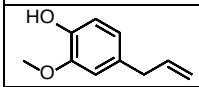	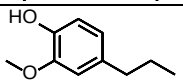	240	-	65%

[a]All information was derived from steel reactor data; all reactions run at 66 rpm unless otherwise specified. [b]After addition of 5 mass % fumed silica.

To confirm that this is truly a metal-free hydrogenation from mechanically treated *dh*-BN, additional steps and analyses were performed. Firstly, the use of the custom mechanochemical hydrogenation reactor made of alumina reduced the likelihood that milling equipment could actively participate in catalytic hydrogenations. As a model test reaction for the custom reactor, propene was chosen as a substrate void of metal impurities that could potentially be carried by

alternative liquid or solid substrates. Lastly, analysis of the *dh*-BN catalyst by inductively coupled plasma atomic emission analysis (ICP-AES) before and after activation revealed only minimal metal incorporation from the milling process. Specifically, while the starting material contained no detectable iron or nickel, the material after activation exhibited no more than 7 ppm of iron and 10 ppm of nickel. To prove it was the defects and not trace metal impurities that are catalytically active, hydrogenation reactions on propene substrates were performed in the custom mill with graphite instead of *dh*-BN, while maintaining similar contents of iron and nickel in the catalyst. Under reaction conditions similar to those used with the *dh*-BN catalyst, the use of mechanically treated graphite to catalyze the hydrogenation of propene showed no hydrogen uptake, and no hydrogenation products were observed. Moving forward, components other than the catalyst, such as a catalyst support or the reaction vessel material, can influence the catalytic capacities of a system and display control over things like yield, selectivity, and reaction rates.

In 2017, Chisholm and coworkers described the mechanochemical synthesis of an ordered mesoporous carbon (OMC) material supporting metal nanoparticles, displaying use as catalysts for the selective hydrogenation of arenes.[69] The OMC support was made beginning with the neat ball milling of Pluronic triblock co-polymers PEO–PPO–PEO (F127) and tannin for 30 minutes, followed by the addition of a divalent metal acetate to the solid mixture to mill for another 30 minutes. Subsequent carbonization under a nitrogen atmosphere yielded the pure OMCs; however, if the pure metal species of the metal acetate chosen has a high enough boiling point then the metallic component will not evaporate during high temperature (450 – 800°C) carbonization and metallic nanoparticles will remain in the final product. The transition metal ions were necessary to crosslink the tannin around the F127 micelles during milling, after which the F127 micelles were completely decomposed and the tannin-metal polymer restructured into a carbon framework

during the carbonization step. From XRD data it was believed that the metal ion during carbonization initially becomes an oxide and is eventually reduced to pure metal by surrounding carbons if the material was carbonized for long enough, after which the pure metal would either evaporate or remain depending on its boiling point. A graphic of the synthesis process is shown in Figure 6 that better visually conveys the structural coordination of the tannin-F127-metal solid-state mixture.

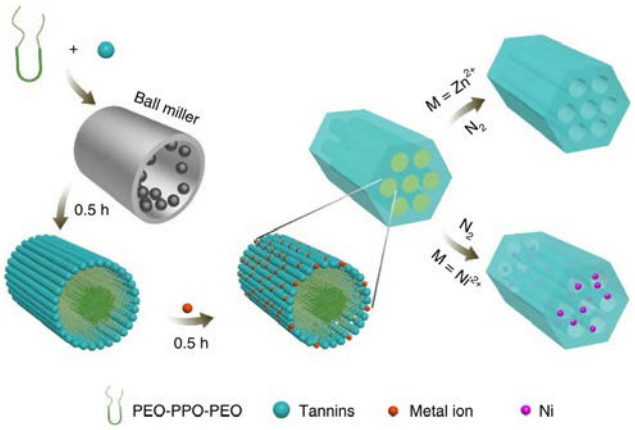

Fig 6. A proposed mechanism for the mechanochemical assembly mediated by coordination crosslinking of tannin, a biomass-derived polyphenol, with divalent metal ions in the presence of Pluronic triblock co-polymers PEO–PPO–PEO. First, the PEO– PPO–PEO and tannin are ball milled for 0.5 h, forming a brown gel. Selected metal acetates are then added to the miller, resulting in homogeneous gel nanocomposites after a short milling time (0.5 h). After carbonization in a N_2 atmosphere, pure OMCs, or metal NP OMCs are obtained depending on the boiling point of the reduced metal species. For example, metallic Zn can evaporate during high-temperature treatment[69]

Nickel (II) acetate was chosen as the metal component of the catalytically active OMC materials, which were prepared using a variety of conditions, including different carbonization temperatures and different tannin-to-F127 weight ratios. These parameters are outlined in the catalyst description Ni-OMC@F127$_w$-c as ‘c’ and ‘w’, respectively. Figure 7 details characterization of the Ni OMCs using STEM-HAADF imaging. The Ni nanoparticles were consistently ultrasmall

and well dispersed, with average particles sizes of 4.35 nm and 5.4 nm for samples carbonized at 450 and 600°C, respectively. Even after being recycled for multiple uses the average particle size (6.24 nm) did not grow substantially.

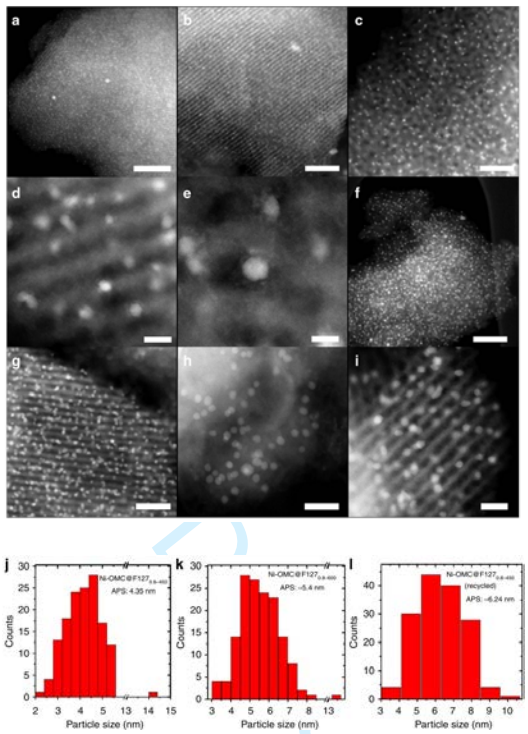

Fig 7. Morphology and structural characterization of nickel OMCs. (a–e) STEM-HAADF images of Ni-OMC@F127$_{0.8}$-450. Scale bar, 200 (a), 100 (b), 50 (c), 10 (d) and 5 nm (e). (f,g) Ni-OMC@F127$_{0.8}$-600. Scale bar, 100 (f) and 50 nm (g). (h) Ni-OMC@F127$_{0.8}$-800. Scale bar, 50 nm. (i) NiOMC@F127$_{0.8}$-450 recycled from hydrogenation reaction; scale bar, 20 nm. (j–l) The corresponding particle size distributions. The particle size distribution was calculated based on 150 particles randomly selected. APS, average particle size[69]

Hydrogenation runs with Ni-OMCs were compared against similar materials such as Ni on commercial activated carbon (Ni-AC) or traditional soft templated OMC (Ni-ST-OMC). The latter two were prepared by a wet impregnation method, maintaining the same Ni content as in Ni-OMC@F127$_{0.8}$-450 (16.1 wt.%). It is worth noting that severe agglomeration of Ni nanoparticles was observed in the AC and ST materials of upwards of 100 nm in diameter. A summary of the

catalytic conversion tests is shown in Table 4. Three different substrates of different sizes were run, and the conversion results clearly demonstrated that the novel Ni-OMCs were unrestricted by substrate size whereas the alternative catalysts performed increasingly worse as the substrate size increased. This wide-ranging size selectivity was attributed to the pore size and structure of the novel carbon framework. Specifically, the catalytic properties of the novel mechanochemically synthesised Ni-OMCs were greatly enhanced by coupling large pore size with 1D pore channel structure, and a high surface area.

Table 4. Selective hydrogenation of alkenes by Ni-based catalysts. Reaction conditions: cyclohexene or 1-octadecene 1 mmol, decane (internal standard: 1 mmol), ethanol 3 ml, Ni catalyst 10 mg, H_2 3MPa, 130 °C, 2 h; or cholesteryl acetate 0.5 mmol, acetone 10 ml, Ni catalyst 10mg, H_2 3MPa, 130 °C, 2 h[69] The three reagents, cyclohexene, 1-Octadecene, Cholesteryl acetate, are represented at the bottom.

Catalyst	Cyclohexene Yield	1-Octadecene Yield	Cholesteryl acetate Yield
Blank	8%	<1%	<1%
Ni-OMC@F127$_{0.8}$-450	98%	96%	92%
Ni-AC@450	97%	65%	10%
Ni-ST-OMC@450	98%	77%	24%

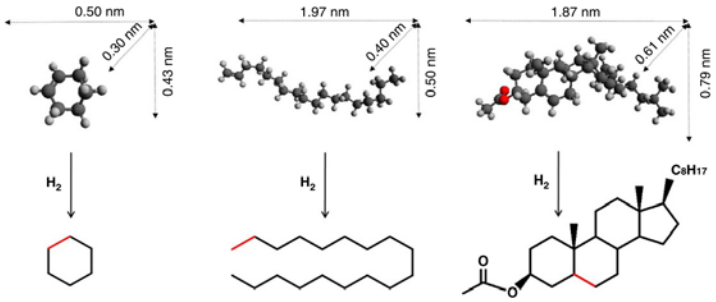

Because the pore structures result from the decomposition of organic polymer regions, the pore sizes and surface areas could be controlled and tuned by varying the weight ratios involving F127 or by changing the choice of polymer: Pluronic F88, F87, F68, F38, P123, P103, P85, P65 and non-ionic surfactants like PEO-based Triton X-100 and Brij-78 were also explored (Table 5).

Table 5. Calculated N_2 at 77K adsorption parameters for the various tannin-based materials obtained with or without metal crosslinkers, using different triblock co-polymers as templates, and under various carbonization temperatures[69]

Sample	V_{SP} (cm^3 g^{-1})*	S_{BET} (m^2 g^{-1})†	V_{mi} (cm^3 g^{-1})‡	S_{mi} (m^2 g^{-1})§	w_{KJS} (nm)‖	V_{mi} CO_2 (cm^3 g^{-1})¶
C@Tannin-Zn	0.23	514	0.20	469	-	-
C@Tannin-F127	0.36	395	0.11	245	-	-
OMC@F127$_{0.4}$-800	0.59	773	0.19	475	7.3	0.22
OMC@F127$_{0.6}$-800	0.76	1057	0.24	601	7.8	0.29
OMC@F127$_{0.8}$-800	0.58	621	0.12	293	6.9	0.29
OMC@F127$_{1.0}$-450	0.66	547	0.08	180	8.6	-
OMC@F127$_{1.0}$-600	0.67	869	0.17	412	8.2	-
OMC@F127$_{1.0}$-800	0.69	734	0.16	390	7.8	0.18
Ni-OMC@F127$_{0.8}$-450	0.96	996	0.19	464	6.9	0.18
NiOMC@F127$_{0.8}$-600	0.73	769	0.15	356	7.8	-
Ni-OMC@F127$_{0.8}$-800	0.52	558	0.14	355	9.2	-
OMC@F38$_{0.8}$-800	0.49	722	0.16	381	5.3	-
OMC@F68$_{0.8}$-800	0.58	770	0.15	350	5.3	-
OMC@F87$_{0.8}$-800	0.62	765	0.17	412	5.9	-
OMC@F88$_{0.8}$-800	0.61	733	0.13	316	5.7	-
OMC@P65$_{0.8}$-800	0.60	851	0.15	340	4.2	-
OMC@P85$_{0.8}$-800	0.66	770	0.17	405	6.6	-
OMC@P103$_{0.8}$-800	0.76	825	0.19	466	7.5	-
OMC@P123$_{0.8}$-800	0.73	811	0.13	310	5.4	-
OMC@Bj78$_1$-800	0.89	695	0.16	382	17	-
OMC@TritonX100$_{0.8}$-800	0.50	782	0.17	407	5.0	-
OMC@(F127+Ph_3P)$_{0.8}$-800	0.57	496	0.10	244	10.4	-

*Single point pore volume at relative pressure of 0.98
†Specific surface area calculated using BET equation in the relative pressure range of 0.02-0.05
‡Micropore volume
§Micropore surface area calculated using the carbon black STSA *t*-plot equation within the thickness range of 0.354-0.500 nm
‖Pore width from the distribution maxima calculated according to the KJS method using carbon black as reference
¶Cumulative plot from NLDFT analysis for CO_2 isotherms for pores up to 1.5 nm

3.2 Carbonyls

3.2.1 Stoichiometric reductant

Due to their prevalence in a variety of value-added products, the investigation of sustainable, mechanochemical routes for the reduction of carbonyl compounds has gained considerable traction in the last two decades. One of the earliest examples of such reactivity was reported in 1989 by Yagi and coworkers who described the reduction of carbonyl compounds to alcohols using $NaBH_4$. The reactions were performed by grinding together ten molar equivalents of $NaBH_4$ with a variety of aliphatic or aromatic ketones, followed by ageing for 5 days with daily stirring, yielding the corresponding alcohol.[70] This work was further expanded upon by Santos and coworkers, who showed that milling of $NaBH_4$ with benzaldehyde and acetophenone derivatives, having both electron-withdrawing and -donating groups, affords the corresponding primary and

secondary alcohols.[71] The reactions were conducted in custom-made stainless-steel milling jars using alumina balls of 0.25 inch diameter as milling media. This work also showcased the *in situ* generation of highly reactive $LiBH_4$ through milling of $NaBH_4$ with LiCl, enabling solid-state reduction of esters *via* mechanochemistry.[71] Since these early examples, the mechanochemical hydrogenation of carbonyls has expanded to use novel reductants, as well as accessing previously difficult products, due to their intrinsic solubility challenges. Apart from using hydrogen gas or reactive metal hydrides, our group had investigated the use of a solid siloxane, polymethylhydrosiloxane (PMHS), as a viable reductant when activated by a solid fluoride in the form of *tert*-butyl ammonium fluoride (TBAF) supported on silica, or a pairing of alkali fluoride salts with crown ethers.[72] This work systematically investigated the hydrogenation of both aliphatic and aromatic aldehydes and ketones. The mechanism of the mechanochemical reduction using PMHS proceeded *via in situ* generation of gaseous methylsilane ($MeSiH_3$), which was further activated into the highly reactive $[H_3SiFMe]^-$ from another equivalent of silica-supported TBAF. This study also showed the effectiveness of mechanochemical hydrogenation towards substrates with challenges regarding solubility. On one hand, polyketones of low solubility are difficult to reduce using solution-based methods, while under mechanochemistry, 54% of available carbonyl bonds could be reduced after milling for 90 minutes followed by 2 days of passive ageing at room temperature. On the other hand, mechanochemistry helps prevent other separation issues. For instance, both 5-hydroxymethylfurfural (HMF) and its corresponding alcohol dihydroxymethylfurfural (DHMF) are highly soluble in water and hard to separate when dissolved. Using mechanochemistry for this reduction prevented contact with water during reaction and facilitated separation afterwards.

Expanding on this study, Forgione and coworkers studied the KOH-driven Cannizzaro disproportionation of HMF and benzaldehyde derivatives with both electron donating and withdrawing substituents. While this report was successful in the equal production of DHMF, as well as the fully oxidized dicarboxylic acid products in under 5 minutes, it was noted that selectivity could be driven entirely towards DHMF, but required the use of 1.2 equivalents of paraformaldehyde as a sacrificial reagent.[73]

3.2.2 Nanocatalysts

In 2015, Luque and coworkers studied the hydroconversion of cinnamaldehyde using mechanochemically-synthesized palladium nanoparticles that were supported on an aluminum incorporated mesoporous silica (Pd/Al-SBA-15).[74] Catalysts of different Pd loadings (0.5, 1, 2, 4 wt.%) were synthesised and a commercial palladium-on-carbon (Pd/C) catalyst was purchased for catalytic activity comparison. To mechanochemically synthesise the catalyst, palladium(II) acetate and pre-formed Al-SBA-15 were milled together in a planetary ball mill at 350 rpm for 10 minutes. After milling, the solid material obtained was calcined at 450°C in air for 2 hours. TEM images of the bare Al-SBA-15 support (Figure 8A) and of three of the differently Pd-loaded catalysts (Figure 8B-D) are shown below. The mesopores of the Al-SBA-15 are shown to be well structured prior to the Pd catalyst being milled in and the ordered nature of the support is mostly kept intact after milling, though some amorphous domains of Si were observed. For catalysts with a low palladium loading the nanoparticles were small, well dispersed with an average diameter <10 nm, and no sintering was observable. However, larger aggregates could be seen for systems with higher palladium loadings.

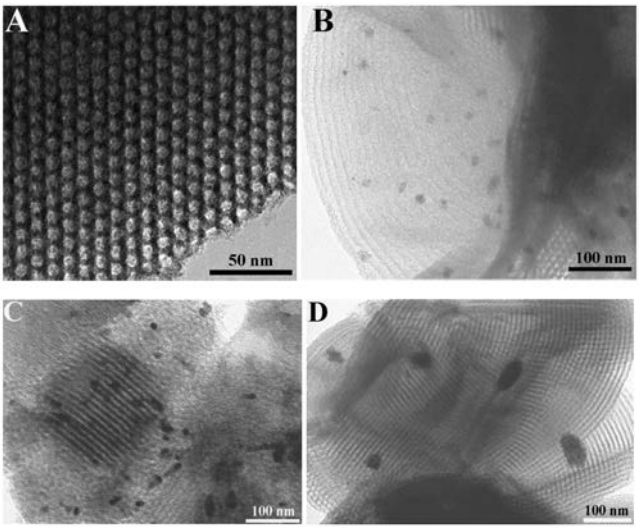

Fig 8. TEM images of A) Al-SBA-15 support; B) Pd1-Al; C) Pd2-Al; D) Pd4-Al[75]

The hydroconversion of cinnamaldehyde was performed with formic acid under conventional heating or microwave irradiation, using acetonitrile as a solvent within the presence of a palladium catalyst. Formic acid was presumed to decompose into CO, CO_2, H_2, and water under heating in the presence of noble metals, providing an *in situ* source of hydrogen. The conversion values of cinnamaldehyde and the multiple product selectivity values in mol% are summarized in Table 6 with detailed reaction conditions. Although both conventional heating and microwave irradiation experiments were both performed, only the microwave trials are presented due to the poor conversion values collected from conventional heating.

Table 6. Total conversion (mol %) and selectivities to products (mol %) of different supported Pd nanoparticles on Al-SBA-15 as compared to a commercial 5%Pd/C material in the microwave-assisted hydroconversion of cinnamaldehyde in formic acid. Reaction conditions: 0.1 mL cinnamaldehyde (0.8 mmol), 0.3 mL formic acid (8 mmol), 2 mL acetonitrile, 0.5 g catalyst, microwave irradiation, 200 W (180 °C maximum temperature reached, averaged temperature 150 °C, 250 PSI maximum pressure), 15 min reaction[75]

Catalyst	Conversion (mol%)	Selectivity (mol%)					
		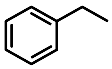		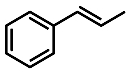	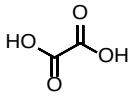	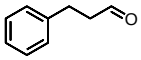	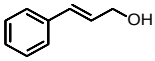
Blank	<5	-	-	-	-	-	-
Pd0.5-Al	97	<5	52	26	16	<5	-
Pd1-Al	>99	<5	64	11	18	-	-
Pd2-Al	98	<5	66	18	13	-	-
Pd4-Al	85	13	44	41	<5	-	-
5% Pd/C	71	21	48	27	-	<5	-

Intriguingly, though only the commercial Pd/C catalyst performed well under conventional heating (96% conversion after 24 hours) while the next best result was the Pd4-Al catalyst (50% conversion after 24 hours), under microwave irradiation the Pd/C catalyst performed worse (by at least 14%) compared to any of the mechanochemically synthesised catalysts. Most of the product quantity was made up of ethylbenzene, β-methylstyrene, cyclohexane, and oxalic acid, the molar composition of which depended on the palladium loading of the catalyst used. For example, production of ethylbenzene increased, while production of oxalic acid generally decreased, with an increase in palladium loading. A possible explanation for the changes in product selectivities might be in sensitivity to changing sizes of palladium nanoparticles due to agglomeration at higher catalyst loadings.

3.3 Carbon monoxide and carbon dioxide

3.3.1 Stoichiometric reductant

From the highlighted early examples of mechanochemical methods being applied towards the hydrogenation of carbonyl functionalities in organic small molecules, the next step in expanding the sustainability and use of mechanochemistry towards a circular economy would be

applications in CO_2 reduction. The hydrogenation of CO_2, while fundamentally different than organic carbonyl reduction, gives access to formates and formic acid, both valuable C_1 building blocks.[76] Initial work done by Mulas and coworkers used olivine, a mixed Mg-Fe silicate ore, for the hydrogenation of CO_2 gas using water as the source of hydrogen.[77] Using a custom-modified SPEX milling jar with sealable valves enabled sampling the atmosphere within the jar using an airtight syringe, followed by gas chromatography (GC) analysis. Conversions of nearly 50% were achievable using an internal CO_2 pressure of 1.5 bar, after 150 minutes of milling, with only slight selectivity to the primary target methane (~0.2% v/v). A tentative explanation for the discrepancies in mass balance is partial hydrogenation to give liquid products, which would not be detectable by GC measurements. While mechanochemical activation of olivine by milling produces 13.5% of magnesium carbonates, there was no evidence of magnetite formation upon milling of a solid catalyst shown to be effective for CO_2 hydrogenation under hydrothermal conditions.[78, 79] This observation indicates that only Fe^{3+} ions are needed as the active metal species, and are most likely released by olivine activation upon extended milling.

Processeses for the activation of CO_2 have been expanded to include solid carbonates as the carbon source, as many inorganic carbonates suffer from solubility limitations in traditional organic solvents.[11, 80] As a stand-in for gaseous CO_2, Jingying and coworkers showed the mechanochemical reduction of several carbonates and bicarbonates with stoichiometric amounts of sodium metal acting as the reductant to give the corresponding formate salts.[81] This work highlighted that ammonium carbonate salts performed the best, giving conversion up to 45% to the corresponding sodium formate. Despite this early success, this process still suffers from low yields as well as the production of undesirable stoichiometric amounts of sodium oxide as a

byproduct. The transition to more air and moisture stable reductants in future works would also be of interest as it allows for more industrially applicable processes.

3.3.2 Nanocatalysts

In 2019, Dai and coworkers detailed the mechanochemical synthesis of single atom catalysts (SACs) using noble metals on metal-oxide supports for hydrogenations. A high entropy (HE) metal oxide [(NiMgCuZnCo)O] was mechanochemically synthesised with a supported catalytically active noble metal element under ambient conditions and was used in the hydrogenation of atmospheric CO_2 to CO.[82] HE oxides, or more descriptively "configurationally disordered and entropy-stabilized mixed metal oxides", are part of a broader class of materials that include both metallic and non-metallic materials. Their single-phase crystal structure has enhanced stability through maximization of the configurational entropy that occurs from the roughly equal inclusion of a large (usually at least five) number of homogenously dispersed metal cations in the solid solution. The resulting changes of the entropic term to the Gibbs free energy of mixing contribute to the high temperature stability of the HE materials. This HE material was made in a two-step mechanochemical process whereby precursor oxide powders are first ball milled for 2 hours, and then the mixed material is calcinated for 2 hours at 500°C: a schematic of the synthesis method is shown in Figure 9.

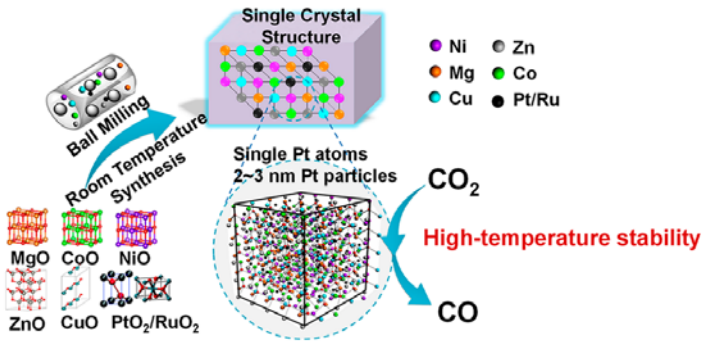

Fig 9. Schematic of the mechanochemical synthesis of Pt/Ru(NiMgCuZnCo)O entropy-stabilized metal oxide solid solution[82]

As the authors stated, this is a notable improvement over other methods to synthesize HE oxide materials, which require long processing times (>48 hours) and/or high temperatures (900 – 1300°C). To evaluate the role of milling in the chemical transformation, X-ray diffraction patterns (Figure 10a) of the milled samples were taken after milling for different times. After 2 hours of milling the base oxide powders (without the catalytically active noble metal), all the precursor phases were successfully converted to a single new phase that was characteristic of the HE oxide material.

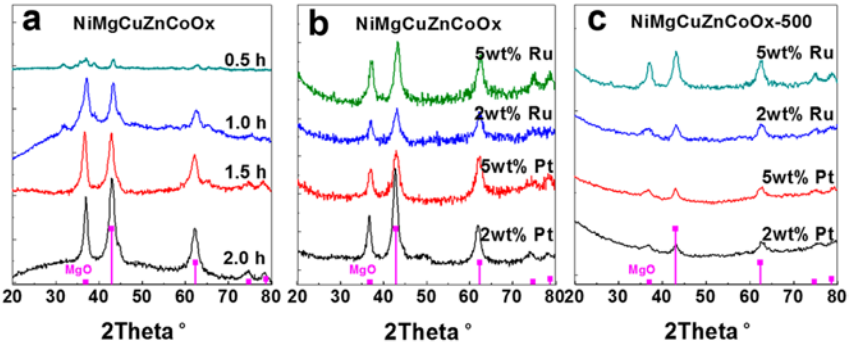

Fig 10. X-ray diffraction patterns for (a) NiMgCuZnCoOx synthesized by ball milling with different times; (b) 2 and 5 wt.% Pt/RuNiMgCuZnCoOx synthesized by ball milling with 2 h; and (c) 2 and 5 wt.% Pt/Ru-NiMgCuZnCoOx synthesized by ball milling with 2 h and 500°C treatment for 2 h[82]

Different loadings of Pt(II) and Ru(II) oxide powders were added to the mixture and X-ray patterns were taken showing good incorporation of the critical noble metal powders (Figure 10b). Lastly, another X-ray pattern was taken after the catalytically active HE solid was calcinated at 500°C for 2 hours and no significant change in the pattern was found that would have indicated the formation of binary platinum or ruthenium oxides (Figure 10c). To help substantiate the dispersity and size of the of catalytic sites, scanning transmission electron microscopy (STEM) images of the milled and calcinated product were taken (Figure 11a-e). Platinum was found both in the form of single atoms, and as ultrasmall (2 – 3 nm) nanoparticles. Morever, there was no evidence of large noble metal particles that could result from sintering, and elemental mapping revealed a balanced distribution of transition metals throughout the solid (Figure 11e).

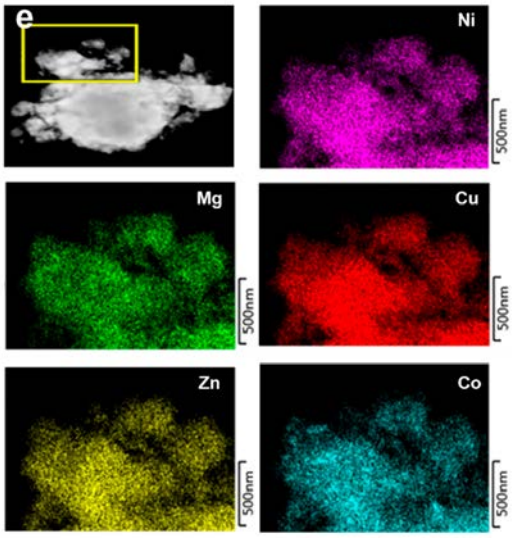

Fig 11. High-angle annular dark-field STEM images for 5 wt.% Pt-(NiMgCuZnCo)O after 500°C treatment with 2 h. Highly dispersed Pt particles in the size range of 2−3 nm on entropy-stabilized metal oxide particles are shown in panels a and b, while panels c and d show atomically dispersed Pt single atoms. Elemental mapping is shown in panel e for 5 wt.% Pt-(NiMgCuZnCo)O after 500°C treatment for 2 h[82]

The catalytic performance and stability of the Pt/Ru-loaded HE oxides were investigated, and are summarized in Figure 12. Hydrogen gas was used to reduce CO_2 into CO with only a small amount

of side-product, as shown by robust selectivity to CO production of over 95% across all catalyst variations. The catalysts containing 2 wt. % Ru-500 and 2 wt. % Pt-500 provided 33.9% and 36.6% yields of CO, with respective conversions of CO_2 of 40.1% and 43.4%. For 5 wt. % Ru-500 and 5 wt. % Pt-500, the yields of CO were increased to 45.7% and 46.1%, with corresponding CO_2 conversions of 45.4% and 47.8%, respectively. Catalytic performance at 500°C was measured over time to investigate the stability of the catalyst, revealing that the conversions and yields remained mostly unchanged over the course of 20 hours.

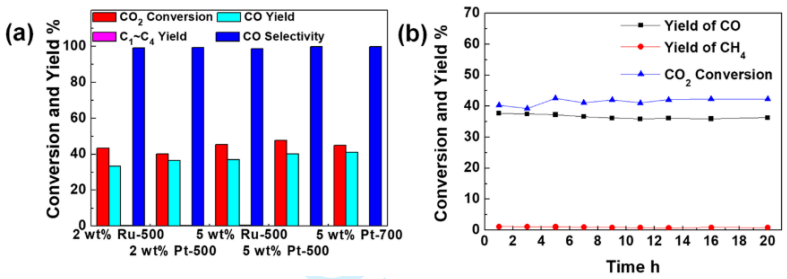

Fig 12. (a) CO_2 hydrogenation activity of 2 wt.% Pt-500, 5 wt.% Pt-500, 2 wt.% Ru-500, and 5 wt.% Ru-500 under 500°C reaction temperature, (b) CO_2 hydrogenation stability at 500°C over 5 wt.% Pt-500, and (c) STEM result of 5 wt.% Pt-500 after hydrogenation of CO_2 at 500°C for 2 h[82]

3.4 Imine/nitro/azides

3.4.1 Stoichiometric reductant or metal complexes

Carbon-nitrogen bonds can be found throughout a variety of molecular structure motifs in the agricultural and pharmaceutical sectors. As previously outlined, direct mechanochemical hydrogenations have already shown great success towards the reduction of olefins and carbonyls, with nitrogen-based functional groups such as imine, azide or nitro moieties, being attractive targets for extending the reaction scope. To the best of our knowledge, the earliest example of such work came from the Wang group in 2005, who described a reductive amination by pairing of a zinc chloride catalyst and a Hanztch ester reductant in order to couple and reduce aromatic

aldehydes and amines[83] bearing electron-withdrawing functionalities. In 2018, Cintas and coworkers demonstrated the reduction of nitrobenzene, as well as alkyl and aryl azides, using formates or hydrazine as model hydrogen sources, without the addition of a catalyst.[84] Their initial investigation explored the reduction of nitrobenzene to aniline using hydrazine as the reductant in order to optimize the reaction conditions for later investigations into the formate-driven hydrogenation of azides. The optimized reaction conditions revealed that quantitative yields were achievable after only 30 minutes of milling in a Retsch planetary mill, using a stainless steel vessel, neutral alumina as a grinding auxiliary, as well as potassium hydroxide and 10 molar equivalents of hydrazine. They also investigated the influence of jar material and ball size, noting that no reactivity occurred when using zirconia implements and that a mixture of 2 and 5 millimeter balls were the most consistent in achieving full conversion. Following the initial optimizations, the highly toxic hydrazine was replaced with much more benign formate as the hydrogen source. This change in reductant led to only a minimal loss in reaction effectiveness, producing aniline in 97% yields. The reactions also showed good selectivity, being applicable to a range of substituted aromatics with no proof of reductive dehalogenation (Table 8). The reaction was also applicable to the reduction of aryl and alkyl azides into their corresponding amines: both benzyl and aryl azides underwent excellent conversions, with yields ranging from 60% to quantitative for both electron-rich and -poor substituents (Tables 7 and 8).

Table 7: Benzyl and alkyl azide reduction scope through the mechanochemical decomposition of hydrazine as a hydrogen source[84]

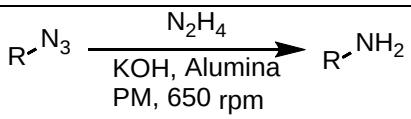

Entry	Alkyl azides	Time (h)	Yield[b] (conv.)[c] %
1	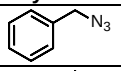	1	98 (100)
2	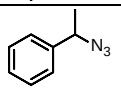	1	100 (100)
3	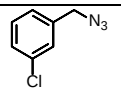	1	100 (100)
4[d]	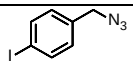	1	- (100)
5	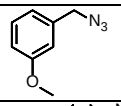	1	99 (100)
6	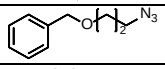	1	80 (100)
7		1	96 (98)
8	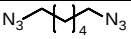	1	90 (100)
9	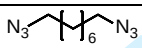	1	94 (100)
10	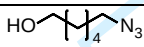	1	60 (100)
11	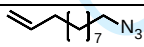	1	81 (90)

[a]Reaction conditions: aryl azide (0.5 mmol), hydrazine (15 mmol), KOH (10 mmol), alumina (1 g), 650 rpm, stainless steel jar (50 mL), 1500 balls (ϕ = 2 mm) and 48 balls (ϕ = 5 mm) [b]Isolated yield, compound purity proven by ^{1}H and ^{13}C NMR. [c]Determined by GC-MS. [d]Benzylamine was formed as the product

Table 8: Aryl azide reduction scope through the mechanochemical decomposition of sodium formate as a hydrogen source[84]

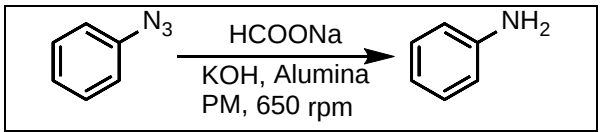

Entry	Alkyl azides	Time (h)	Yield[b] (conv.)[c] %
1	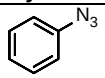	1.5	98 (100)
2	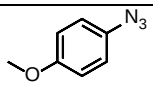	1.5	85 (98)
3	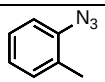	1	100 (100)
4	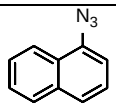	1	87 (92)
5	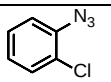	1.5	95 (98)

[a]Reaction conditions: aryl azide (0.5 mmol), sodium formate (10 mmol), KOH (1 mmol), basic alumina (1 g), 650 rpm, stainless steel jar (50 mL), 1500 balls (ϕ = 2 mm) and 48 balls (ϕ = 5 mm) [b]Isolated yield, compound purity proven by ^{1}H and ^{13}C NMR. [c]Determined by GC-MS.

It is worth noting that ICP analysis confirmed that the stainless steel milling assembly was leaching Cr, Fe and Ni during the reaction, as had previously been discussed for hydrogenation reactions involving water-splitting or activation of ethers and light alkenes.

Direct transfer hydrogenation using a supported metal catalyst was also investigated towards the mechanochemical reduction of nitro groups, as demonstrated by the work of Štrukil and coworkers. The use of a traditional Pd/C catalyst was shown to be effective, with ammonium formate being used as a solid-state source of hydrogen.[59] Previous work had shown that in the presence of a palladium catalyst, formate salts would decompose, giving off gaseous NH_3, CO_2 and H_2.[85] As a result, the heterogeneous palladium catalyst functioned as both the generator of the hydrogen gas, and as the catalyst for the hydrogenation of nitroarenes. This catalytic system was readily applied to nearly 20 substrates, some with multiple isomers, with up to ≥90% conversions. Firstly, in addition to using a commercial Pd/C catalyst the authors also fabricated and employed a milled pure Pd/C catalyst and a milled in silica Pd/C catalyst. The morphological and size differences were examined under SEM as shown in Figure 13.

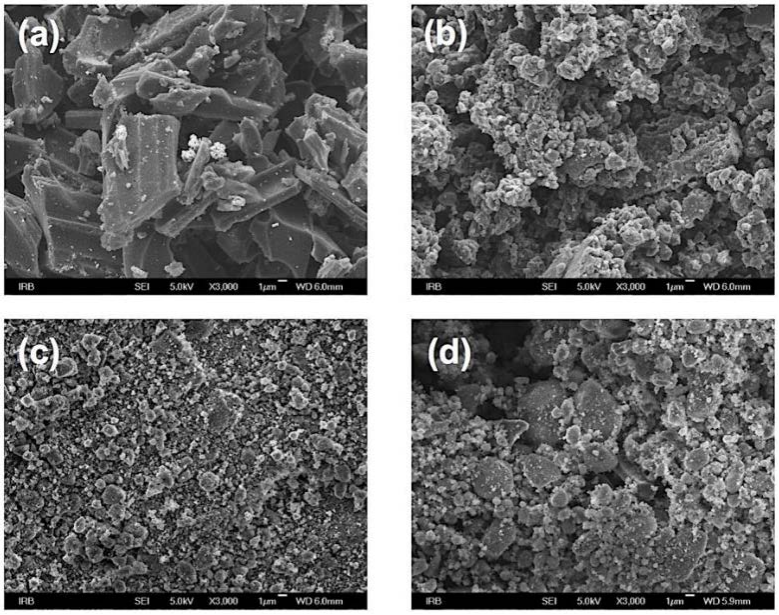

Fig 13. SEM images (3000×) of (a) commercial and (b) milled samples of 10 wt. % Pd/C catalyst; (c) The catalyst milled with silica under LAG conditions for 60 min and (d) post-workup sample after CTH of 3-nitrobenzonitrile[59]

The catalysts milled with silica (regardless of the use of a liquid additive) offered the best benefits in terms of size and homogeneity, being generally smaller and more evenly dispersed compared to the other samples, and was chosen for the substrate scope investigation. Secondly, the use of a LAG additive in the catalytic reaction (Figure 14a) demonstrated an exceptional improvement in conversion, not only compared to neat mechanochemistry but also in comparison to reactivity in solution.

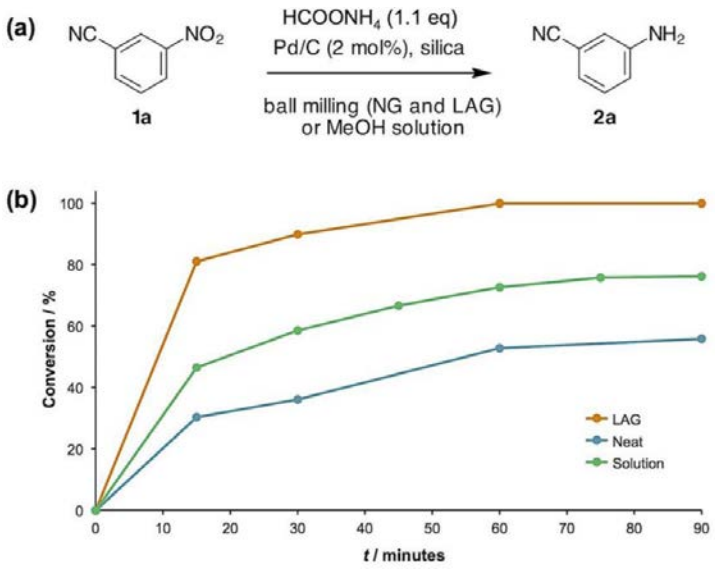

Fig 14. (a) Mechanochemical CTH model reaction; (b) Conversion of 3-nitro-benzonitrile during CTH determined by HPLC analysis[59]

The mechanochemical method enabled a considerable improvement over reactivity in solution, with LAG providing at least 20% higher conversion (Figure 14). This work demonstrated the versatility of mechanochemistry by adapting to a solid-state hydrogen source from a gaseous one, the simple effectiveness of milling by significantly reducing the catalyst size and increasing particle dispersity in a relatively short milling time, and the power of LAG by significantly and quantitatively improving on the solution conversion with only a tiny fraction of the solvent waste. The catalyst did show some limitations with nitro-functionalized thioureas due to catalyst poisoning, as well as nitro-substituted polycyclic aromatic hydrocarbons. In specific cases with halogenated nitroarenes, a mixture of both the dehalogenated and reduced product was noted, due to the high reactivity of the palladium catalyst towards the competitive dehalogenation reaction.

3.4.2 Nanocatalysts

In 2016, Hapiot and coworkers reported the use of cyclodextrins (CDs) and other saccharide additives as simultaneous reducing and stabilizing agents for the mechanosynthesis of

CD supported gold nanoparticles used to catalyse the reduction of substituted nitrobenzene derivatives to aniline products.[86] To synthesize the AuNPs/β-CD complex, 10 mL zirconia grinding jars containing a 9 mm zirconia ball were shaken in a vibrational mill for 5 minutes at a frequency of 30 Hz. The jars were filled with a cationic gold source, 0.016 mmol of $AuCl_3$, and 0.881 mmol of a saccharide additive as a reductive and capping agent. TEM images of the mechanochemical product and a size histogram of Au nanoparticle diameters are shown in Figure 15; the particles are ultrasmall and very monodisperse, averaging 1.54 ± 0.4 nm in diameter.

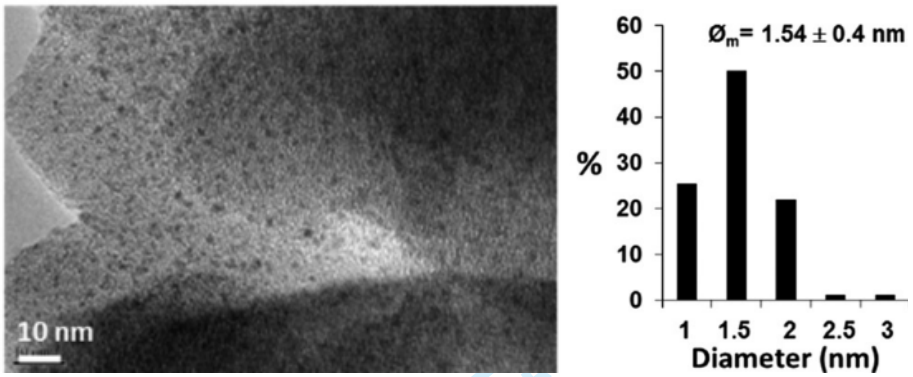

Fig 15. TEM of beta-cyclodextrin stabilised gold nanoparticles and particle size histogram[86]

The as-made saccharide-stabilized Au nanoparticles were then used to catalyze the hydrogenation of 1-chloro-2-nitrobenzene and other closely related halogenonitrobenzene and methoxynitrobenzene derivatives reduced by $NaBH_4$. Variables such as the saccharide additive, the milling frequency and time, and the saccharide hydration were explored in attempts to maximize conversion values and widen the scope of compatible substrates. Among the best conversion results of 100% in 15 minutes for a substrate, the necessary conditions were a combination of milling at 30 Hz for 15 minutes and using hydrous β-CD (10 wt.% water) as a capping agent. Regarding the scope of substrates as seen in Figure 16 that are accessible to hydrogenation, the authors found an interesting regioselectivity in the hydrogenation of

nitrophenols: para isomers were disfavored while meta and ortho isomers reacted well. A poisoning effect, illustrated in Figure 16, was evoked as a possible mechanism.

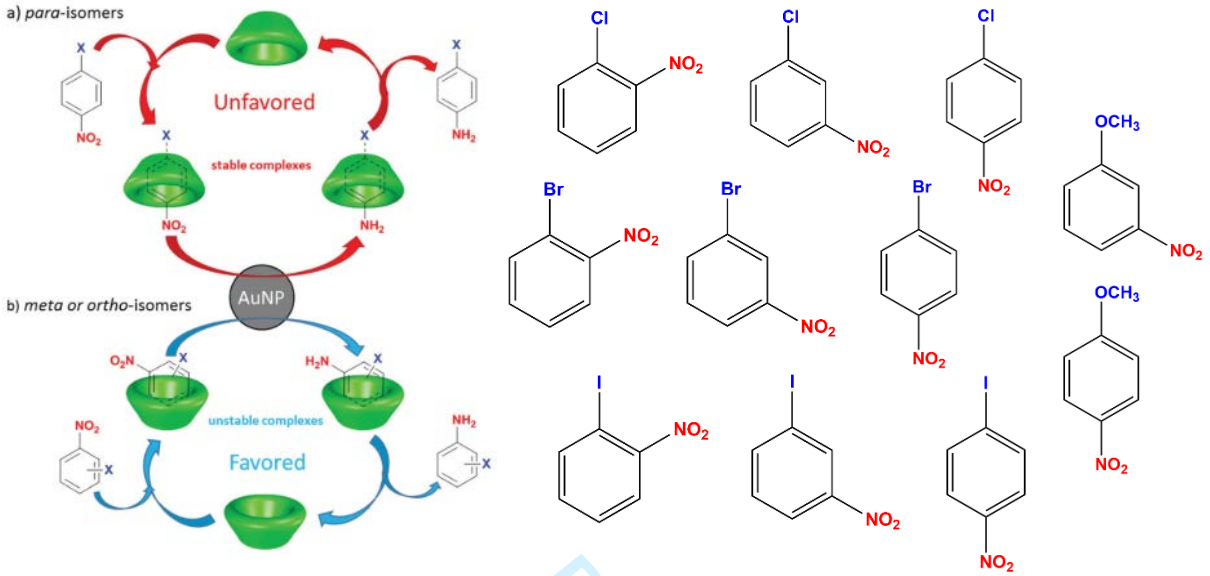

Fig 16. (Left) Schematic representation of dynamics of exchange between CDs and halogenonitrobenzene derivatives. (Right) Full scope of substrates investigated[86]

It was determined that a strong interaction between the substrate and the saccharide that is stabilizing the catalytically-active nanoparticle can slow down or even halt the conversion process. This was attributed to the importance of a dynamic exchange process created by the formation of saccharide/substrate complexes that boost the mobility of the substrate in the solid mixture. The mechanochemical hydrogenation method displayed several advantages to previous methods, including catalyst reusability over multiple cycles, complete substrate conversion in reaction times as low as 15 minutes, and lower amounts of required reducing agents relative to wet methods.

In 2019, Chung and coworkers reported the synthesis of ultrasmall nickel nanoparticles dispersed on a graphene oxide (GO) support from nickel (II) acetate ($Ni(acac)_2$) salts.[87] Graphene has been an explosively popular material in recent research, known for its 2-dimensional (2D) structure, conductive properties, and good mechanical strength. As a result of this interest in graphene, its cost of production has been gradually reducing, making this substance a potentially

economical alternative to metal oxide particle supports. The Ni/GO catalysts were used to catalyse the hydrogenation of 2-nitrophenol and 4-nitrophenol to aminophenols. To prepare the Ni/GO materials, a nickel (II) acetate solution is mixed with ground GO by grinding in a mortar and pestle for 30 minutes. The resulting paste was dried through thermally accelerated evaporation at 130°C for several hours. Finally, the dried product was ground for 15 minutes using mortar and pestle and was subsequently calcinated under N_2 atmosphere at 400°C for 3 hours.

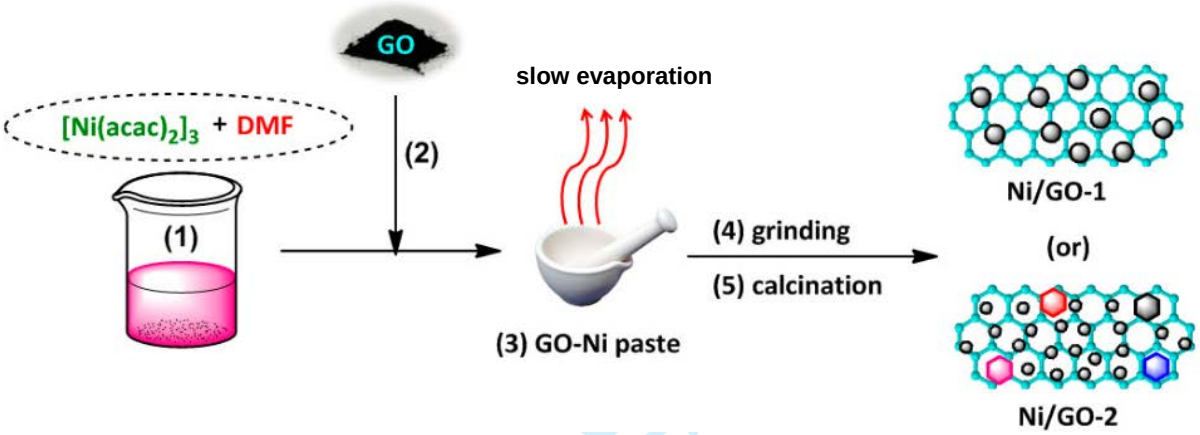

Fig 17. Schematic of Ni/GO preparation[87]

The synthesis of the catalyst was conducted through a low nickel loading (Ni/GO-1), 3 wt.%, and through a high nickel loading (Ni/GO-2), 8 wt.%, pathway shown in Figure 17, only one of which produced the ultrasmall particles. The Ni/GO-1 catalyst displayed a unimodal size distribution centered around ~20.5 nm particles, on the contrary the Ni/GO-2 catalyst displayed a bimodal size distribution centered around ~2.9 nm particles with spherical morphology and around ~25.5 nm particles with irregular morphology. Particle characteristics have been summarized in Figure 18, where TEM images and particle size histograms for each of the catalyst types is provided.

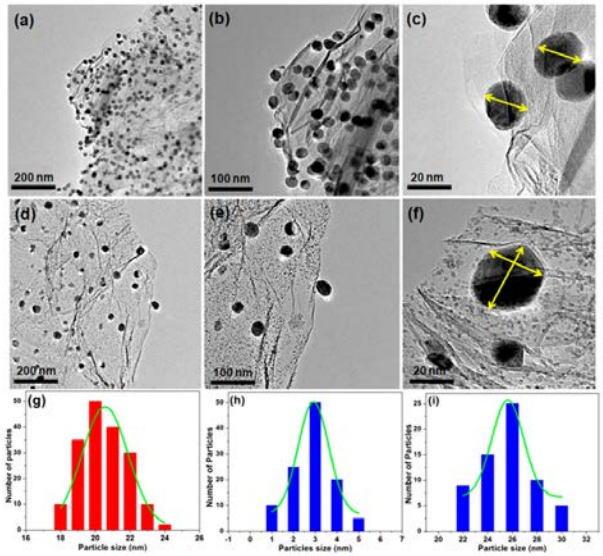

Fig 18. TEM images of (a–c) Ni/GO-1 and (d–f) Ni/GO-2, and particle-size distribution histogram of NiO nanoparticles in (g) Ni/GO-1 and (h,i) Ni/GO-2[87]

The catalytic results from hydrogenation tests are highlighted as follows. Though limited in reactant scope, the quantitative results show comparable or improved efficiency of the new Ni/GO catalyst relative to other noble metal or highly loaded catalysts. In comparing reaction rates, though silica nanotubes supported Ni nanocomposites (Ni/SNTs) showed quantitative conversion with faster kinetics than the Ni/GO catalysts, the Ni/GO catalysts were run with a much lower metal loading (3% or 8%) than the Ni/SNT catalysts (15% or 23%) and thus had improved turn over frequencies (TOF). A similar catalyst to the Ni/GO was prepared with reduced graphene oxide supported Ni catalyst (RGO/Ni) by a wet synthesis method. In comparison to the RGO/Ni catalyst made by wet synthesis, the mechanochemically made Ni/GO catalysts showed an approximate 330-fold increase in the k_{app} and k′ values. Beyond these, the optimized Ni/GO catalyst managed to outperform some catalysts with gold,[88] silver,[89] or platinum[90] alloy metal nanoparticles. It is also worth noting the environmental and economical benefits of the Ni/GO catalysts; both of the catalysts, Ni/GO-1 and Ni/GO-2, displayed excellent reusability over ten cycles of hydrogenation and maintained 95% conversion.

4. Conclusions

Mechanochemistry has demonstrated clear benefits over solution reactivity for many organic transformation, and in particular for hydrogenation reactions of substrates whose specific solubilities make them challenging to use in solution, at the same time decreasing reaction times, temperature, and the production of bulk solvent waste. For the design of novel molecular and nanostructured catalysts, mechanochemical methods have also shown a clear benefit in the ability to access solid-state structures not easily accessible in solution, or the direct synthesis of ultrasmall and highly reactive supported and free nanoparticle catalysts whose solution synthesis often involves energy intensive high temperature annealing or sintering steps. While mechanochemistry has already demonstrated a number of new opportunities and advantages in catalytic hydrogenation, it is also clear that the use of mechanochemical techniques for conducting this fundamental chemical transformation is at a very early stage of development. Consequently, we hope that, by highlighting existing work as well as outlining open questions and limitations, this Review will also serve as an inspiration for the further exploration and development of this field of mechanochemistry and Green Chemistry.

5. Perspectives

The outlined successes of ball milling in conducting hydrogenation reactions have demonstrated mechanochemistry as a viable strategy for this type of chemical transformations, setting the stage for further development. In this section, we highlight several recently emerged instrumental techniques that show high promise for further improving various aspects of mechanochemical reactivity and, consequently, would be attractive targets for further development of mechanochemical hydrogenation techniques.

As has been previously discussed, milling in stainless-steel vessels can often leach metal nanoparticles and metal ions, providing parts per billion (ppb) or parts per million (ppm) amounts of catalyst during the milling process. This leaching can be a detriment, however, especially towards pharmaceutical applications where there are strict regulations on the amount of residual metal allowed in active pharmaceutical ingredients (APIs). A potential route to reduce or completely avoid metal contamination resulting from the wear of milling media in mechanochemical synthesis is offered by resonant acoustic mixing (RAM). The RAM methodology relies on the use of acoustic vibrations as a means to achieve intense and localized mixing zones. The use of RAM technology has recently been demonstrated in the context of pharmaceutically relevant cocrystals,[91, 92] as well as metal-organic frameworks,[21] and it is anticipated it could be of considerable value as a general tool for mechanochemical reactions.

As mechanochemistry expands its potential towards large scale and industrial implementation, the ability to scale-up the space-time yield of organic transformations has become a crucial goal. The first logical step for increasing the scale of a mechanochemical reaction would be to implement a planetary mill. This method is the most easily accessible, however it still works on a batch-process, with a low space-time yield. Flow chemistry for solution processes has seen a surge in industrial processes to limit waste, as well as increasing the throughput of pharmaceutical APIs while seeing a considerable decrease in the footprint of the process, both physical and environmental.[93] The mirror of continuous flow processes in solid-state mechanochemical techniques is possible through the application of twin screw extrusion (TSE). The apparatus for TSE (Figure 19) allows for control of both mixing zones and heating and is already widely used in the polymer industry[94] and pharmaceutical cocrystal formation.[20, 95] Various groups have employed TSE towards high-throughput organic synthesis,[96-99] the formation of peptide bonds,[100]

deep-eutectic solvents,[101] metal-organic[16, 102] and covalent-organic frameworks,[103, 104] as well as the synthesis of API molecules.[105]

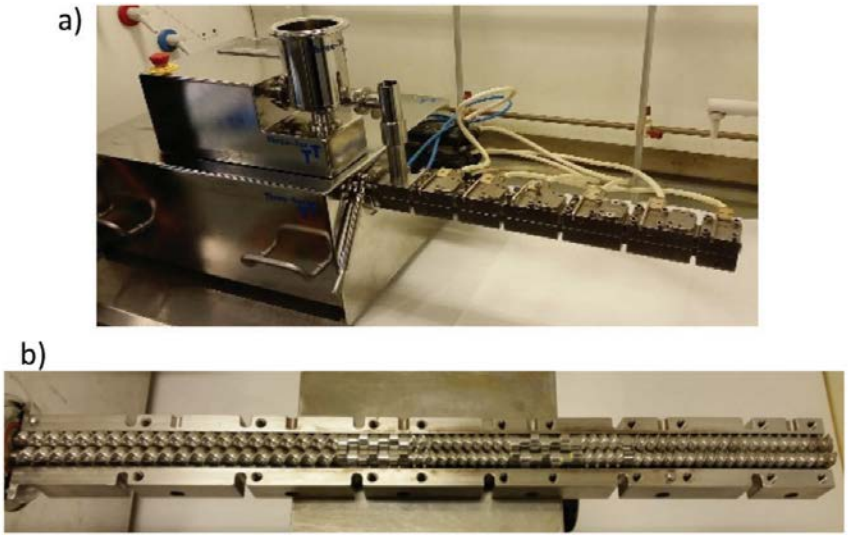

Fig 19. Twin screw extruder (TSE) apparatus employed for continuous, solid-state organic transformations[96]

These initial studies, which include processes at the milligram as well as work towards larger scale continuous processes, provide a framework for future development in mechanochemical hydrogenations. The development of mechanochemical strategies to conduct asymmetric or late-stage hydrogenations that show functional group selectivity are important future research goals. Mechanochemistry has already shown potential for organocatalytic asymmetric bond forming reactions,[106, 107] but has yet to be applied for asymmetric hydrogenations. Alongside the need to improve enantioselectivity, methods which produce hydrogen *in situ* also struggle with chemoselectivity when being applied to substrates with multiple reducible functionalities. This selectivity can be influenced both by the nature of the catalyst as well as the hydrogen source.

Advancements and experimentation in the field of hydrogenation/dehydrogenation catalysis design and in mechanochemical methods have no doubt been bountiful for the growth of mechanochemistry as a field. The improvements made in terms of energy efficiency, catalytic activity, reaction selectivity, and atom efficiency, are likely to enable an significant increase in

mechanochemically-synthesised catalysts and hydrogenation reactions under mechanochemical conditions. These improvements present economical opportunities that may allow for eventual replacement of traditional processing methods and infrastructure, a pathway towards commercialisation that would provide greener, safer, and more sustainable chemistry in the future.

Acknowledgements

B.G. F. acknowledges the financial support of the Walter C. Sumner Memorial Fellowship. We thank the Natural Science and Engineering Research Council of Canada (NSERC) Discovery Grant and accelerator programs, the Canada Foundation for Innovation (CFI), the Canada Research Chairs (CRC), the Centre for Green Chemistry and Catalysis (CGCC), and McGill University for their financial support.

References

(1) Blaser, H.-U.; Spindler, F.; Thommen, M. Industrial Applications. In *The Handbook of Homogeneous Hydrogenation*, de Vries, J. G.; Elsevier, C. J. Eds.; Wiley-VCH Verlag GmbH & Co. KGaA: Weinheim, 2007; pp 1279-1324.

(2) Sabatier, P.; Senderens, J.-B. Action du nickel sur l'éthylène. Sythèse de l'éthane. *C. R. Hebd. Séances Acad. Sci.* **1897,** *124,* 616.

(3) Sabatier, P. Hydrogénations et déshydrogénations par catalyse. *Ber. Dtsch. Chem. Ges.* **1911,** *44*, 1984.

(4) Hudson, R.; Hamasaka, G.; Osako, T.; Yamada, Y. M. A.; Li, C.-J.; Uozumi, Y.; Moores, A. Highly efficient iron(0) nanoparticle-catalyzed hydrogenation in water in flow. *Green Chem.* **2013,** *15,* 2141.

(5) Li, A. Y.; Kaushik, M.; Li, C. J.; Moores, A. Microwave-Assisted Synthesis of Magnetic Carboxymethyl Cellulose-Embedded Ag-Fe_3O_4 Nanocatalysts for Selective Carbonyl Hydrogenation. *ACS Sustainable Chem. Eng.* **2016,** *4,* 965.

(6) Hudson, R.; Chazelle, V.; Bateman, M.; Roy, R.; Li, C. J.; Moores, A. Sustainable Synthesis of Magnetic Ruthenium-Coated Iron Nanoparticles and Application in the Catalytic Transfer Hydrogenation of Ketones. *ACS Sustainable Chem. Eng.* **2015,** *3,* 814.

(7) Torres Galvis, H. M.; Bitter, J. H.; Khare, C. B.; Ruitenbeek, M.; Dugulan, A. I.; de Jong, K. P. Supported Iron Nanoparticles as Catalysts for Sustainable Production of Lower Olefins. *Science* **2012,** *335,* 835.

(8) Li, Y.-Y.; Yu, S.-L.; Shen, W.-Y.; Gao, J.-X., Iron-, Cobalt-, and Nickel-Catalyzed Asymmetric Transfer Hydrogenation and Asymmetric Hydrogenation of Ketones. *Acc. Chem. Res.* **2015,** *48,* 2587.

(9) Kallmeier, F.; Kempe, R. Manganese Complexes for (De)Hydrogenation Catalysis: A Comparison to Cobalt and Iron Catalysts. *Angew. Chem. Int. Ed.* **2018,** *57,* 46.

(10) Constable, D. J.; Jimenez-Gonzalez, C.; Henderson, R. K. Perspective on solvent use in the pharmaceutical industry. *Org. Process Res. Dev.* **2007,** *11,* 133.

(11) Do, J.-L.; Friščić, T. Mechanochemistry: A Force of Synthesis. *ACS Cent. Sci.* **2017,** *3,* 13.

(12) Fischer, F.; Fendel, N.; Greiser, S.; Rademann, K.; Emmerling, F., Impact Is Important-Systematic Investigation of the Influence of Milling Balls in Mechanochemical Reactions. *Org. Process Res. Dev.* **2017,** *21,* 655.

(13) Friščić, T.; Mottillo, C.; Titi, H. M. Mechanochemistry for Synthesis. *Angew. Chem. Int. Ed.* **2020,** *59,* 1018.

(14) Hasa, D.; Carlino, E.; Jones, W. Polymer-assisted grinding, a versatile method for polymorph control of cocrystallization. *Cryst. Growth Des.* **2016,** *16,* 1772.

(15) Muñoz-Batista, M. J.; Rodriguez-Padron, D.; Puente-Santiago, A. R.; Luque, R. Mechanochemistry: Toward Sustainable Design of Advanced Nanomaterials for Electrochemical Energy Storage and Catalytic Applications. *ACS Sustainable Chem. Eng.* **2018,** *6,* 9530.

(16) Crawford, D.; Casaban, J.; Haydon, R.; Giri, N.; McNally, T.; James, S. L. Synthesis by extrusion: continuous, large-scale preparation of MOFs using little or no solvent. *Chem. Sci.* **2015,** *6,* 1645.

(17) Crawford, D. E.; Miskimmin, C. K.; Albadarin, A. B.; Walker, G.; James, S. L., Organic synthesis by Twin Screw Extrusion (TSE): continuous, scalable and solvent-free. *Green Chem.* **2017,** *19,* 1507.

(18) Margetić, D.; Štrukil, V. Recent Advances in Mechanochemical Organic Synthesis. In *Organic Synthesis-A Nascent Relook,* Nandeshwarappam B. P. Eds.; IntechOpen: London, 2020; pp 1-23.

(19) Martina, K.; Rotolo, L.; Porcheddu, A.; Delogu, F.; Bysouth, S. R.; Cravotto, G.; Colacino, E. High throughput mechanochemistry: application to parallel synthesis of benzoxazines. *Chem. Commun.* **2018,** *54,* 551.

(20) Tan, D.; Loots, L.; Friščić, T. Towards medicinal mechanochemistry: evolution of milling from pharmaceutical solid form screening to the synthesis of active pharmaceutical ingredients (APIs). *Chem. Commun.* **2016,** *52,* 7760.

(21) Titi, H. M.; Do, J.-L.; Howarth, A. J.; Nagapudi, K.; Friščić, T. Simple, scalable mechanosynthesis of metal–organic frameworks using liquid-assisted resonant acoustic mixing (LA-RAM). *Chem. Sci.* **2020,** *11,* 7578.

(22) Parkin, I. P. Solid state metathesis reaction for metal borides, silicides, pnictides and chalcogenides: Ionic or elemental pathways. *Chem. Soc. Rev.* **1996,** *25,* 199.

(23) Rightmire, N. R.; Hanusa, T. P. Advances in organometallic synthesis with mechanochemical methods. *Dalton Trans.* **2016,** *45,* 2352.

(24) Tan, D.; Friščić, T. Mechanochemistry for Organic Chemists: An Update. *Eur. J. Org. Chem.* **2018,** *2018,* 18.

(25) Tan, D.; Garcia, F. Main group mechanochemistry: from curiosity to established protocols. *Chem. Soc. Rev.* **2019,** *48,* 2274.

(26) Hasa, D.; Jones, W. Screening for new pharmaceutical solid forms using mechanochemistry: A practical guide. *Adv. Drug Deliv. Rev.* **2017,** *117,* 147.

(27) Hasa, D.; Schneider Rauber, G.; Voinovich, D.; Jones, W. Cocrystal Formation through Mechanochemistry: from Neat and Liquid-Assisted Grinding to Polymer-Assisted Grinding. *Angew. Chem. Int. Ed.* **2015,** *54,* 7371.

(28) Porcheddu, A.; Colacino, E.; De Luca, L.; Delogu, F., Metal-Mediated and Metal-Catalyzed Reactions Under Mechanochemical Conditions. *ACS Catal.* **2020,** *10,* 8344.

(29) Takacs, L. Quicksilver from Cinnabar: The First Documented Mechanochemical Reaction? *JOM.* **2000,** *52,* 12.

(30) Takacs, L. The mechanochemical reduction of AgCl with metals. *J. Therm. Anal. Calorim.* **2007,** *90,* 81.

(31) Faraday, M. On the Decomposition of Chloride of Silver, by Hydrogen, and by Zinc. *Q. J. Sci. Lit. Arts.* **1820,** *8,* 374.

(32) Lea, M. C. Disruption of the silver haloid molecule by mechanical force. *Am. J. Sci.* **1892,** *43,* 527.

(33) Wöhler, F. Ueber künstliche Bildung des Harnstoffs. *Ann. Phys.* **1828,** *87,* 253.

(34) Cao, Q.; Crawford, D. E.; Shi, C.; James, S. L. Greener Dye Synthesis: Continuous, Solvent-Free Synthesis of Commodity Perylene Diimides by Twin-Screw Extrusion. *Angew. Chem. Int. Ed.* **2020,** *59,* 4478.

(35) Friščić, T.; Reid, D. G.; Halasz, I.; Stein, R. S.; Dinnebier, R. E.; Duer, M. J. Ion-and Liquid-Assisted Grinding: Improved Mechanochemical Synthesis of Metal–Organic Frameworks Reveals Salt Inclusion and Anion Templating. *Angew. Chem. Int. Ed.* **2010,** *49,* 712.

(36) Mukherjee, A.; Rogers, R. D.; Myerson, A. Cocrystal formation by ionic liquid-assisted grinding: case study with cocrystals of caffeine. *CrystEngComm* **2018,** *20,* 3817.

(37) Friščić, T.; Childs, S. L.; Rizvi, S. A. A.; Jones, W. The role of solvent in mechanochemical and sonochemical cocrystal formation: a solubility-based approach for predicting cocrystallisation outcome. *CrystEngComm* **2009,** *11,* 418.

(38) Hernández, J. G.; Bolm, C. Altering Product Selectivity by Mechanochemistry. *J. Org. Chem.* **2017,** *82,* 4007.

(39) Julien, P. A.; Mottillo, C.; Friščić, T. Metal–organic frameworks meet scalable and sustainable synthesis. *Green Chem.* **2017,** *19,* 2729.

(40) Lv, D.; Chen, Y.; Li, Y.; Shi, R.; Wu, H.; Sun, X.; Xiao, J.; Xi, H.; Xia, Q.; Li, Z. Efficient Mechanochemical Synthesis of MOF-5 for Linear Alkanes Adsorption. *J. Chem. Eng. Data* **2017,** *62,* 2030.

(41) Klimakow, M.; Klobes, P.; Thünemann, A. F.; Rademann, K.; Emmerling, F. Mechanochemical Synthesis of Metal−Organic Frameworks: A Fast and Facile Approach toward Quantitative Yields and High Specific Surface Areas. *Chem. Mater.* **2010,** *22,* 5216.

(42) Mukherjee, A.; Rogers, R. D.; Myerson, A. S. Cocrystal formation by ionic liquid-assisted grinding: case study with cocrystals of caffeine. *CrystEngComm* **2018,** *20,* 3817.

(43) Hasa, D.; Rauber, G. S.; Voinovich, D.; Jones, W. Cocrystal Formation through Mechanochemistry : from Neat and Liquid-Assisted Grinding to Polymer-Assisted Grinding. *Angew. Chem. Int. Ed.* **2015,** *54,* 7371.

(44) Fiss, B. G.; Hatherly, L.; Stein, R. S.; Friščić, T.; Moores, A. Mechanochemical Phosphorylation of Polymers and Synthesis of Flame-Retardant Cellulose Nanocrystals. *ACS Sustainable Chem. Eng.* **2019,** *7,* 7951.

(45) Huang, J.; Moore, J. A.; Acquaye, J. H.; Kaner, R. B., Mechanochemical Route to the Conducting Polymer Polyaniline. *Macromolecules* **2005,** *38,* 317.

(46) Ravnsbæk, J. B.; Swager, T. M. Mechanochemical Synthesis of Poly(phenylene vinylenes). *ACS Macro Lett.* **2014,** *3,* 305.

(47) Malca, M. Y.; Ferko, P. O.; Friščić, T.; Moores, A. Solid-state mechanochemical ω-functionalization of poly(ethylene glycol). *Beilstein J. Org. Chem.* **2017,** *13,* 1963.

(48) Ashlin, M.; Hobbs, C. E. Post-Polymerization Thiol Substitutions Facilitated by Mechanochemistry. *Macromol. Chem. Phys.* **2019,** *220,* 1900350.

(49) Malca, M. Y.; Bao, H.; Bastaille, T.; Saadé, N. K.; Kinsella, J. M.; Friščić, T.; Moores, A. Mechanically Activated Solvent-Free Assembly of Ultrasmall Bi_2S_3 Nanoparticles: A Novel, Simple, and Sustainable Means to Access Chalcogenide Nanoparticles. *Chem. Mater.* **2017,** *29,* 7766.

(50) Rak, M. J.; Saadé, N. K.; Friščić, T.; Moores, A. Mechanosynthesis of ultra-small monodisperse amine-stabilized gold nanoparticles with controllable size. *Green Chem.* **2014,** *16,* 86.

(51) Fiss, B. G.; Vu, N.-N.; Douglas, G.; Do, T.-O.; Friščić, T.; Moores, A., Solvent-Free Mechanochemical Synthesis of Ultrasmall Nickel Phosphide Nanoparticles and Their Application as a Catalyst for the Hydrogen Evolution Reaction (HER). *ACS Sustainable Chem. Eng.* **2020,** *8,* 12014.

(52) Wang, G.-W. Mechanochemical organic synthesis. *Chem. Soc. Rev.* **2013,** *42,* 7668.

(53) Häussinger, P.; Lohmüller, R.; Watson, A. M., Hydrogen, 6. Uses. In *Ullmann's Encyclopedia of Industrial Chemistry,* Wiley-VCH Verlag GmbH & Co. KGaA: Weinheim, 2011; 18, pp 353-390.

(54) Bolm, C.; Hernández, J. G., Mechanochemistry of Gaseous Reactants. *Angew. Chem. Int. Ed.* **2019,** *58,* 3285.

(55) Sawama, Y.; Niikawa, M.; Yabe, Y.; Goto, R.; Kawajiri, T.; Marumoto, T.; Takahashi, T.; Itoh, M.; Kimura, Y.; Sasai, Y.; Yamauchi, Y.; Kondo, S.-I.; Kuzuya, M.; Monguchi, Y.; Sajiki, H. Stainless-Steel-Mediated Quantitative Hydrogen Generation from Water under Ball Milling Conditions. *ACS Sustainable Chem. Eng.* **2015,** *3,* 683.

(56) Sawama, Y.; Kawajiri, T.; Niikawa, M.; Goto, R.; Yabe, Y.; Takahashi, T.; Marumoto, T.; Itoh, M.; Kimura, Y.; Monguchi, Y.; Kondo, S.; Sajiki, H. Stainless-Steel Ball-Milling Method for Hydro-/Deutero-genation using H_2O/D_2O as a Hydrogen/Deuterium Source. *ChemSusChem* **2015,** *8,* 3773.

(57) Sawama, Y.; Yasukawa, N.; Ban, K.; Goto, R.; Niikawa, M.; Monguchi, Y.; Itoh, M.; Sajiki, H. Stainless Steel-Mediated Hydrogen Generation from Alkanes and Diethyl Ether and Its Application for Arene Reduction. *Org. Lett.* **2018,** *20,* 2892.

(58) Schumacher, C.; Crawford, D. E.; Ragu, Z. B.; Glaum, R.; James, S. L.; Bolm, C.; Hernández, J. G., Mechanochemical Dehydrocoupling of Dimethylamine Borane and Hydrogenation Reactions Using Wilkinson's Catalyst. *Chem. Commun.* **2018,** *54,* 8355.

(59) Portada, T.; Margetic, D.; Štrukil, V. Mechanochemical Catalytic Transfer Hydrogenation of Aromatic Nitro Derivatives. *Molecules* **2018,** *23,* 3163.

(60) Baláž, P.; Achimovičová, M.; Baláž, M.; Billik, P.; Cherkezova-Zheleva, Z.; Criado, J. M.; Delogu, F.; Dutková, E.; Gaffet, E.; Gotor, F. J. Hallmarks of mechanochemistry: from nanoparticles to technology. *Chem. Soc. Rev.* **2013,** *42,* 7571.

(61) Haley, R. A.; Mack, J.; Guan, H. 2-in-1: catalyst and reaction medium. *Inorg. Chem. Front.* **2017,** *4,* 52.

(62) Goodman, J.; Grushin, V. V.; Larichev, R. B.; Macgregor, S. A.; Marshall, W. J.; Roe, D. C. Fluxionality of [(Ph_3P) 3M (X)](M= Rh, Ir). The Red and Orange Forms of [$(Ph3P)_3$Ir (Cl)]. Which Phosphine Dissociates Faster from Wilkinson's Catalyst? *J. Am. Chem. Soc.* **2010,** *132,* 12013.

(63) Osborn, J. A.; Jardine, F.; Young, J. F.; Wilkinson, G. The preparation and properties of tris (triphenylphosphine) halogenorhodium (I) and some reactions thereof including catalytic

homogeneous hydrogenation of olefins and acetylenes and their derivatives. *J. Chem. Soc. A* **1966,** 1711.

(64) Golubkova, G.; Bazanova, I.; Gostikin, V.; Nischenkova, L.; Lomovsky, O. Mechanochemical promotion with molybdenum and catalytic activity of skeletal nickel catalysts in hydrogenation reactions. *React. Kinet. and Catal. Lett.* **1999,** *67,* 169.

(65) Trovarelli, A.; Matteazzi, P.; Dolcetti, G.; Lutman, A.; Miani, F. Nanophase iron carbides as catalysts for carbon dioxide hydrogenation. *Appl. Catal. A* **1993,** *95,* L9.

(66) Mulas, G.; Conti, L.; Scano, G.; Schiffini, L.; Cocco, G. Mechanically driven CO hydrogenation over NiZr amorphous catalysts. *Mater. Sci. Eng. A* **1994,** *181-182,* 1085.

(67) Alonso, F.; Osante, I.; Yus, M. Highly selective hydrogenation of multiple carbon–carbon bonds promoted by nickel(0) nanoparticles. *Tetrahedron* **2007,** *63,* 93.

(68) Nash, D. J.; Restrepo, D. T.; Parra, N. S.; Giesler, K. E.; Penabade, R. A.; Aminpour, M.; Le, D.; Li, Z.; Farha, O. K.; Harper, J. K.; Rahman, T. S.; Blair, R. G. Heterogeneous metal-free hydrogenation over defect-laden hexagonal boron nitride. *ACS Omega* **2016,** *1,* 1343.

(69) Zhang, P.; Wang, L.; Yang, S.; Schott, J. A.; Liu, X.; Mahurin, S. M.; Huang, C.; Zhang, Y.; Fulvio, P. F.; Chisholm, M. F. Solid-state synthesis of ordered mesoporous carbon catalysts via a mechanochemical assembly through coordination cross-linking. *Nat. Comm.* **2017,** *8,* 1.

(70) Toda, F.; Kiyoshige, K.; Yagi, M. $NaBH_4$ Reduction of Ketones in the Solid State. *Angew. Chem. Int. Ed. Engl.* **1989,** *28,* 320.

(71) Mack, J.; Fulmer, D.; Stofel, S.; Santos, N., The first solvent-free method for the reduction of esters. *Green Chem.* **2007,** *9,* 1041.

(72) Li, A. Y.; Segalla, A.; Li, C.-J.; Moores, A. Mechanochemical Metal-Free Transfer Hydrogenation of Carbonyls Using Polymethylhydrosiloxane as the Hydrogen Source. *ACS Sustainable Chem. Eng.* **2017,** *5,* 11752.

(73) Chacón-Huete, F.; Messina, C.; Chen, F.; Cuccia, L.; Ottenwaelder, X.; Forgione, P. Solvent-Free Mechanochemical Oxidation and Reduction of Biomass-Derived 5-Hydroxymethyl Furfural. *Green Chem.* **2018,** *20,* 5261.

(74) Yepez, A.; Hidalgo, J. M.; Pineda, A.; Černý, R.; Jíša, P.; Garcia, A.; Romero, A. A.; Luque, R., Mechanistic insights into the hydroconversion of cinnamaldehyde using mechanochemically-synthesized Pd/Al-SBA-15 catalysts. *Green Chem.* **2015,** *17,* 565.

(75) Al5-Naji, M.; Balu, A. M.; Roibu, A.; Goepel, M.; Einicke, W. D.; Luque, R.; Gläser, R. Mechanochemical preparation of advanced catalytically active bifunctional Pd-containing nanomaterials for aqueous phase hydrogenation. *Catal. Sci. Technol.* **2015,** *5,* 2085.

(76) Balaraman, E.; Gunanathan, C.; Zhang, J.; Shimon, L. J. W.; Milstein, D. Efficient hydrogenation of organic carbonates, carbamates and formates indicates alternative routes to methanol based on CO_2 and CO. *Nat. Chem.* **2011,** *3,* 609.

(77) Farina, V.; Gamba, N. S.; Gennari, F.; Garroni, S.; Torre, F.; Taras, A.; Enzo, S.; Mulas, G. O_2 Hydrogenation Induced by Mechanochemical Activation of Olivine with Water Under CO_2 Atmosphere. *Front. Energy Res.* **2019,** *7,* 107.

(78) Giammar, D. E.; Bruant, R. G.; Peters, C. A. Forsterite dissolution and magnesite precipitation at conditions relevant for deep saline aquifer storage and sequestration of carbon dioxide. *Chem. Geol.* **2005,** *217,* 257.

(79) Camille Jones, L.; Rosenbauer, R.; Goldsmith, J. I.; Oze, C. Carbonate control of H_2 and CH_4 production in serpentinization systems at elevated P-Ts. *Geophys. Res. Lett.* **2010,** *37,* L14306.

(80) Adams, C. J.; Kurawa, M. A.; Lusi, M.; Orpen, A. G. Solid state synthesis of coordination compounds from basic metal salts. *CrystEngComm* **2008,** *10,* 1790.

(81) Zhou, D.; Yu, M.; Fan, Y.; Wang, Z.; Dang, G.; Zhang, Q.; Xie, J. Sodium-induced solid-phase hydrogenation of carbon dioxide to formate by mechanochemistry. *Environ. Chem. Lett.* **2020,** *18,* 905.

(82) Chen, H.; Lin, W.; Zhang, Z.; Jie, K.; Mullins, D. R.; Sang, X.; Yang, S.-Z.; Jafta, C. J.; Bridges, C. A.; Hu, X.; Unocic, R. R.; Fu, J.; Zhang, P.; Dai, S. Mechanochemical Synthesis of High Entropy Oxide Materials under Ambient Conditions: Dispersion of Catalysts *via* Entropy Maximization. *ACS Mater. Lett.* **2019,** *1,* 83.

(83) Zhang, Z.; Gao, J.; Xia, J.-J.; Wang, G.-W. Solvent-free mechanochemical and one-pot reductive benzylizations of malononitrile and 4-methylaniline using Hantzsch 1,4-dihydropyridine as the reductant. Org. Biomol. Chem. **2005,** *3,* 1617.

(84) Martina, K.; Baricco, F.; Tagliapietra, S.; Moran, M. J.; Cravotto, G.; Cintas, P. Highly efficient nitrobenzene and alkyl/aryl azide reduction in stainless steel jars without catalyst addition. *New J. Chem.* **2018,** *42,* 18881.

(85) Dobrovolná, Z.; Červený, L. Ammonium formate decomposition using palladium catalyst. *Res. Chem. Intermed.* **2000,** *26,* 489.

(86) Menuel, S.; Leger, B.; Addad, A.; Monflier, E.; Hapiot, F. Cyclodextrins as Effective Additives in AuNP-Catalyzed Reduction of Nitrobenzene Derivatives in a Ball-Mill. *Green Chem.* **2016,** *18,* 5500.

(87) Gopiraman, M.; Saravanamoorthy, S.; Deng, D.; Ilangovan, A.; Kim, I. S.; Chung, I. M. Facile Mechanochemical Synthesis of Nickel/Graphene Oxide Nanocomposites with Unique and Tunable Morphology: Applications in Heterogeneous Catalysis and Supercapacitors. *Catalysts* **2019,** *9,* 486.

(88) Vellaichamy, B.; Prakash, P.; Thomas, J. Synthesis of AuNPs@RGO nanosheets for sustainable catalysis toward nitrophenols reduction. *Ultrason. Sonochem.* **2018,** *48,* 362.

(89) Zhang, Y.; Yuan, X.; Wang, Y.; Chen, Y. One-pot photochemical synthesis of graphene composites uniformly deposited with silver nanoparticles and their high catalytic activity towards the reduction of 2-nitroaniline. *J. Mater. Chem.* **2012,** *22,* 7245.

(90) Zhao, F.; Kong, W.; Hu, Z.; Liu, J.; Zhao, Y.; Zhang, B. Tuning the performance of Pt–Ni alloy/reduced graphene oxide catalysts for 4-nitrophenol reduction. *RSC Adv.* **2016,** *6,* 79028.

(91) am Ende, D. J.; Anderson, S. R.; Salan, J. S. Development and Scale-Up of Cocrystals Using Resonant Acoustic Mixing. *Org. Process Res. Dev.* **2014,** *18,* 331.

(92) Michalchuk, A. A.; Hope, K. S.; Kennedy, S. R.; Blanco, M. V.; Boldyreva, E. V.; Pulham, C. R. Ball-free mechanochemistry: *in situ* real-time monitoring of pharmaceutical co-crystal formation by resonant acoustic mixing. *ChemComm.* **2018,** *54,* 4033.

(93) Porta, R.; Benaglia, M.; Puglisi, A. Flow Chemistry: Recent Developments in the Synthesis of Pharmaceutical Products. *Org. Process Res. Dev.* **2015,** 20, 2.

(94) Vlachopoulos, J.; Strutt, D. Polymer processing. *Mater. Sci. Technol.* **2003,** *19,* 1161.

(95) Daurio, D.; Nagapudi, K.; Li, L.; Quan, P.; Nunez, F.-A. Application of twin screw extrusion to the manufacture of cocrystals: scale-up of AMG 517–sorbic acid cocrystal production. *Faraday Discuss.* **2014,** *170,* 235.

(96) Crawford, D. E.; Miskimmin, C. K. G.; Albadarin, A. B.; Walker, G.; James, S. L. Organic synthesis by Twin Screw Extrusion (TSE): Continuous, Scalable and Solvent-Free. *Green Chem.* **2017,** *19,* 1507.

(97) Crawford, D. E. Extrusion–back to the future: Using an established technique to reform automated chemical synthesis. *Beilstein J. Org. Chem.* **2017,** *13,* 65.

(98) Cao, Q.; Howard, J. L.; Crawford, D. E.; James, S. L.; Browne, D. L. Translating solid state organic synthesis from a mixer mill to a continuous twin screw extruder. *Green Chem.* **2018,** 20, 4443.

(99) Crawford, D. E.; Miskimmin, C. K.; Cahir, J.; James, S. Continuous multi-step synthesis by extrusion–telescoping solvent-free reactions for greater efficiency. *ChemComm.* **2017,** *53,* 13067.

(100) Yeboue, Y.; Gallard, B.; Le Moigne, N.; Jean, M.; Lamaty, F.; Martinez, J.; Métro, T.-X. Peptide Couplings by Reactive Extrusion: Solid-Tolerant and Free from Carcinogenic, Mutagenic and Reprotoxic Chemicals. *ACS Sustainable Chem. Eng.* **2018,** *6,* 16001.

(101) Crawford, D. E.; Wright, L.; James, S.; Abbott, A. Efficient continuous synthesis of high purity deep eutectic solvents by twin screw extrusion. *ChemComm.* **2016,** *52,* 4215.

(102) Karadeniz, B.; Howarth, A. J.; Stolar, T.; Islamoglu, T.; Dejanovic, I.; Tireli, M.; Wasson, M. C.; Moon, S.-Y.; Farha, O. K.; Friščić, T.; Užarević, K. Benign by design: green and scalable synthesis of zirconium UiO-metal–organic frameworks by water-assisted mechanochemistry. *ACS Sustainable Chem. Eng.* **2018,** *6,* 15841.

(103) Egleston, B. D.; Brand, M. C.; Greenwell, F.; Briggs, M. E.; James, S. L.; Cooper, A. I.; Crawford, D. E.; Greenaway, R. L. Continuous and scalable synthesis of a porous organic cage by twin screw extrusion (TSE). *Chem. Sci.* **2020,** *11,* 6582.

(104) Karak, S.; Kandambeth, S.; Biswal, B. P.; Sasmal, H. S.; Kumar, S.; Pachfule, P.; Banerjee, R. Constructing Ultraporous Covalent Organic Frameworks in Seconds via an Organic Terracotta Process. *J. Am. Chem. Soc.* **2017,** *139,* 1856.

(105) Crawford, D. E.; Porcheddu, A.; McCalmont, A. S.; Delogu, F.; James, S. L.; Colacino, E. Solvent-Free, Continuous Synthesis of Hydrazone-Based Active Pharmaceutical Ingredients by Twin-Screw Extrusion. *ACS Sustainable Chem. Eng.* **2020,** *8,* 12230.

(106) Chauhan, P.; Chimni, S. S. Mechanochemistry assisted asymmetric organocatalysis: A sustainable approach. *Beilstein J. Org. Chem.* **2012,** *8,* 2132.

(107) Krištofíková, D.; Mečiarová, M.; Rakovský, E.; Šebesta, R. Mechanochemically Activated Asymmetric Organocatalytic Domino Mannich Reaction-Fluorination. *ACS Sustainable Chem. Eng.* **2020,** *8*¸14417.

Mechanochemistry for sustainable, efficient dehydrogenation/hydrogenation

Blaine G. Fiss[1], Austin J. Richard[1], Tomislav Friščić[1*], Audrey Moores[1,2*]

1. Centre in Green Chemistry and Catalysis, Department of Chemistry, McGill University, 801 Sherbrooke Street West, Montréal, Québec H3A 0B8, Canada

2. Department of Materials Engineering, McGill University, 3610 University Street, Montréal, Québec H3A 0C5, Canada

Keywords: Ball-milling, solvent-free, organic synthesis, catalysis, green chemistry

tomislav.friscic@mcgill.ca

audrey.moores@mcgill.ca

Abstract

Hydrogenation reactions are one of the pillars of the chemical industry, with applications from bulk chemicals to pharmaceuticals manufacturing. The ability to selectively add hydrogen across double and/or triple bonds is key in the chemist's toolbox, and the enabling component in the development of sustainable processes. Traditional solution-based approaches to hydrogenation reactions are tainted by significant consumption of energy and production of solvent waste. This review highlights the development and applications of recently emerged solvent-free approaches to conduct the hydrogenation of organic molecules using mechanochemistry, *i.e.* chemical transformations induced or sustained by mechanical force. In particular, we will show how mechanochemical techniques such as ball-milling enable catalytic or stoichiometric metal-mediated hydrogenation reactions that are simple, fast, and are conducted under significantly milder conditions compared to traditional solution routes. Importantly, we highlight the current challenges and opportunities in this field, while also identifying exciting cases in which mechanochemical hydrogenation strategies lead to new, unique targets and reactivity.

1. Introduction

Hydrogenation reactions have long been a staple of the chemical industry, ranging from the bulk chemical manufacturing to the pharmaceutical and agrochemical sectors.[1] The scope of bond types that can be transformed through hydrogenation reactions include carbon-carbon, carbon-oxygen, carbon-nitrogen and nitrogen-oxygen bonds, allowing access to a variety of products, often in a stereo- or regio-controlled fashion. Along with π-bonded motifs, such as carbonyl moieties, as well as carbon-carbon double (C=C) and triple (C≡C) bonds often seen in organic chemistry, sustainable approaches to hydrogenation have also made advances towards the conversion of small molecule feedstocks, such as carbon monoxide (CO) and carbon dioxide (CO_2)

into value-added products. Since the early development of catalytic processes based on solid platinum and palladium as catalysts, highlighted in the seminal work of Sabatier in 1897,[2, 3] significant strides have been made towards the development of more reactive, selective and recyclable catalysts in the form of organometallic complexes and nanoparticles (NPs).[4-7] Such development has at the same time included a shift towards the use of more sustainable, less toxic, and Earth-abundant metals as active catalyst components.[8, 9]

The development of cleaner and more sustainable catalytic processes is not focused only on creation of new, more efficient catalysts, but also seeks to ameliorate or completely eliminate the overall negative environmental impacts of many traditional synthetic procedures. Among these negative impacts, particular attention has been given to reducing the production of waste, either due to excess solvent[10] or to the loss of energy associated with reactor heating. This has made way for the development of synthetic methodologies which are both solvent-free, and have a low energy demand. Particularly successful among these emergent approaches to cleaner, solvent-free chemistry are mechanochemical techniques, in which chemical and/or materials transformations are induced and/or sustained by mechanical agitation in the form of grinding, milling or other types of shear and extrusion, with or without the need for milling media.[11-28]

Mechanochemical transformations have a long history, with one of the earliest reports coming from Theophrastus of Eresus, who described a methodology for mechanochemical production of mercury metal by manual grinding of cinnabarite (mercury(II) sulfide) using a mortar and pestle made from copper or bronze.[29] While inorganic materials, such as ores and minerals, have been processed through mechanical grinding since Antiquity, the underlying chemical transformations have not been systematically investigated until the late 19th century, when Faraday described the mechanically-induced transformations of metal salts (1820),[30, 31] and

Carey Lea demonstrated that mechanical treatment of silver and mercury halides leads to different outcomes compared to treatment by heat or pressure.[32] This work, together with pioneering investigations by Wöhler in mechanically-inducted transformations of organic solids,[33] provides the foundation for the development of solid-state, solvent-free chemistry by mechanical grinding.

Mechanochemical reactions can be conducted using diverse equipment, ranging from simple and readily accessible mortar and pestle, to much more sophisticated and automated equipment, such as shaker mills, planetary mills, extruders or devices operating through (ultra)sonic irradiation (Figure 1).

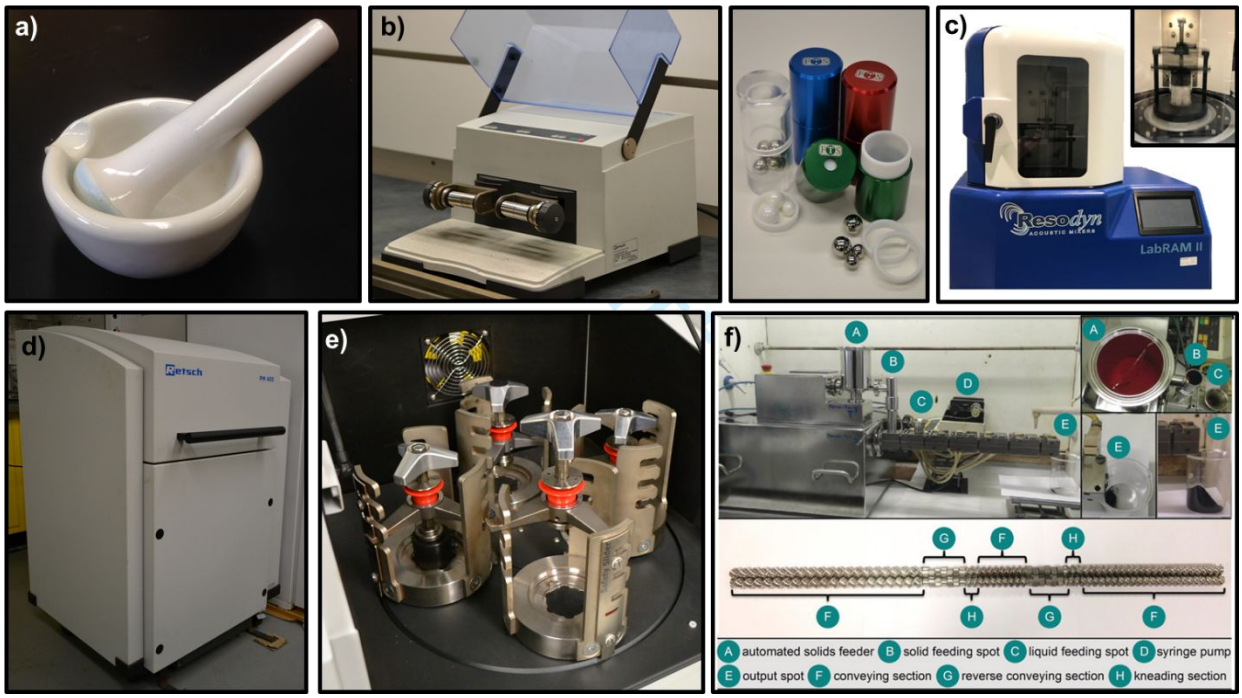

Fig 1. Equipment for mechanochemical reactions a) mortar and pestle b) vibrational mill and small-scale milling jars and balls c) resonant acoustic mixer (RAM) exterior and in operation (insert) d) planetary mill external and e) internal f) twin-screw extruder (TSE)[34] allowing for continuous processing

Mechanochemical reactions can be performed using neat substrates, or in the presence of a small amount of a liquid additive, stoichiometrically comparable to or even lower than the amount of reacting substrate, in a process known as liquid-assisted grinding (LAG). The amount of liquid

additive in LAG and related methods (*e.g.* ion- and liquid-assisted grinding, ILAG[35] or ionic liquid-assisted grinding, IL-AG[36]) is measured using the parameter η, which is the ratio of liquid additive volume to the mass of solid reactants, expressed in μL/mg.[37] The exact mechanisms through which the liquid additive promotes reactivity in LAG are not yet known, but are generally considered to be based on surface activation and improvement of molecular mobility. The ability to improve, optimize and direct the course of a mechanochemical process by varying the choice or amount of liquid additive has provided unprecedented generality to chemical reactions by milling, providing tolerance to molecular size, shape and functionality in solvent-free synthesis. At the same time, the unique mechanically-agitated environment of neat or LAG reactions has enabled access to molecular targets, materials and chemical transformations that are difficult or perhaps even considered impossible in conventional solution processes.[38] In the area of materials science, mechanochemistry has proven paramount in making readily accessible a range of materials, including novel metal-organic frameworks,[39-41] cocrystals,[42, 43] polymers, enabling the efficient functionalization of inorganic and organic substrates,[44-48] as well as the solvent-free, room-temperature synthesis and functionalization of discrete metal NPs.[49-51]

Over the past two decades, the applications of mechanochemistry to organic synthesis have been rapidly expanding, and it is now well established that the mechanochemical reaction environment sustains and promotes a wide range of transformations, including organocatalytic, enzyme- and metal-catalyzed reactions, and can often lead to selectivities that are very different from those encountered in solution. While the scope of mechanochemistry in organic synthesis has been extensively reviewed within the last decade,[18, 24, 52] this review focuses specifically on the emergent applications of ball-milling for conducting the reactions of hydrogenation and/or dehydrogenation which are critical for the development of cleaner, more sustainable chemical

manufacturing. For that reason, we will particularly highlight the recent applications of mechanochemistry to key transformations, such as the reduction of carbon monoxide (CO) and carbon dioxide (CO_2).

2. Typical reductants and catalyst design

2.1 Reductant choice

Hydrogen gas is the most atom-economic reagent for hydrogenation reaction and, therefore, a staple of chemical industry.[53] While hydrogen gas is readily deployed in laboratory and industrial scale applications, its use in mechanochemical processes has been limited by the lack of equipment designed to handle gaseous reagents. The development of such equipment is an area of rising importance, as described in the recent review of gas-based mechanochemical milling reactions by Bolm and Hernández.[54] An alternative to gaseous H_2 as a reactant in milling reactions is the use of simpler and safer to handle solid or liquid reagents that can be used as *in situ* sources of hydrogen. The generation of hydrogen gas *in situ* has recently been investigated using both water,[55, 56] as well as ethers and short alkanes as sources of H_2.[57] In 2015, the Sajiki group showed how the mechanochemical treatment of water in a planetary mill, using milling vessels (jars) and milling media (balls) made of SUS304 stainless steel could lead to production of H_2 gas *via* galvanic splitting of water due to the pairing of chromium and nickel in the milling assembly.[55] This work demonstrated quantitative conversion of H_2O into H_2 (Table 1), which was subsequently collected and quantified using gas chromatography and pressure measurement.

Table 1. Galvanic generation of H_2 gas by milling of water in a Ni- and Cr-containing stainless steel assembly[55]

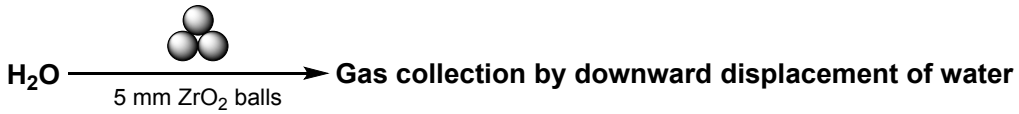

						Gas proportions (%)[a]		
Entry	**Reaction vessel**	**H_2O (μL)**	**Number of balls**	**Additive**	**Collected gas volume (mL)**	**N_2**	**H_2**	**O_2**
1	SUS304 (80 mL)	270, 15 mmol	100[b]	None	120	44	51	1.5
2	SUS304 (80 mL)	270, 15 mmol	100	None	100	35	50	1.3
3	ZrO_2 (20 mL)	68, 3.8 mmol	25[b]	None	23	78	0.3	20
4	ZrO_2 (20 mL)	68, 3.8 mmol	25	None	40	62	33	3.8
5	ZrO_2 (20 mL)	68, 3.8 mmol	25	Ni (1.88 mmol, 0.5 equiv.)	20	89	2.2	8.0
6	ZrO_2 (20 mL)	68, 3.8 mmol	25	Fe (1.88 mmol, 0.5 equiv.)	20	86	>0.1	13
7	ZrO_2 (20 mL)	68, 3.8 mmol	25	Cr (0.38 mmol, 0.1 equiv.)	35	62	20	13
8	ZrO_2 (20 mL)	68, 3.8 mmol	25	Cr (0.76 mmol, 0.2 equiv.)	45	50	39	8.9
9	ZrO_2 (20 mL)	68, 3.8 mmol	25	Cr (1.88 mmol, 0.5 equiv.)	56	42	47	4.7
10	ZrO_2 (20 mL)	68, 3.8 mmol	25	Cr (3.75 mmol, 1.0 equiv.)	65	40	47	4.3
11	ZrO_2 (20 mL)	68, 3.8 mmol	25	SUS304 58.5 mg (0.21 mmol as Cr)[c]	35	63	29	3.6

[a]Determined by Shimadzu gas chromatograph. [b]SUS304 balls were used. [c]18.89% of Cr was contained in SUS304 purchased from Fritsch Japan Co. Ltd.

A subsequent report expanded the use of SUS304 milling assembly for mechanochemical reduction or deuteration of a range of substrates, by milling in the presence of H_2O or D_2O, respectively.[56] The same approach, based on pairing of chromium and nickel in the stainless steel milling assembly, was also reported to enable the use of alkanes and diethyl ether as liquid sources of hydrogen. In this process, the chromium is thought to lead to galvanic generation of hydrogen gas from simple alkanes or diethyl ether, while the presence of nickel catalyzes subsequent hydrogenation. In 2018, Hernández and coworkers employed *in situ* generation of H_2 *via* the dehydrogenation of ammonia-borane,[58] while the work by Štrukil and coworkers in 2018 described the use of ammonium formate as a solid reductant.[59]

2.2 Mechanochemical catalyst design

Mechanochemists working in methodology and catalyst design have shown successful methods towards making catalytically viable organometallic complexes (Figure 2a), as well as obtaining unique size control of a variety of earth-abundant or noble metal nanoparticles,[15, 60] (Figure 2b) both of which we will highlight in this review. Mechanochemistry, however, also has the unique advantage of employing the materials of the milling assembly, to act as the metal source for chemical transformations (Figure 2c). While we will only highlight a handful of specific examples where the milling assembly plays an active role, other groups have highlighted the advantages of this technique.[61] Herein we have outlined key examples where either catalyst reactivity or selectivity was improved through mechanochemical catalyst synthesis or where employing mechanochemical reduction reactions allowed the reduction of challenging substrates, while reducing bulk solvent waste.

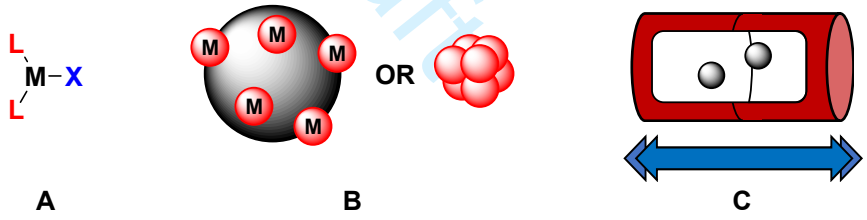

Fig 2. Possible catalysts for mechanochemical reduction reactions. A) molecular species B) nanocatalysts, either supported or free C) the material of the milling assembly itself

2.2.1 Molecular catalysts

Since Sabatier's Nobel Prize winning demonstration of catalytic hydrogenation reactions,[2, 3] the use of organometallic complexes for hydrogenation has been at the forefront of this field. Mechanochemistry has seen a range of utility in fundamental organometallic chemistry, enabling reactivities not previously seen in solution synthesis.[38] However, the mechanochemical application of such complexes towards hydrogenation/dehydrogenation reactions is not very developed . A

seminal example of the successful application of organometallic complexes towards catalytic dehydrogenation and subsequent hydrogenation reactions in mechanochemistry was presented by Hernández et al. of the *in situ* synthesis and use of Wilkinson's catalyst, $[RhCl(PPh_3)_3]$, under ball-milling conditions.[58] Uniquely, the mechanochemical method gave exclusively the orange polymorph of Wilkinson's catalyst, previously known to form when the quantity of solvent used to make the catalyst was reduced.[62, 63] This study demonstrated the overall versatility of ball-milling, demonstrating that the catalyst synthesis, the ammonia-borane dehydrogenation and the catalytic reduction of *trans*-stilbene could all be conducted successfully using a ball mill. Several control reactions were conducted to ensure the release of hydrogen gas through the dehydrogenation of ammonia-borane, which was confirmed both through $^{11}B\{^1H\}$ NMR studies as well as through a modified milling jar that allowed for the capture and volume measurement of the produced hydrogen gas (Figure 3).

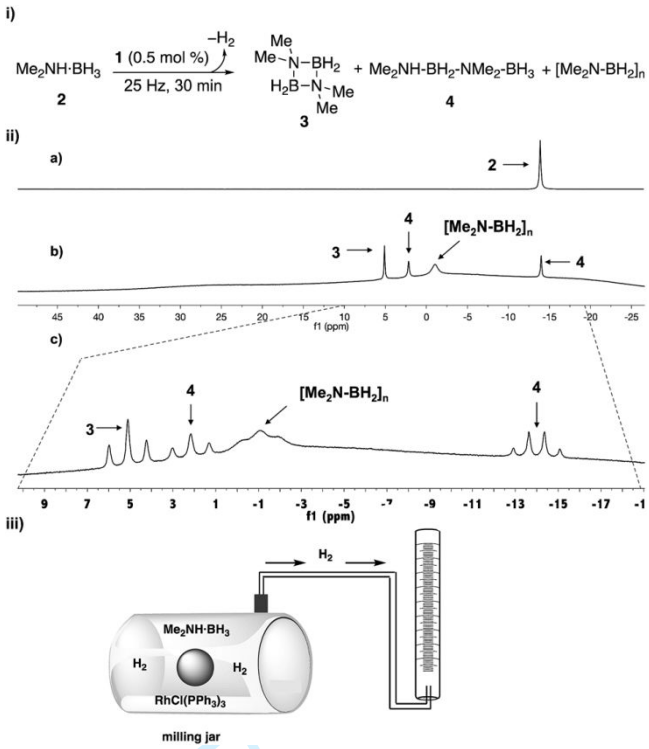

Fig 3. Control experiments showing i) the dehydrogenation of ammonia borane in the presence of Wilkinson's catalyst, as seen from ii) $^{11}B\{^{1}H\}$ NMR a) before and b) after. iii) apparatus to measure hydrogen release[58]

2.2.2 Nanoparticle catalysts

Early works in applied mechanochemical methods to hydrogenation catalysis research focused on comparing mechanical to traditional thermal and solvent based methods. For instance in 1999 by Lomovsky and coworkers synthesised Ni-Al-Mo alloy catalysts pyrometallurgically and mechanically, and studied their application to the hydrogenation of sodium maleate and sodium p-nitrophenolate.[64] They measured better average reaction rates and faster synthesis times for the mechanical version. Particle size reduction was limited and bottomed out at the order of single digit micrometer particle diameters. Due to the top-down approach to synthesis that was taken, ultrasmall sizes less than 10 nm in diameter were simply inaccessible and the particle size dispersity went uncontrolled and non-uniform. Particle characteristics such as these can be typical of mechanical methods where the process is mainly physical, like mechanical alloying of elemental

powders without a chemical change, or where there is either no particle capping agent to nullify aggregation, or no support structure to effectively disperse the particles. Similar works were published in 1993 and in 1994 by the groups of Miani and Cocco respectively, where elemental iron and carbon were ball-milled into nanophase iron carbides,[65] and where mechanically alloyed nickel-zirconium catalysts were ball-milled from their elemental precursors,[66] both as catalysts for the hydrogenation of carbon dioxide and carbon monoxide respectively.

3. Applications towards organic reduction reactions

3.1 Alkenes/Alkynes

3.1.1 Stoichiometric reductant or metal complexes

A methodology for the reduction of alkynes, alkenes, carbonyls, nitro groups and dehalogenation of aryl halides using *in situ* galvanic reduction of water to produce hydrogen was demonstrated by the Sakiji group. The selectivity of the process was limited, most likely due to high reactivity of nickel metal towards hydrogenations.[67] In 2018, the same group demonstrated that diethyl ether, as well as short-chain alkanes in a large excess (20 molar equivalents) could act as liquid sources of hydrogen gas when milled in the same SUS304 stainless-steel milling jars.[57] This work improved reaction yields, giving conversions in the range 29-86% for alkene, as well as full arene hydrogenations within 24 hours (Table 2). With this initial viability to produce stoichiometric amounts of hydrogen gas and the use of the milling vessel and media itself as the metal source to drive this reaction, there were some major setbacks which would need to be improved in future works. Using Entry 2 from Table 2 for example, the η value equates to 13.6 μL mg^{-1}, well within the limit of a traditional solution reaction, as opposed to traditional LAG ranges of 0.1-1 μL mg^{-1}. The galvanic oxidation of the jars in order to drive these reactions also leads to eventual degradation of the reaction vessel, limiting the long-term application of these methods.

Table 2. Substrate scope presented from the in situ generation of H_2 gas, using ethyl ether as a sacrificial source[57]

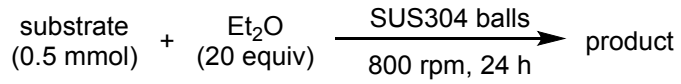

Entry	Substrate	Product	Yield (%)
1	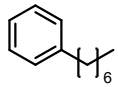	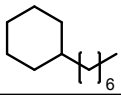	67
2	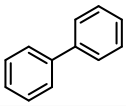	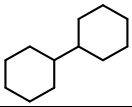	56
3	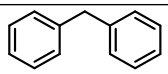	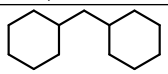	61
4	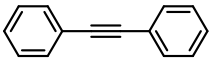	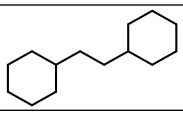	48
5	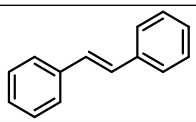	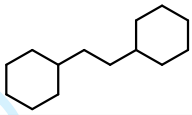	49
6	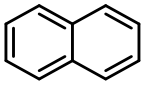	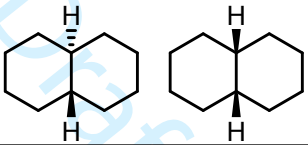	27 (30:70)
7	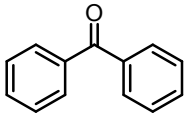	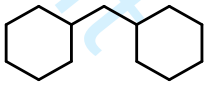	43
8	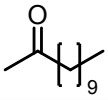	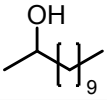	32 (61)[b]
9	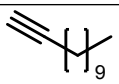	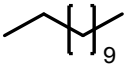	86
10	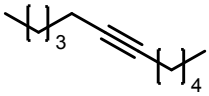	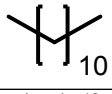	64

[a]The reaction was carried out using a Fritsch Pulverisette 7 Classic Line Ball Mill (PL-7) equipped a 12 mL SUS304 vessel and 50 SUS304 balls (diameter: ca. 5 mm). Et_2O was purchased from commercial sources and used without further purification. [b]Recovery of the substrate.

The work of Hernández et al. in 2018, in which they were able to obtain an orange polymorph of Wilkinson's catalyst as discussed in Section 2.2.1, highlights the fact that both the orange and red polymorphs showed vastly different reactivities towards the mechanochemical hydrogenation of *trans*-stilbene, giving 78% isolated yield after only 90 minutes milling at 25 Hz with the commercial catalyst as opposed to 13% with the catalyst synthesized using the LAG method. The

orange polymorph also showed unique reactivity towards *cis*-stilbene, having comparable yields as well as isomerization to *trans*-stilbene (Figure 4).[58] This highlights the utility of mechanochemical techniques for discovering the reactivity of catalysts in the solid state, not possible by traditional solution-based methods.

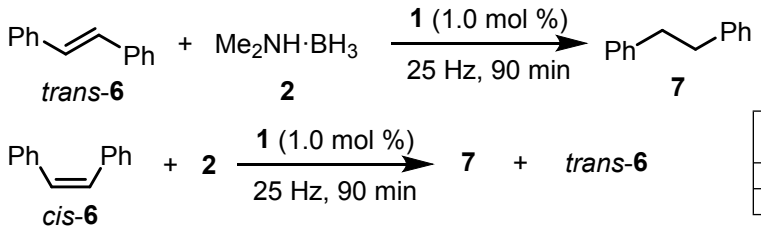

$RhCl(PPh_3)_3$	Yield[a]
LAG WC	13%
Red WC	99% (78%)[b]

$RhCl(PPh_3)_3$	Yield[a]	
	7	*trans*-**6**
LAG WC	62%	30%
Red WC	77%	23%

[a]Determined by ^{1}H NMR spectroscopy using 1,3,5-trimethoxybenzene as an internal standard. [b]After isolation by column chromatography.

Fig 4. Catalytic reactivity comparing the commercially available Wilkinson's catalyst to the catalyst made by milling (LAG WC) for both *cis* and *trans* stilbene hydrogenation and isomerization[58]

To the best of our knowledge, while mechanochemistry has shown broad and unique applicability in organometallic synthesis, this is the only example in which different polymorphic forms of a discrete metal complex were made mechanochemically and investigated as catalysts towards hydrogenation.

3.1.2 Nanocatalysts

In 2016, the Blair group reported metal-free mechanochemical hydrogenation using defect-laden hexagonal boron nitride (*dh*-BN) as a catalyst for the hydrogenation of olefins with H_2.[68] Boron nitride is not catalytically active until after the defects are introduced into the structure; in order to prepare the catalyst, pristine *h*-BN was milled in a zirconia jar for 30 minutes, yielding nanosheets with defect-rich structure (Figure 5).

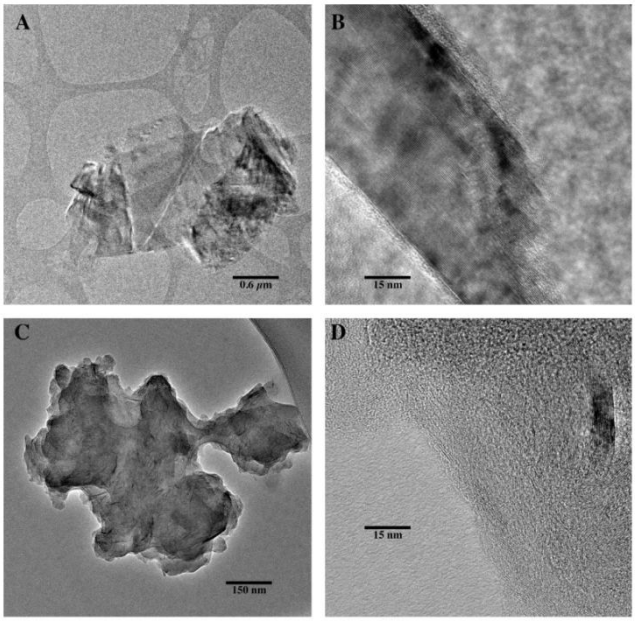

Fig 5. TEM images of as received *h*-BN (A and B) and *dh*-BN (C and D). The as received material is large flakes (A) with well ordered staking of the BN sheets (B). The *dh*-BN is much smaller and thinner flakes (C) with much less order in the c direction. Evidence of delamination and curling of the BN sheet can be seen in (C)[68]

With density functional theory (DFT) calculations as support, and with already existing work on hydrogen sorption energies to *dh*-BN sheets and nanotubes,[58] the authors identified the particular types of defect sites that contributed most to the catalytic activity of the *dh*-BN. If the binding energy of the site is too strong or too weak then the reactivity will be hindered. The nitrogen vacancies (V_N) and sites where boron atoms substituted for nitrogen (B_N) were found to be the most energetically similar to the binding energies of known metal catalysts, indicating their favourability for catalytic olefin hydrogenation. Solid-state NMR (ssNMR) spectroscopy revealed that the concentration of B_N sites is low compared to that of V_N sites, supporting the view that catalytic activity originates from nitrogen vacancies.

Outcomes of mechanochemical catalytic hydrogenation of various olefins are presented in Table 3; hydrogenations took place inside a temperature controlled and air-sealed custom alumina

pebble mill shaped like a double truncated cone. Full conversion could be reached in some cases with temperatures as low as 20°C, in stark contrast to typical industrial hydroprocessing that can require much higher temperatures (300 – 400°C). Conversion values across the ten different substrates were generally good; turnover frequencies (TOFs) and turnover numbers (TONs) were also calculated based on an assumption that the catalysis is deactivated after first use, but in practice the authors were able to recycle the catalyst at least three times with minimal loss of catalytic activity.

Table 3. Mechanochemical hydrogenation Yields, TOFs, and Single-Use TONs of Various Substrates over dh-BN with a Mill Speed of 66 rpm Unless Otherwise Specified [68]

Reactant	Products(s)	Reaction Temp. (°C)	TOF (s^{-1})/TON	Yield/Comments
		20	1.25×10^{-3}/16.10	100%; 114 RPM
		200	4.15×10^{-3}/90.69	100%
		20	2.88×10^{-4}/15.88	100%; 114 RPM
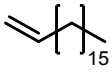	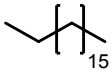	150	4.15×10^{-5}/90.69	35% at 150°C
		220	2.88×10^{-4}/15.88	100% at 220°C[a]
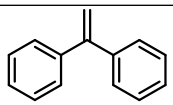	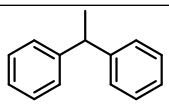	170	1.17×10^{-3}/21.07	97%
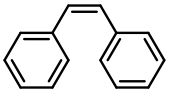	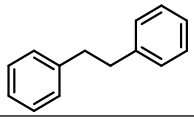	170	1.41×10^{-3}/14.49	100%
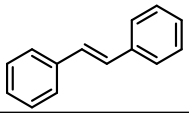	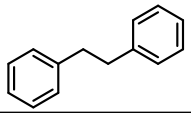	135	1.09×10^{-3}/5.00	99%
			1.15×10^{-3}/13.47	99%
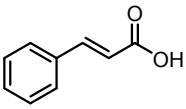	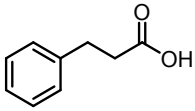	170	1.19×10^{-4}/10.28	55.1% hydrocinnamic acid after catalyst recycle
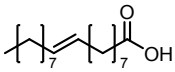	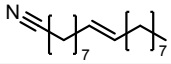	170	5.79×10^{-5}/5.00	58% olyel nitrile
				33% steryl nitrile
	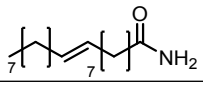			10% oleylamide
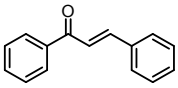	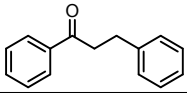	240	1.56×10^{-4}/13.56	90%
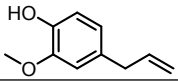	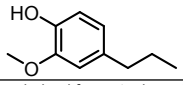	240	-	65%

[a]All information was derived from steel reactor data; all reactions run at 66 rpm unless otherwise specified. [b]After addition of 5 mass % fumed silica.

To confirm that this is truly a metal-free hydrogenation from mechanically treated *dh*-BN, additional steps and analyses were performed. Firstly, the use of the custom mechanochemical hydrogenation reactor made of alumina reduced the likelihood that milling equipment could actively participate in catalytic hydrogenations. As a model test reaction for the custom reactor, propene was chosen as a substrate void of metal impurities that could potentially be carried by

alternative liquid or solid substrates. Lastly, analysis of the *dh*-BN catalyst by inductively coupled plasma atomic emission analysis (ICP-AES) before and after activation revealed only minimal metal incorporation from the milling process. Specifically, while the starting material contained no detectable iron or nickel, the material after activation exhibited no more than 7 ppm of iron and 10 ppm of nickel. To prove it was the defects and not trace metal impurities that are catalytically active, hydrogenation reactions on propene substrates were performed in the custom mill with graphite instead of *dh*-BN, while maintaining similar contents of iron and nickel in the catalyst. Under reaction conditions similar to those used with the *dh*-BN catalyst, the use of mechanically treated graphite to catalyze the hydrogenation of propene showed no hydrogen uptake, and no hydrogenation products were observed. Moving forward, components other than the catalyst, such as a catalyst support or the reaction vessel material, can influence the catalytic capacities of a system and display control over things like yield, selectivity, and reaction rates.

In 2017, Chisholm and coworkers described the mechanochemical synthesis of an ordered mesoporous carbon (OMC) material supporting metal nanoparticles, displaying use as catalysts for the selective hydrogenation of arenes.[69] The OMC support was made beginning with the neat ball milling of Pluronic triblock co-polymers PEO–PPO–PEO (F127) and tannin for 30 minutes, followed by the addition of a divalent metal acetate to the solid mixture to mill for another 30 minutes. Subsequent carbonization under a nitrogen atmosphere yielded the pure OMCs; however, if the pure metal species of the metal acetate chosen has a high enough boiling point then the metallic component will not evaporate during high temperature (450 – 800°C) carbonization and metallic nanoparticles will remain in the final product. The transition metal ions were necessary to crosslink the tannin around the F127 micelles during milling, after which the F127 micelles were completely decomposed and the tannin-metal polymer restructured into a carbon framework

during the carbonization step. From XRD data it was believed that the metal ion during carbonization initially becomes an oxide and is eventually reduced to pure metal by surrounding carbons if the material was carbonized for long enough, after which the pure metal would either evaporate or remain depending on its boiling point. A graphic of the synthesis process is shown in Figure 6 that better visually conveys the structural coordination of the tannin-F127-metal solid-state mixture.

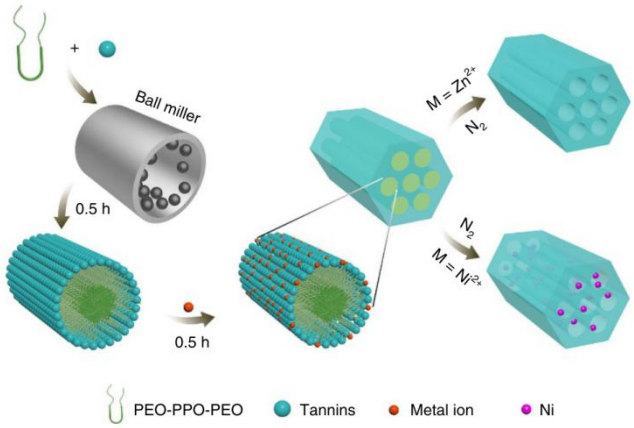

Fig 6. A proposed mechanism for the mechanochemical assembly mediated by coordination crosslinking of tannin, a biomass-derived polyphenol, with divalent metal ions in the presence of Pluronic triblock co-polymers PEO–PPO–PEO. First, the PEO– PPO–PEO and tannin are ball milled for 0.5 h, forming a brown gel. Selected metal acetates are then added to the miller, resulting in homogeneous gel nanocomposites after a short milling time (0.5 h). After carbonization in a N_2 atmosphere, pure OMCs, or metal NP OMCs are obtained depending on the boiling point of the reduced metal species. For example, metallic Zn can evaporate during high-temperature treatment[69]

Nickel (II) acetate was chosen as the metal component of the catalytically active OMC materials, which were prepared using a variety of conditions, including different carbonization temperatures and different tannin-to-F127 weight ratios. These parameters are outlined in the catalyst description Ni-OMC@F127$_w$-c as 'c' and 'w', respectively. Figure 7 details characterization of the Ni OMCs using STEM-HAADF imaging. The Ni nanoparticles were consistently ultrasmall

and well dispersed, with average particles sizes of 4.35 nm and 5.4 nm for samples carbonized at 450 and 600°C, respectively. Even after being recycled for multiple uses the average particle size (6.24 nm) did not grow substantially.

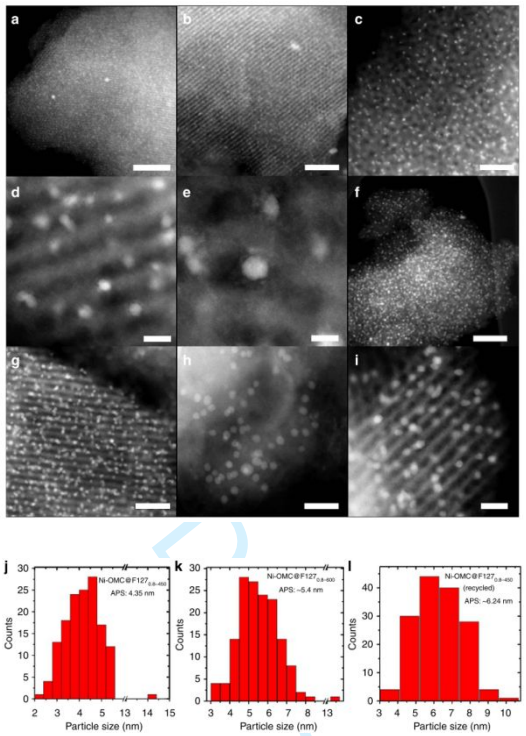

Fig 7. Morphology and structural characterization of nickel OMCs. (a–e) STEM-HAADF images of Ni-OMC@F127$_{0.8}$-450. Scale bar, 200 (a), 100 (b), 50 (c), 10 (d) and 5 nm (e). (f,g) Ni-OMC@F127$_{0.8}$-600. Scale bar, 100 (f) and 50 nm (g). (h) Ni-OMC@F127$_{0.8}$-800. Scale bar, 50 nm. (i) NiOMC@F127$_{0.8}$-450 recycled from hydrogenation reaction; scale bar, 20 nm. (j–l) The corresponding particle size distributions. The particle size distribution was calculated based on 150 particles randomly selected. APS, average particle size[69]

Hydrogenation runs with Ni-OMCs were compared against similar materials such as Ni on commercial activated carbon (Ni-AC) or traditional soft templated OMC (Ni-ST-OMC). The latter two were prepared by a wet impregnation method, maintaining the same Ni content as in Ni-OMC@F127$_{0.8}$-450 (16.1 wt.%). It is worth noting that severe agglomeration of Ni nanoparticles was observed in the AC and ST materials of upwards of 100 nm in diameter. A summary of the

catalytic conversion tests is shown in Table 4. Three different substrates of different sizes were run, and the conversion results clearly demonstrated that the novel Ni-OMCs were unrestricted by substrate size whereas the alternative catalysts performed increasingly worse as the substrate size increased. This wide-ranging size selectivity was attributed to the pore size and structure of the novel carbon framework. Specifically, the catalytic properties of the novel mechanochemically synthesised Ni-OMCs were greatly enhanced by coupling large pore size with 1D pore channel structure, and a high surface area.

Table 4. Selective hydrogenation of alkenes by Ni-based catalysts. Reaction conditions: cyclohexene or 1-octadecene 1 mmol, decane (internal standard: 1 mmol), ethanol 3 ml, Ni catalyst 10 mg, H_2 3MPa, 130 °C, 2 h; or cholesteryl acetate 0.5 mmol, acetone 10 ml, Ni catalyst 10mg, H_2 3MPa, 130 °C, 2 h[69] The three reagents, cyclohexene, 1-Octadecene, Cholesteryl acetate, are represented at the bottom.

Catalyst	Cyclohexene Yield	1-Octadecene Yield	Cholesteryl acetate Yield
Blank	8%	<1%	<1%
Ni-OMC@F127$_{0.8}$-450	98%	96%	92%
Ni-AC@450	97%	65%	10%
Ni-ST-OMC@450	98%	77%	24%

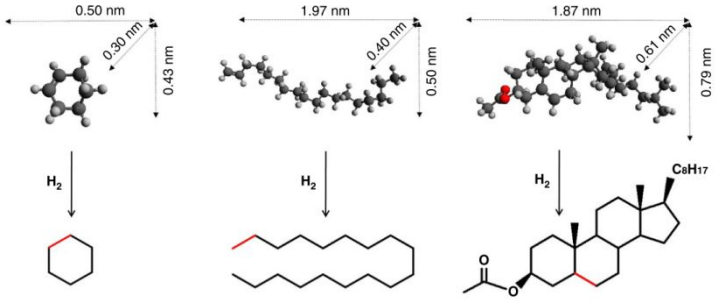

Because the pore structures result from the decomposition of organic polymer regions, the pore sizes and surface areas could be controlled and tuned by varying the weight ratios involving F127 or by changing the choice of polymer: Pluronic F88, F87, F68, F38, P123, P103, P85, P65 and non-ionic surfactants like PEO-based Triton X-100 and Brij-78 were also explored (Table 5).

Table 5. Calculated N_2 at 77K adsorption parameters for the various tannin-based materials obtained with or without metal crosslinkers, using different triblock co-polymers as templates, and under various carbonization temperatures[69]

Sample	V_{SP} (cm³ g⁻¹)*	S_{BET} (m² g⁻¹)†	V_{mi} (cm³ g⁻¹)‡	S_{mi} (m² g⁻¹)§	w_{KJS} (nm)‖	V_{mi} CO_2 (cm³ g⁻¹)¶
C@Tannin-Zn	0.23	514	0.20	469	-	-
C@Tannin-F127	0.36	395	0.11	245	-	-
OMC@F127$_{0.4}$-800	0.59	773	0.19	475	7.3	0.22
OMC@F127$_{0.6}$-800	0.76	1057	0.24	601	7.8	0.29
OMC@F127$_{0.8}$-800	0.58	621	0.12	293	6.9	0.29
OMC@F127$_{1.0}$-450	0.66	547	0.08	180	8.6	-
OMC@F127$_{1.0}$-600	0.67	869	0.17	412	8.2	-
OMC@F127$_{1.0}$-800	0.69	734	0.16	390	7.8	0.18
Ni-OMC@F127$_{0.8}$-450	0.96	996	0.19	464	6.9	0.18
NiOMC@F127$_{0.8}$-600	0.73	769	0.15	356	7.8	-
Ni-OMC@F127$_{0.8}$-800	0.52	558	0.14	355	9.2	-
OMC@F38$_{0.8}$-800	0.49	722	0.16	381	5.3	-
OMC@F68$_{0.8}$-800	0.58	770	0.15	350	5.3	-
OMC@F87$_{0.8}$-800	0.62	765	0.17	412	5.9	-
OMC@F88$_{0.8}$-800	0.61	733	0.13	316	5.7	-
OMC@P65$_{0.8}$-800	0.60	851	0.15	340	4.2	-
OMC@P85$_{0.8}$-800	0.66	770	0.17	405	6.6	-
OMC@P103$_{0.8}$-800	0.76	825	0.19	466	7.5	-
OMC@P123$_{0.8}$-800	0.73	811	0.13	310	5.4	-
OMC@Bj78$_1$-800	0.89	695	0.16	382	17	-
OMC@TritonX100$_{0.8}$-800	0.50	782	0.17	407	5.0	-
OMC@(F127+Ph_3P)$_{0.8}$-800	0.57	496	0.10	244	10.4	-

*Single point pore volume at relative pressure of 0.98
†Specific surface area calculated using BET equation in the relative pressure range of 0.02-0.05
‡Micropore volume
§Micropore surface area calculated using the carbon black STSA *t*-plot equation within the thickness range of 0.354-0.500 nm
‖Pore width from the distribution maxima calculated according to the KJS method using carbon black as reference
¶Cumulative plot from NLDFT analysis for CO_2 isotherms for pores up to 1.5 nm

3.2 Carbonyls

3.2.1 Stoichiometric reductant

Due to their prevalence in a variety of value-added products, the investigation of sustainable, mechanochemical routes for the reduction of carbonyl compounds has gained considerable traction in the last two decades. One of the earliest examples of such reactivity was reported in 1989 by Yagi and coworkers who described the reduction of carbonyl compounds to alcohols using $NaBH_4$. The reactions were performed by grinding together ten molar equivalents of $NaBH_4$ with a variety of aliphatic or aromatic ketones, followed by ageing for 5 days with daily stirring, yielding the corresponding alcohol.[70] This work was further expanded upon by Santos and coworkers, who showed that milling of $NaBH_4$ with benzaldehyde and acetophenone derivatives, having both electron-withdrawing and -donating groups, affords the corresponding primary and

secondary alcohols.[71] The reactions were conducted in custom-made stainless-steel milling jars using alumina balls of 0.25 inch diameter as milling media. This work also showcased the *in situ* generation of highly reactive $LiBH_4$ through milling of $NaBH_4$ with LiCl, enabling solid-state reduction of esters *via* mechanochemistry.[71] Since these early examples, the mechanochemical hydrogenation of carbonyls has expanded to use novel reductants, as well as accessing previously difficult products, due to their intrinsic solubility challenges. Apart from using hydrogen gas or reactive metal hydrides, our group had investigated the use of a solid siloxane, polymethylhydrosiloxane (PMHS), as a viable reductant when activated by a solid fluoride in the form of *tert*-butyl ammonium fluoride (TBAF) supported on silica, or a pairing of alkali fluoride salts with crown ethers.[72] This work systematically investigated the hydrogenation of both aliphatic and aromatic aldehydes and ketones. The mechanism of the mechanochemical reduction using PMHS proceeded *via in situ* generation of gaseous methylsilane ($MeSiH_3$), which was further activated into the highly reactive $[H_3SiFMe]^-$ from another equivalent of silica-supported TBAF. This study also showed the effectiveness of mechanochemical hydrogenation towards substrates with challenges regarding solubility. On one hand, polyketones of low solubility are difficult to reduce using solution-based methods, while under mechanochemistry, 54% of available carbonyl bonds could be reduced after milling for 90 minutes followed by 2 days of passive ageing at room temperature. On the other hand, mechanochemistry helps prevent other separation issues. For instance, both 5-hydroxymethylfurfural (HMF) and its corresponding alcohol dihydroxymethylfurfural (DHMF) are highly soluble in water and hard to separate when dissolved. Using mechanochemistry for this reduction prevented contact with water during reaction and facilitated separation afterwards.

Expanding on this study, Forgione and coworkers studied the KOH-driven Cannizzaro disproportionation of HMF and benzaldehyde derivatives with both electron donating and withdrawing substituents. While this report was successful in the equal production of DHMF, as well as the fully oxidized dicarboxylic acid products in under 5 minutes, it was noted that selectivity could be driven entirely towards DHMF, but required the use of 1.2 equivalents of paraformaldehyde as a sacrificial reagent.[73]

3.2.2 Nanocatalysts

In 2015, Luque and coworkers studied the hydroconversion of cinnamaldehyde using mechanochemically-synthesized palladium nanoparticles that were supported on an aluminum incorporated mesoporous silica (Pd/Al-SBA-15).[74] Catalysts of different Pd loadings (0.5, 1, 2, 4 wt.%) were synthesised and a commercial palladium-on-carbon (Pd/C) catalyst was purchased for catalytic activity comparison. To mechanochemically synthesise the catalyst, palladium(II) acetate and pre-formed Al-SBA-15 were milled together in a planetary ball mill at 350 rpm for 10 minutes. After milling, the solid material obtained was calcined at 450°C in air for 2 hours. TEM images of the bare Al-SBA-15 support (Figure 8A) and of three of the differently Pd-loaded catalysts (Figure 8B-D) are shown below. The mesopores of the Al-SBA-15 are shown to be well structured prior to the Pd catalyst being milled in and the ordered nature of the support is mostly kept intact after milling, though some amorphous domains of Si were observed. For catalysts with a low palladium loading the nanoparticles were small, well dispersed with an average diameter <10 nm, and no sintering was observable. However, larger aggregates could be seen for systems with higher palladium loadings.

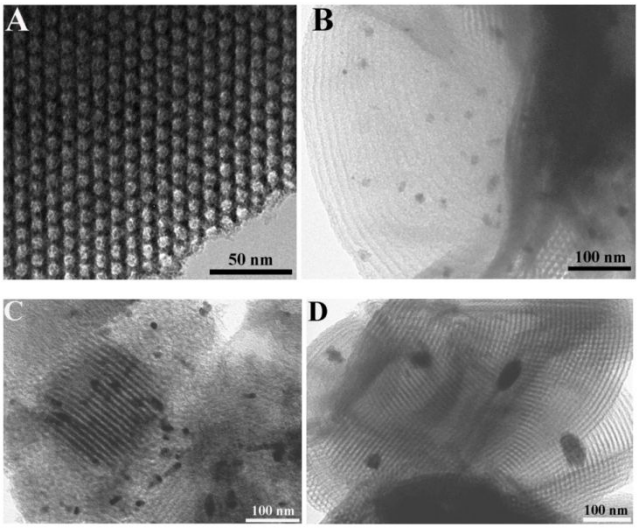

Fig 8. TEM images of A) Al-SBA-15 support; B) Pd1-Al; C) Pd2-Al; D) Pd4-Al[75]

The hydroconversion of cinnamaldehyde was performed with formic acid under conventional heating or microwave irradiation, using acetonitrile as a solvent within the presence of a palladium catalyst. Formic acid was presumed to decompose into CO, CO_2, H_2, and water under heating in the presence of noble metals, providing an *in situ* source of hydrogen. The conversion values of cinnamaldehyde and the multiple product selectivity values in mol% are summarized in Table 6 with detailed reaction conditions. Although both conventional heating and microwave irradiation experiments were both performed, only the microwave trials are presented due to the poor conversion values collected from conventional heating.

Table 6. Total conversion (mol %) and selectivities to products (mol %) of different supported Pd nanoparticles on Al-SBA-15 as compared to a commercial 5%Pd/C material in the microwave-assisted hydroconversion of cinnamaldehyde in formic acid. Reaction conditions: 0.1 mL cinnamaldehyde (0.8 mmol), 0.3 mL formic acid (8 mmol), 2 mL acetonitrile, 0.5 g catalyst, microwave irradiation, 200 W (180 ºC maximum temperature reached, averaged temperature 150 ºC, 250 PSI maximum pressure), 15 min reaction[75]

Catalyst	Conversion (mol%)	Selectivity (mol%)					
		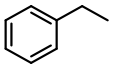		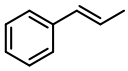	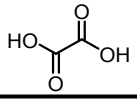	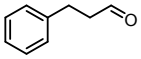	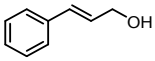
Blank	<5	-	-	-	-	-	-
Pd0.5-Al	97	<5	52	26	16	<5	-
Pd1-Al	>99	<5	64	11	18	-	-
Pd2-Al	98	<5	66	18	13	-	-
Pd4-Al	85	13	44	41	<5	-	-
5% Pd/C	71	21	48	27	-	<5	-

Intriguingly, though only the commercial Pd/C catalyst performed well under conventional heating (96% conversion after 24 hours) while the next best result was the Pd4-Al catalyst (50% conversion after 24 hours), under microwave irradiation the Pd/C catalyst performed worse (by at least 14%) compared to any of the mechanochemically synthesised catalysts. Most of the product quantity was made up of ethylbenzene, β-methylstyrene, cyclohexane, and oxalic acid, the molar composition of which depended on the palladium loading of the catalyst used. For example, production of ethylbenzene increased, while production of oxalic acid generally decreased, with an increase in palladium loading. A possible explanation for the changes in product selectivities might be in sensitivity to changing sizes of palladium nanoparticles due to agglomeration at higher catalyst loadings.

3.3 Carbon monoxide and carbon dioxide

3.3.1 Stoichiometric reductant

From the highlighted early examples of mechanochemical methods being applied towards the hydrogenation of carbonyl functionalities in organic small molecules, the next step in expanding the sustainability and use of mechanochemistry towards a circular economy would be

applications in CO_2 reduction. The hydrogenation of CO_2, while fundamentally different than organic carbonyl reduction, gives access to formates and formic acid, both valuable C_1 building blocks.[76] Initial work done by Mulas and coworkers used olivine, a mixed Mg-Fe silicate ore, for the hydrogenation of CO_2 gas using water as the source of hydrogen.[77] Using a custom-modified SPEX milling jar with sealable valves enabled sampling the atmosphere within the jar using an airtight syringe, followed by gas chromatography (GC) analysis. Conversions of nearly 50% were achievable using an internal CO_2 pressure of 1.5 bar, after 150 minutes of milling, with only slight selectivity to the primary target methane (~0.2% v/v). A tentative explanation for the discrepancies in mass balance is partial hydrogenation to give liquid products, which would not be detectable by GC measurements. While mechanochemical activation of olivine by milling produces 13.5% of magnesium carbonates, there was no evidence of magnetite formation upon milling of a solid catalyst shown to be effective for CO_2 hydrogenation under hydrothermal conditions.[78, 79] This observation indicates that only Fe^{3+} ions are needed as the active metal species, and are most likely released by olivine activation upon extended milling.

Processeses for the activation of CO_2 have been expanded to include solid carbonates as the carbon source, as many inorganic carbonates suffer from solubility limitations in traditional organic solvents.[11, 80] As a stand-in for gaseous CO_2, Jingying and coworkers showed the mechanochemical reduction of several carbonates and bicarbonates with stoichiometric amounts of sodium metal acting as the reductant to give the corresponding formate salts.[81] This work highlighted that ammonium carbonate salts performed the best, giving conversion up to 45% to the corresponding sodium formate. Despite this early success, this process still suffers from low yields as well as the production of undesirable stoichiometric amounts of sodium oxide as a

byproduct. The transition to more air and moisture stable reductants in future works would also be of interest as it allows for more industrially applicable processes.

3.3.2 Nanocatalysts

In 2019, Dai and coworkers detailed the mechanochemical synthesis of single atom catalysts (SACs) using noble metals on metal-oxide supports for hydrogenations. A high entropy (HE) metal oxide [(NiMgCuZnCo)O] was mechanochemically synthesised with a supported catalytically active noble metal element under ambient conditions and was used in the hydrogenation of atmospheric CO_2 to CO.[82] HE oxides, or more descriptively "configurationally disordered and entropy-stabilized mixed metal oxides", are part of a broader class of materials that include both metallic and non-metallic materials. Their single-phase crystal structure has enhanced stability through maximization of the configurational entropy that occurs from the roughly equal inclusion of a large (usually at least five) number of homogenously dispersed metal cations in the solid solution. The resulting changes of the entropic term to the Gibbs free energy of mixing contribute to the high temperature stability of the HE materials. This HE material was made in a two-step mechanochemical process whereby precursor oxide powders are first ball milled for 2 hours, and then the mixed material is calcinated for 2 hours at 500°C: a schematic of the synthesis method is shown in Figure 9.

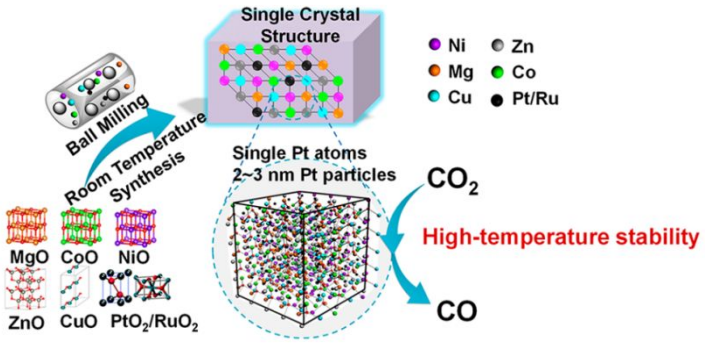

Fig 9. Schematic of the mechanochemical synthesis of Pt/Ru(NiMgCuZnCo)O entropy-stabilized metal oxide solid solution[82]

As the authors stated, this is a notable improvement over other methods to synthesize HE oxide materials, which require long processing times (>48 hours) and/or high temperatures (900 – 1300°C). To evaluate the role of milling in the chemical transformation, X-ray diffraction patterns (Figure 10a) of the milled samples were taken after milling for different times. After 2 hours of milling the base oxide powders (without the catalytically active noble metal), all the precursor phases were successfully converted to a single new phase that was characteristic of the HE oxide material.

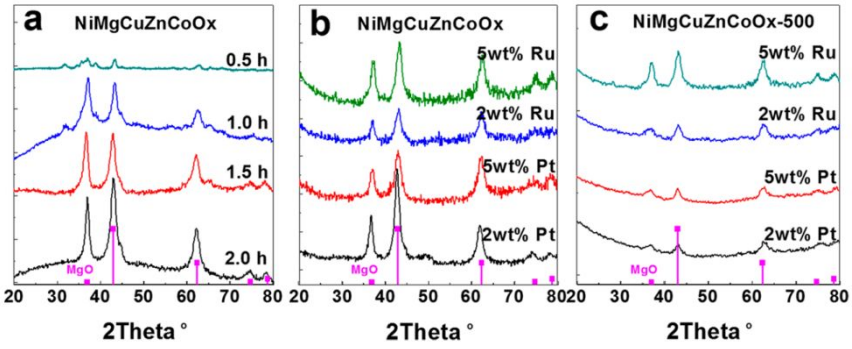

Fig 10. X-ray diffraction patterns for (a) NiMgCuZnCoOx synthesized by ball milling with different times; (b) 2 and 5 wt.% Pt/RuNiMgCuZnCoOx synthesized by ball milling with 2 h; and (c) 2 and 5 wt.% Pt/Ru-NiMgCuZnCoOx synthesized by ball milling with 2 h and 500°C treatment for 2 h[82]

Different loadings of Pt(II) and Ru(II) oxide powders were added to the mixture and X-ray patterns were taken showing good incorporation of the critical noble metal powders (Figure 10b). Lastly, another X-ray pattern was taken after the catalytically active HE solid was calcinated at 500°C for 2 hours and no significant change in the pattern was found that would have indicated the formation of binary platinum or ruthenium oxides (Figure 10c). To help substantiate the dispersity and size of the of catalytic sites, scanning transmission electron microscopy (STEM) images of the milled and calcinated product were taken (Figure 11a-e). Platinum was found both in the form of single atoms, and as ultrasmall (2 – 3 nm) nanoparticles. Morever, there was no evidence of large noble metal particles that could result from sintering, and elemental mapping revealed a balanced distribution of transition metals throughout the solid (Figure 11e).

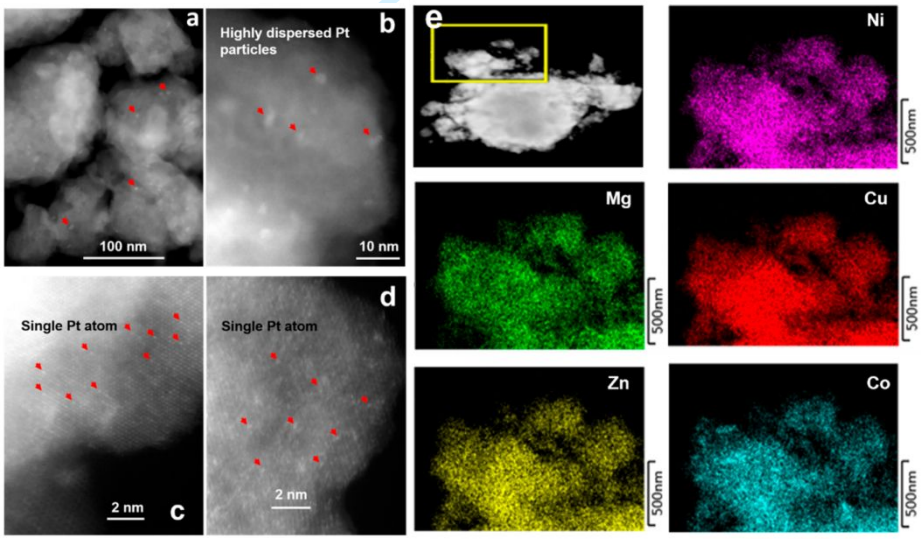

Fig 11. High-angle annular dark-field STEM images for 5 wt.% Pt-(NiMgCuZnCo)O after 500°C treatment with 2 h. Highly dispersed Pt particles in the size range of 2−3 nm on entropy-stabilized metal oxide particles are shown in panels a and b, while panels c and d show atomically dispersed Pt single atoms. Elemental mapping is shown in panel e for 5 wt.% Pt-(NiMgCuZnCo)O after 500°C treatment for 2 h[82]

The catalytic performance and stability of the Pt/Ru-loaded HE oxides were investigated, and are summarized in Figure 12. Hydrogen gas was used to reduce CO_2 into CO with only a small amount

of side-product, as shown by robust selectivity to CO production of over 95% across all catalyst variations. The catalysts containing 2 wt. % Ru-500 and 2 wt. % Pt-500 provided 33.9% and 36.6% yields of CO, with respective conversions of CO_2 of 40.1% and 43.4%. For 5 wt. % Ru-500 and 5 wt. % Pt-500, the yields of CO were increased to 45.7% and 46.1%, with corresponding CO_2 conversions of 45.4% and 47.8%, respectively. Catalytic performance at 500°C was measured over time to investigate the stability of the catalyst, revealing that the conversions and yields remained mostly unchanged over the course of 20 hours.

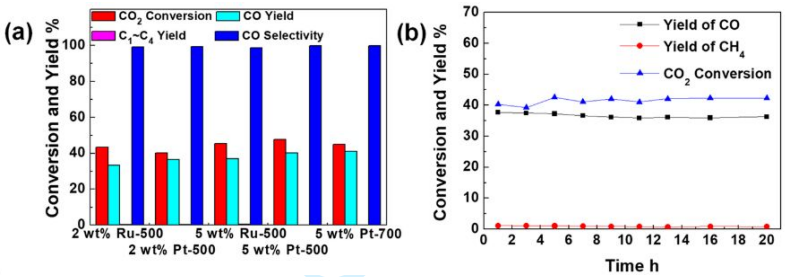

Fig 12. (a) CO_2 hydrogenation activity of 2 wt.% Pt-500, 5 wt.% Pt-500, 2 wt.% Ru-500, and 5 wt.% Ru-500 under 500°C reaction temperature, (b) CO_2 hydrogenation stability at 500°C over 5 wt.% Pt-500, and (c) STEM result of 5 wt.% Pt-500 after hydrogenation of CO_2 at 500°C for 2 h[82]

3.4 Imine/nitro/azides

3.4.1 Stoichiometric reductant or metal complexes

Carbon-nitrogen bonds can be found throughout a variety of molecular structure motifs in the agricultural and pharmaceutical sectors. As previously outlined, direct mechanochemical hydrogenations have already shown great success towards the reduction of olefins and carbonyls, with nitrogen-based functional groups such as imine, azide or nitro moieties, being attractive targets for extending the reaction scope. To the best of our knowledge, the earliest example of such work came from the Wang group in 2005, who described a reductive amination by pairing of a zinc chloride catalyst and a Hanztch ester reductant in order to couple and reduce aromatic

aldehydes and amines[83] bearing electron-withdrawing functionalities. In 2018, Cintas and coworkers demonstrated the reduction of nitrobenzene, as well as alkyl and aryl azides, using formates or hydrazine as model hydrogen sources, without the addition of a catalyst.[84] Their initial investigation explored the reduction of nitrobenzene to aniline using hydrazine as the reductant in order to optimize the reaction conditions for later investigations into the formate-driven hydrogenation of azides. The optimized reaction conditions revealed that quantitative yields were achievable after only 30 minutes of milling in a Retsch planetary mill, using a stainless steel vessel, neutral alumina as a grinding auxiliary, as well as potassium hydroxide and 10 molar equivalents of hydrazine. They also investigated the influence of jar material and ball size, noting that no reactivity occurred when using zirconia implements and that a mixture of 2 and 5 millimeter balls were the most consistent in achieving full conversion. Following the initial optimizations, the highly toxic hydrazine was replaced with much more benign formate as the hydrogen source. This change in reductant led to only a minimal loss in reaction effectiveness, producing aniline in 97% yields. The reactions also showed good selectivity, being applicable to a range of substituted aromatics with no proof of reductive dehalogenation (Table 8). The reaction was also applicable to the reduction of aryl and alkyl azides into their corresponding amines: both benzyl and aryl azides underwent excellent conversions, with yields ranging from 60% to quantitative for both electron-rich and -poor substituents (Tables 7 and 8).

Table 7: Benzyl and alkyl azide reduction scope through the mechanochemical decomposition of hydrazine as a hydrogen source[84]

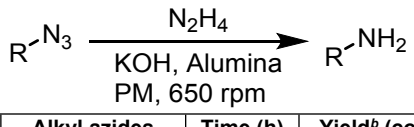

Entry	Alkyl azides	Time (h)	Yield[b] (conv.)[c] %
1	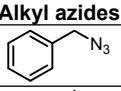	1	98 (100)
2	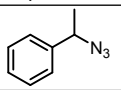	1	100 (100)
3	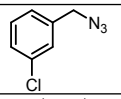	1	100 (100)
4[d]	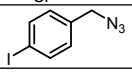	1	- (100)
5	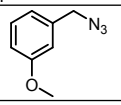	1	99 (100)
6	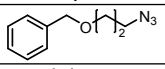	1	80 (100)
7		1	96 (98)
8	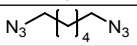	1	90 (100)
9	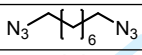	1	94 (100)
10	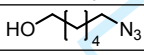	1	60 (100)
11	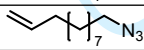	1	81 (90)

[a]Reaction conditions: aryl azide (0.5 mmol), hydrazine (15 mmol), KOH (10 mmol), alumina (1 g), 650 rpm, stainless steel jar (50 mL), 1500 balls (ϕ = 2 mm) and 48 balls (ϕ = 5 mm) [b]Isolated yield, compound purity proven by ^{1}H and ^{13}C NMR. [c]Determined by GC-MS. [d]Benzylamine was formed as the product

Table 8: Aryl azide reduction scope through the mechanochemical decomposition of sodium formate as a hydrogen source[84]

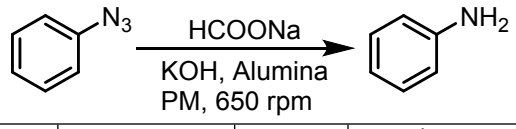

Entry	Alkyl azides	Time (h)	Yield[b] (conv.)[c] %
1		1.5	98 (100)
2	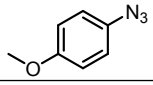	1.5	85 (98)
3		1	100 (100)
4	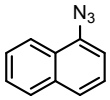	1	87 (92)
5	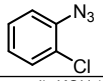	1.5	95 (98)

[a]Reaction conditions: aryl azide (0.5 mmol), sodium formate (10 mmol), KOH (1 mmol), basic alumina (1 g), 650 rpm, stainless steel jar (50 mL), 1500 balls (ϕ = 2 mm) and 48 balls (ϕ = 5 mm) [b]Isolated yield, compound purity proven by ^{1}H and ^{13}C NMR. [c]Determined by GC-MS.

It is worth noting that ICP analysis confirmed that the stainless steel milling assembly was leaching Cr, Fe and Ni during the reaction, as had previously been discussed for hydrogenation reactions involving water-splitting or activation of ethers and light alkenes.

Direct transfer hydrogenation using a supported metal catalyst was also investigated towards the mechanochemical reduction of nitro groups, as demonstrated by the work of Štrukil and coworkers. The use of a traditional Pd/C catalyst was shown to be effective, with ammonium formate being used as a solid-state source of hydrogen.[59] Previous work had shown that in the presence of a palladium catalyst, formate salts would decompose, giving off gaseous NH_3, CO_2 and H_2.[85] As a result, the heterogeneous palladium catalyst functioned as both the generator of the hydrogen gas, and as the catalyst for the hydrogenation of nitroarenes. This catalytic system was readily applied to nearly 20 substrates, some with multiple isomers, with up to ≥90% conversions. Firstly, in addition to using a commercial Pd/C catalyst the authors also fabricated and employed a milled pure Pd/C catalyst and a milled in silica Pd/C catalyst. The morphological and size differences were examined under SEM as shown in Figure 13.

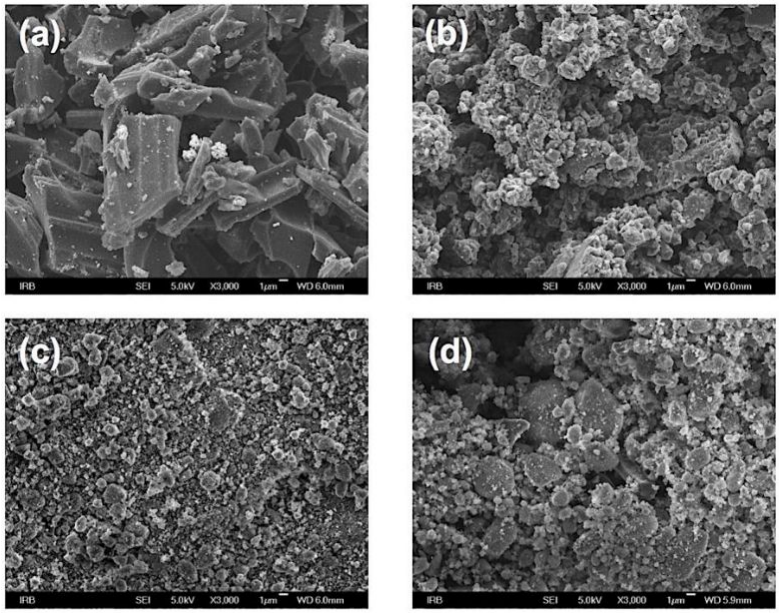

Fig 13. SEM images (3000×) of (a) commercial and (b) milled samples of 10 wt. % Pd/C catalyst; (c) The catalyst milled with silica under LAG conditions for 60 min and (d) post-workup sample after CTH of 3-nitrobenzonitrile[59]

The catalysts milled with silica (regardless of the use of a liquid additive) offered the best benefits in terms of size and homogeneity, being generally smaller and more evenly dispersed compared to the other samples, and was chosen for the substrate scope investigation. Secondly, the use of a LAG additive in the catalytic reaction (Figure 14a) demonstrated an exceptional improvement in conversion, not only compared to neat mechanochemistry but also in comparison to reactivity in solution.

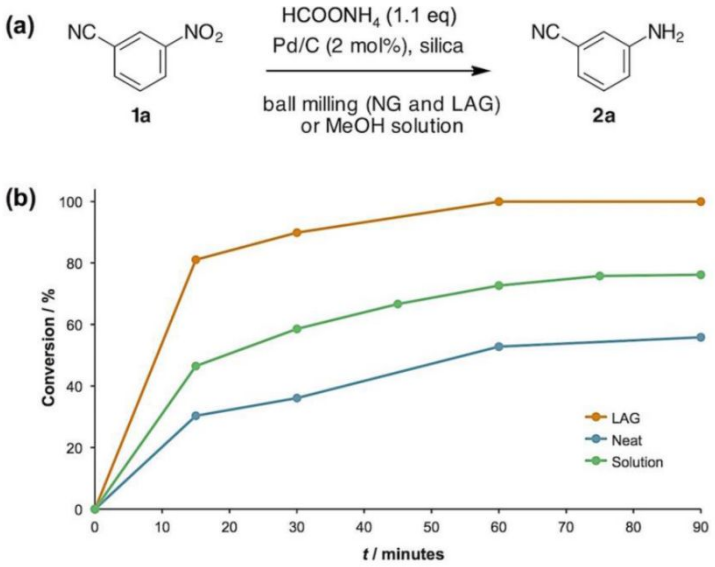

Fig 14. (a) Mechanochemical CTH model reaction; (b) Conversion of 3-nitro-benzonitrile during CTH determined by HPLC analysis[59]

The mechanochemical method enabled a considerable improvement over reactivity in solution, with LAG providing at least 20% higher conversion (Figure 14). This work demonstrated the versatility of mechanochemistry by adapting to a solid-state hydrogen source from a gaseous one, the simple effectiveness of milling by significantly reducing the catalyst size and increasing particle dispersity in a relatively short milling time, and the power of LAG by significantly and quantitatively improving on the solution conversion with only a tiny fraction of the solvent waste. The catalyst did show some limitations with nitro-functionalized thioureas due to catalyst poisoning, as well as nitro-substituted polycyclic aromatic hydrocarbons. In specific cases with halogenated nitroarenes, a mixture of both the dehalogenated and reduced product was noted, due to the high reactivity of the palladium catalyst towards the competitive dehalogenation reaction.

3.4.2 Nanocatalysts

In 2016, Hapiot and coworkers reported the use of cyclodextrins (CDs) and other saccharide additives as simultaneous reducing and stabilizing agents for the mechanosynthesis of

CD supported gold nanoparticles used to catalyse the reduction of substituted nitrobenzene derivatives to aniline products.[86] To synthesize the AuNPs/β-CD complex, 10 mL zirconia grinding jars containing a 9 mm zirconia ball were shaken in a vibrational mill for 5 minutes at a frequency of 30 Hz. The jars were filled with a cationic gold source, 0.016 mmol of $AuCl_3$, and 0.881 mmol of a saccharide additive as a reductive and capping agent. TEM images of the mechanochemical product and a size histogram of Au nanoparticle diameters are shown in Figure 15; the particles are ultrasmall and very monodisperse, averaging 1.54 ± 0.4 nm in diameter.

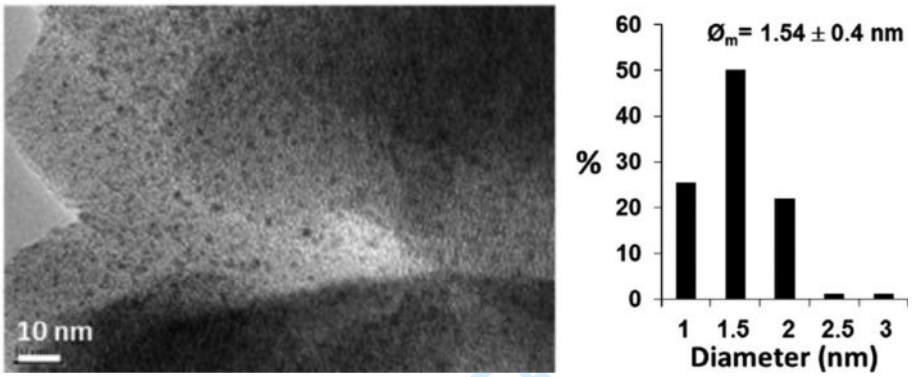

Fig 15. TEM of beta-cyclodextrin stabilised gold nanoparticles and particle size histogram[86]

The as-made saccharide-stabilized Au nanoparticles were then used to catalyze the hydrogenation of 1-chloro-2-nitrobenzene and other closely related halogenonitrobenzene and methoxynitrobenzene derivatives reduced by $NaBH_4$. Variables such as the saccharide additive, the milling frequency and time, and the saccharide hydration were explored in attempts to maximize conversion values and widen the scope of compatible substrates. Among the best conversion results of 100% in 15 minutes for a substrate, the necessary conditions were a combination of milling at 30 Hz for 15 minutes and using hydrous β-CD (10 wt.% water) as a capping agent. Regarding the scope of substrates as seen in Figure 16 that are accessible to hydrogenation, the authors found an interesting regioselectivity in the hydrogenation of

nitrophenols: para isomers were disfavored while meta and ortho isomers reacted well. A poisoning effect, illustrated in Figure 16, was evoked as a possible mechanism.

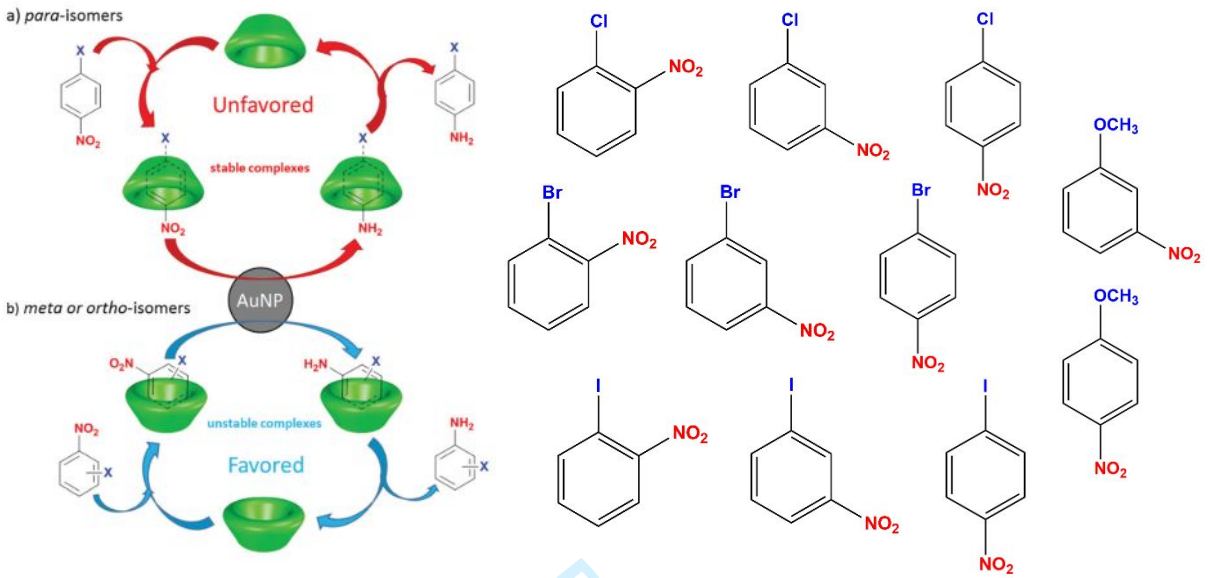

Fig 16. (Left) Schematic representation of dynamics of exchange between CDs and halogenonitrobenzene derivatives. (Right) Full scope of substrates investigated[86]

It was determined that a strong interaction between the substrate and the saccharide that is stabilizing the catalytically-active nanoparticle can slow down or even halt the conversion process. This was attributed to the importance of a dynamic exchange process created by the formation of saccharide/substrate complexes that boost the mobility of the substrate in the solid mixture. The mechanochemical hydrogenation method displayed several advantages to previous methods, including catalyst reusability over multiple cycles, complete substrate conversion in reaction times as low as 15 minutes, and lower amounts of required reducing agents relative to wet methods.

In 2019, Chung and coworkers reported the synthesis of ultrasmall nickel nanoparticles dispersed on a graphene oxide (GO) support from nickel (II) acetate ($Ni(acac)_2$) salts.[87] Graphene has been an explosively popular material in recent research, known for its 2-dimensional (2D) structure, conductive properties, and good mechanical strength. As a result of this interest in graphene, its cost of production has been gradually reducing, making this substance a potentially

economical alternative to metal oxide particle supports. The Ni/GO catalysts were used to catalyse the hydrogenation of 2-nitrophenol and 4-nitrophenol to aminophenols. To prepare the Ni/GO materials, a nickel (II) acetate solution is mixed with ground GO by grinding in a mortar and pestle for 30 minutes. The resulting paste was dried through thermally accelerated evaporation at 130°C for several hours. Finally, the dried product was ground for 15 minutes using mortar and pestle and was subsequently calcinated under N_2 atmosphere at 400°C for 3 hours.

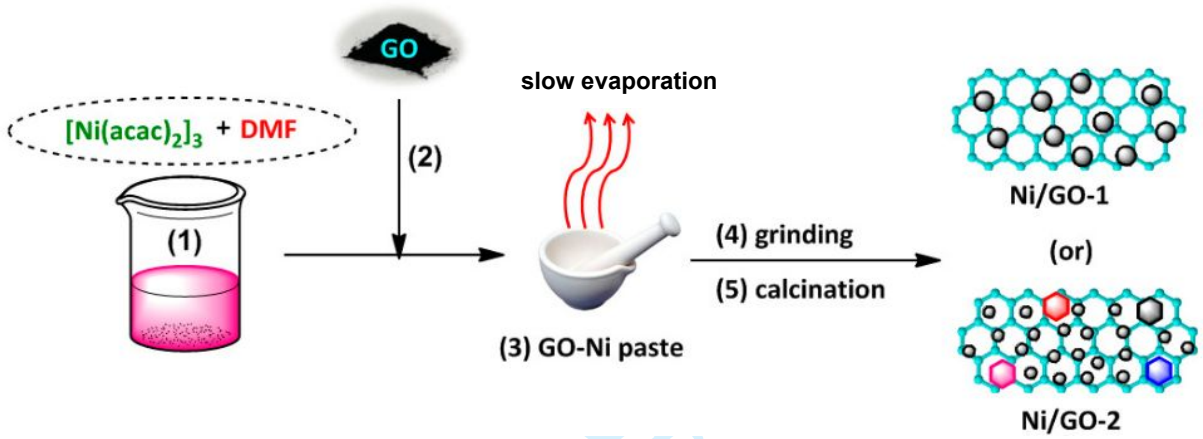

Fig 17. Schematic of Ni/GO preparation[87]

The synthesis of the catalyst was conducted through a low nickel loading (Ni/GO-1), 3 wt.%, and through a high nickel loading (Ni/GO-2), 8 wt.%, pathway shown in Figure 17, only one of which produced the ultrasmall particles. The Ni/GO-1 catalyst displayed a unimodal size distribution centered around ~20.5 nm particles, on the contrary the Ni/GO-2 catalyst displayed a bimodal size distribution centered around ~2.9 nm particles with spherical morphology and around ~25.5 nm particles with irregular morphology. Particle characteristics have been summarized in Figure 18, where TEM images and particle size histograms for each of the catalyst types is provided.

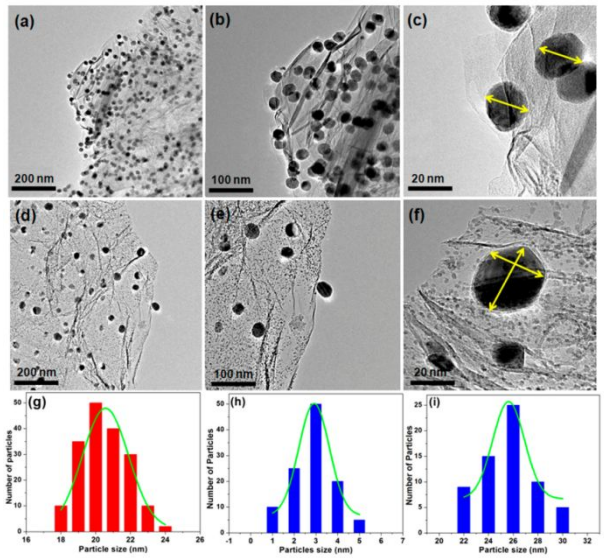

Fig 18. TEM images of (a–c) Ni/GO-1 and (d–f) Ni/GO-2, and particle-size distribution histogram of NiO nanoparticles in (g) Ni/GO-1 and (h,i) Ni/GO-2[87]

The catalytic results from hydrogenation tests are highlighted as follows. Though limited in reactant scope, the quantitative results show comparable or improved efficiency of the new Ni/GO catalyst relative to other noble metal or highly loaded catalysts. In comparing reaction rates, though silica nanotubes supported Ni nanocomposites (Ni/SNTs) showed quantitative conversion with faster kinetics than the Ni/GO catalysts, the Ni/GO catalysts were run with a much lower metal loading (3% or 8%) than the Ni/SNT catalysts (15% or 23%) and thus had improved turn over frequencies (TOF). A similar catalyst to the Ni/GO was prepared with reduced graphene oxide supported Ni catalyst (RGO/Ni) by a wet synthesis method. In comparison to the RGO/Ni catalyst made by wet synthesis, the mechanochemically made Ni/GO catalysts showed an approximate 330-fold increase in the k_{app} and k′ values. Beyond these, the optimized Ni/GO catalyst managed to outperform some catalysts with gold,[88] silver,[89] or platinum[90] alloy metal nanoparticles. It is also worth noting the environmental and economical benefits of the Ni/GO catalysts; both of the catalysts, Ni/GO-1 and Ni/GO-2, displayed excellent reusability over ten cycles of hydrogenation and maintained 95% conversion.

4. Conclusions

Mechanochemistry has demonstrated clear benefits over solution reactivity for many organic transformation, and in particular for hydrogenation reactions of substrates whose specific solubilities make them challenging to use in solution, at the same time decreasing reaction times, temperature, and the production of bulk solvent waste. For the design of novel molecular and nanostructured catalysts, mechanochemical methods have also shown a clear benefit in the ability to access solid-state structures not easily accessible in solution, or the direct synthesis of ultrasmall and highly reactive supported and free nanoparticle catalysts whose solution synthesis often involves energy intensive high temperature annealing or sintering steps. While mechanochemistry has already demonstrated a number of new opportunities and advantages in catalytic hydrogenation, it is also clear that the use of mechanochemical techniques for conducting this fundamental chemical transformation is at a very early stage of development. Consequently, we hope that, by highlighting existing work as well as outlining open questions and limitations, this Review will also serve as an inspiration for the further exploration and development of this field of mechanochemistry and Green Chemistry.

5. Perspectives

The outlined successes of ball milling in conducting hydrogenation reactions have demonstrated mechanochemistry as a viable strategy for this type of chemical transformations, setting the stage for further development. In this section, we highlight several recently emerged instrumental techniques that show high promise for further improving various aspects of mechanochemical reactivity and, consequently, would be attractive targets for further development of mechanochemical hydrogenation techniques.

As has been previously discussed, milling in stainless-steel vessels can often leach metal nanoparticles and metal ions, providing parts per billion (ppb) or parts per million (ppm) amounts of catalyst during the milling process. This leaching can be a detriment, however, especially towards pharmaceutical applications where there are strict regulations on the amount of residual metal allowed in active pharmaceutical ingredients (APIs). A potential route to reduce or completely avoid metal contamination resulting from the wear of milling media in mechanochemical synthesis is offered by resonant acoustic mixing (RAM). The RAM methodology relies on the use of acoustic vibrations as a means to achieve intense and localized mixing zones. The use of RAM technology has recently been demonstrated in the context of pharmaceutically relevant cocrystals,[91, 92] as well as metal-organic frameworks,[21] and it is anticipated it could be of considerable value as a general tool for mechanochemical reactions.

As mechanochemistry expands its potential towards large scale and industrial implementation, the ability to scale-up the space-time yield of organic transformations has become a crucial goal. The first logical step for increasing the scale of a mechanochemical reaction would be to implement a planetary mill. This method is the most easily accessible, however it still works on a batch-process, with a low space-time yield. Flow chemistry for solution processes has seen a surge in industrial processes to limit waste, as well as increasing the throughput of pharmaceutical APIs while seeing a considerable decrease in the footprint of the process, both physical and environmental.[93] The mirror of continuous flow processes in solid-state mechanochemical techniques is possible through the application of twin screw extrusion (TSE). The apparatus for TSE (Figure 19) allows for control of both mixing zones and heating and is already widely used in the polymer industry[94] and pharmaceutical cocrystal formation.[20, 95] Various groups have employed TSE towards high-throughput organic synthesis,[96-99] the formation of peptide bonds,[100]

deep-eutectic solvents,[101] metal-organic[16, 102] and covalent-organic frameworks,[103, 104] as well as the synthesis of API molecules.[105]

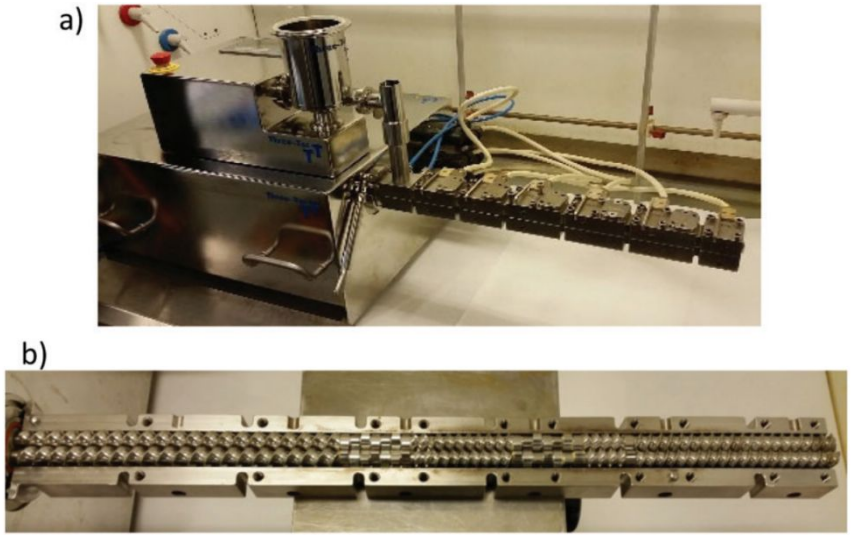

Fig 19. Twin screw extruder (TSE) apparatus employed for continuous, solid-state organic transformations[96]

These initial studies, which include processes at the milligram as well as work towards larger scale continuous processes, provide a framework for future development in mechanochemical hydrogenations. The development of mechanochemical strategies to conduct asymmetric or late-stage hydrogenations that show functional group selectivity are important future research goals. Mechanochemistry has already shown potential for organocatalytic asymmetric bond forming reactions,[106, 107] but has yet to be applied for asymmetric hydrogenations. Alongside the need to improve enantioselectivity, methods which produce hydrogen *in situ* also struggle with chemoselectivity when being applied to substrates with multiple reducible functionalities. This selectivity can be influenced both by the nature of the catalyst as well as the hydrogen source.

Advancements and experimentation in the field of hydrogenation/dehydrogenation catalysis design and in mechanochemical methods have no doubt been bountiful for the growth of mechanochemistry as a field. The improvements made in terms of energy efficiency, catalytic activity, reaction selectivity, and atom efficiency, are likely to enable an significant increase in

mechanochemically-synthesised catalysts and hydrogenation reactions under mechanochemical conditions. These improvements present economical opportunities that may allow for eventual replacement of traditional processing methods and infrastructure, a pathway towards commercialisation that would provide greener, safer, and more sustainable chemistry in the future.

Acknowledgements

B.G. F. acknowledges the financial support of the Walter C. Sumner Memorial Fellowship. We thank the Natural Science and Engineering Research Council of Canada (NSERC) Discovery Grant and accelerator programs, the Canada Foundation for Innovation (CFI), the Canada Research Chairs (CRC), the Centre for Green Chemistry and Catalysis (CGCC), and McGill University for their financial support.

References

(1) Blaser, H.-U.; Spindler, F.; Thommen, M. Industrial Applications. In *The Handbook of Homogeneous Hydrogenation*, de Vries, J. G.; Elsevier, C. J. Eds.; Wiley-VCH Verlag GmbH & Co. KGaA: Weinheim, 2007; pp 1279-1324.

(2) Sabatier, P.; Senderens, J.-B. Action du nickel sur l'éthylène. Sythèse de l'éthane. *C. R. Hebd. Séances Acad. Sci.* **1897,** *124,* 616.

(3) Sabatier, P. Hydrogénations et déshydrogénations par catalyse. *Ber. Dtsch. Chem. Ges.* **1911,** *44*, 1984.

(4) Hudson, R.; Hamasaka, G.; Osako, T.; Yamada, Y. M. A.; Li, C.-J.; Uozumi, Y.; Moores, A. Highly efficient iron(0) nanoparticle-catalyzed hydrogenation in water in flow. *Green Chem.* **2013,** *15,* 2141.

(5) Li, A. Y.; Kaushik, M.; Li, C. J.; Moores, A. Microwave-Assisted Synthesis of Magnetic Carboxymethyl Cellulose-Embedded Ag-Fe_3O_4 Nanocatalysts for Selective Carbonyl Hydrogenation. *ACS Sustainable Chem. Eng.* **2016,** *4*, 965.

(6) Hudson, R.; Chazelle, V.; Bateman, M.; Roy, R.; Li, C. J.; Moores, A. Sustainable Synthesis of Magnetic Ruthenium-Coated Iron Nanoparticles and Application in the Catalytic Transfer Hydrogenation of Ketones. *ACS Sustainable Chem. Eng.* **2015,** *3,* 814.

(7) Torres Galvis, H. M.; Bitter, J. H.; Khare, C. B.; Ruitenbeek, M.; Dugulan, A. I.; de Jong, K. P. Supported Iron Nanoparticles as Catalysts for Sustainable Production of Lower Olefins. *Science* **2012,** *335,* 835.

(8) Li, Y.-Y.; Yu, S.-L.; Shen, W.-Y.; Gao, J.-X., Iron-, Cobalt-, and Nickel-Catalyzed Asymmetric Transfer Hydrogenation and Asymmetric Hydrogenation of Ketones. *Acc. Chem. Res.* **2015,** *48,* 2587.

(9) Kallmeier, F.; Kempe, R. Manganese Complexes for (De)Hydrogenation Catalysis: A Comparison to Cobalt and Iron Catalysts. *Angew. Chem. Int. Ed.* **2018,** *57,* 46.

(10) Constable, D. J.; Jimenez-Gonzalez, C.; Henderson, R. K. Perspective on solvent use in the pharmaceutical industry. *Org. Process Res. Dev.* **2007,** *11,* 133.

(11) Do, J.-L.; Friščić, T. Mechanochemistry: A Force of Synthesis. *ACS Cent. Sci.* **2017,** *3,* 13.

(12) Fischer, F.; Fendel, N.; Greiser, S.; Rademann, K.; Emmerling, F., Impact Is Important-Systematic Investigation of the Influence of Milling Balls in Mechanochemical Reactions. *Org. Process Res. Dev.* **2017,** *21,* 655.

(13) Friščić, T.; Mottillo, C.; Titi, H. M. Mechanochemistry for Synthesis. *Angew. Chem. Int. Ed.* **2020,** *59,* 1018.

(14) Hasa, D.; Carlino, E.; Jones, W. Polymer-assisted grinding, a versatile method for polymorph control of cocrystallization. *Cryst. Growth Des.* **2016,** *16,* 1772.

(15) Muñoz-Batista, M. J.; Rodriguez-Padron, D.; Puente-Santiago, A. R.; Luque, R. Mechanochemistry: Toward Sustainable Design of Advanced Nanomaterials for Electrochemical Energy Storage and Catalytic Applications. *ACS Sustainable Chem. Eng.* **2018,** *6,* 9530.

(16) Crawford, D.; Casaban, J.; Haydon, R.; Giri, N.; McNally, T.; James, S. L. Synthesis by extrusion: continuous, large-scale preparation of MOFs using little or no solvent. *Chem. Sci.* **2015,** *6,* 1645.

(17) Crawford, D. E.; Miskimmin, C. K.; Albadarin, A. B.; Walker, G.; James, S. L., Organic synthesis by Twin Screw Extrusion (TSE): continuous, scalable and solvent-free. *Green Chem.* **2017,** *19,* 1507.

(18) Margetić, D.; Štrukil, V. Recent Advances in Mechanochemical Organic Synthesis. In *Organic Synthesis-A Nascent Relook*, Nandeshwarappam B. P. Eds.; IntechOpen: London, 2020; pp 1-23.

(19) Martina, K.; Rotolo, L.; Porcheddu, A.; Delogu, F.; Bysouth, S. R.; Cravotto, G.; Colacino, E. High throughput mechanochemistry: application to parallel synthesis of benzoxazines. *Chem. Commun.* **2018,** *54,* 551.

(20) Tan, D.; Loots, L.; Friščić, T. Towards medicinal mechanochemistry: evolution of milling from pharmaceutical solid form screening to the synthesis of active pharmaceutical ingredients (APIs). *Chem. Commun.* **2016,** *52,* 7760.

(21) Titi, H. M.; Do, J.-L.; Howarth, A. J.; Nagapudi, K.; Friščić, T. Simple, scalable mechanosynthesis of metal–organic frameworks using liquid-assisted resonant acoustic mixing (LA-RAM). *Chem. Sci.* **2020,** *11,* 7578.

(22) Parkin, I. P. Solid state metathesis reaction for metal borides, silicides, pnictides and chalcogenides: Ionic or elemental pathways. *Chem. Soc. Rev.* **1996,** *25,* 199.

(23) Rightmire, N. R.; Hanusa, T. P. Advances in organometallic synthesis with mechanochemical methods. *Dalton Trans.* **2016,** *45,* 2352.

(24) Tan, D.; Friščić, T. Mechanochemistry for Organic Chemists: An Update. *Eur. J. Org. Chem.* **2018,** *2018,* 18.

(25) Tan, D.; Garcia, F. Main group mechanochemistry: from curiosity to established protocols. *Chem. Soc. Rev.* **2019,** *48,* 2274.

(26) Hasa, D.; Jones, W. Screening for new pharmaceutical solid forms using mechanochemistry: A practical guide. *Adv. Drug Deliv. Rev.* **2017,** *117,* 147.

(27) Hasa, D.; Schneider Rauber, G.; Voinovich, D.; Jones, W. Cocrystal Formation through Mechanochemistry: from Neat and Liquid-Assisted Grinding to Polymer-Assisted Grinding. *Angew. Chem. Int. Ed.* **2015,** *54,* 7371.

(28) Porcheddu, A.; Colacino, E.; De Luca, L.; Delogu, F., Metal-Mediated and Metal-Catalyzed Reactions Under Mechanochemical Conditions. *ACS Catal.* **2020,** *10,* 8344.

(29) Takacs, L. Quicksilver from Cinnabar: The First Documented Mechanochemical Reaction? *JOM*. **2000,** *52,* 12.

(30) Takacs, L. The mechanochemical reduction of AgCl with metals. *J. Therm. Anal. Calorim.* **2007,** *90,* 81.

(31) Faraday, M. On the Decomposition of Chloride of Silver, by Hydrogen, and by Zinc. *Q. J. Sci. Lit. Arts.* **1820,** *8,* 374.

(32) Lea, M. C. Disruption of the silver haloid molecule by mechanical force. *Am. J. Sci.* **1892,** *43,* 527.

(33) Wöhler, F. Ueber künstliche Bildung des Harnstoffs. *Ann. Phys.* **1828,** *87*, 253.

(34) Cao, Q.; Crawford, D. E.; Shi, C.; James, S. L. Greener Dye Synthesis: Continuous, Solvent-Free Synthesis of Commodity Perylene Diimides by Twin-Screw Extrusion. *Angew. Chem. Int. Ed.* **2020,** *59*, 4478.

(35) Friščić, T.; Reid, D. G.; Halasz, I.; Stein, R. S.; Dinnebier, R. E.; Duer, M. J. Ion-and Liquid-Assisted Grinding: Improved Mechanochemical Synthesis of Metal–Organic Frameworks Reveals Salt Inclusion and Anion Templating. *Angew. Chem. Int. Ed.* **2010,** *49,* 712.

(36) Mukherjee, A.; Rogers, R. D.; Myerson, A. Cocrystal formation by ionic liquid-assisted grinding: case study with cocrystals of caffeine. *CrystEngComm* **2018,** *20,* 3817.

(37) Friščić, T.; Childs, S. L.; Rizvi, S. A. A.; Jones, W. The role of solvent in mechanochemical and sonochemical cocrystal formation: a solubility-based approach for predicting cocrystallisation outcome. *CrystEngComm* **2009,** *11,* 418.

(38) Hernández, J. G.; Bolm, C. Altering Product Selectivity by Mechanochemistry. *J. Org. Chem.* **2017,** *82,* 4007.

(39) Julien, P. A.; Mottillo, C.; Friščić, T. Metal–organic frameworks meet scalable and sustainable synthesis. *Green Chem.* **2017,** *19,* 2729.

(40) Lv, D.; Chen, Y.; Li, Y.; Shi, R.; Wu, H.; Sun, X.; Xiao, J.; Xi, H.; Xia, Q.; Li, Z. Efficient Mechanochemical Synthesis of MOF-5 for Linear Alkanes Adsorption. *J. Chem. Eng. Data* **2017,** *62,* 2030.

(41) Klimakow, M.; Klobes, P.; Thünemann, A. F.; Rademann, K.; Emmerling, F. Mechanochemical Synthesis of Metal−Organic Frameworks: A Fast and Facile Approach toward Quantitative Yields and High Specific Surface Areas. *Chem. Mater.* **2010,** *22,* 5216.

(42) Mukherjee, A.; Rogers, R. D.; Myerson, A. S. Cocrystal formation by ionic liquid-assisted grinding: case study with cocrystals of caffeine. *CrystEngComm* **2018,** *20,* 3817.

(43) Hasa, D.; Rauber, G. S.; Voinovich, D.; Jones, W. Cocrystal Formation through Mechanochemistry : from Neat and Liquid-Assisted Grinding to Polymer-Assisted Grinding. *Angew. Chem. Int. Ed.* **2015,** *54,* 7371.

(44) Fiss, B. G.; Hatherly, L.; Stein, R. S.; Friščić, T.; Moores, A. Mechanochemical Phosphorylation of Polymers and Synthesis of Flame-Retardant Cellulose Nanocrystals. *ACS Sustainable Chem. Eng.* **2019,** *7,* 7951.

(45) Huang, J.; Moore, J. A.; Acquaye, J. H.; Kaner, R. B., Mechanochemical Route to the Conducting Polymer Polyaniline. *Macromolecules* **2005,** *38,* 317.

(46) Ravnsbæk, J. B.; Swager, T. M. Mechanochemical Synthesis of Poly(phenylene vinylenes). *ACS Macro Lett.* **2014,** *3,* 305.

(47) Malca, M. Y.; Ferko, P. O.; Friščić, T.; Moores, A. Solid-state mechanochemical ω-functionalization of poly(ethylene glycol). *Beilstein J. Org. Chem.* **2017,** *13,* 1963.

(48) Ashlin, M.; Hobbs, C. E. Post-Polymerization Thiol Substitutions Facilitated by Mechanochemistry. *Macromol. Chem. Phys.* **2019,** *220,* 1900350.

(49) Malca, M. Y.; Bao, H.; Bastaille, T.; Saadé, N. K.; Kinsella, J. M.; Friščić, T.; Moores, A. Mechanically Activated Solvent-Free Assembly of Ultrasmall Bi_2S_3 Nanoparticles: A Novel, Simple, and Sustainable Means to Access Chalcogenide Nanoparticles. *Chem. Mater.* **2017,** *29,* 7766.

(50) Rak, M. J.; Saadé, N. K.; Friščić, T.; Moores, A. Mechanosynthesis of ultra-small monodisperse amine-stabilized gold nanoparticles with controllable size. *Green Chem.* **2014,** *16,* 86.

(51) Fiss, B. G.; Vu, N.-N.; Douglas, G.; Do, T.-O.; Friščić, T.; Moores, A., Solvent-Free Mechanochemical Synthesis of Ultrasmall Nickel Phosphide Nanoparticles and Their Application as a Catalyst for the Hydrogen Evolution Reaction (HER). *ACS Sustainable Chem. Eng.* **2020,** *8,* 12014.

(52) Wang, G.-W. Mechanochemical organic synthesis. *Chem. Soc. Rev.* **2013,** *42,* 7668.

(53) Häussinger, P.; Lohmüller, R.; Watson, A. M., Hydrogen, 6. Uses. In *Ullmann's Encyclopedia of Industrial Chemistry,* Wiley-VCH Verlag GmbH & Co. KGaA: Weinheim, 2011; 18, pp 353-390.

(54) Bolm, C.; Hernández, J. G., Mechanochemistry of Gaseous Reactants. *Angew. Chem. Int. Ed.* **2019,** *58,* 3285.

(55) Sawama, Y.; Niikawa, M.; Yabe, Y.; Goto, R.; Kawajiri, T.; Marumoto, T.; Takahashi, T.; Itoh, M.; Kimura, Y.; Sasai, Y.; Yamauchi, Y.; Kondo, S.-I.; Kuzuya, M.; Monguchi, Y.; Sajiki, H. Stainless-Steel-Mediated Quantitative Hydrogen Generation from Water under Ball Milling Conditions. *ACS Sustainable Chem. Eng.* **2015,** *3,* 683.

(56) Sawama, Y.; Kawajiri, T.; Niikawa, M.; Goto, R.; Yabe, Y.; Takahashi, T.; Marumoto, T.; Itoh, M.; Kimura, Y.; Monguchi, Y.; Kondo, S.; Sajiki, H. Stainless-Steel Ball-Milling Method for Hydro-/Deutero-genation using H_2O/D_2O as a Hydrogen/Deuterium Source. *ChemSusChem* **2015,** *8,* 3773.

(57) Sawama, Y.; Yasukawa, N.; Ban, K.; Goto, R.; Niikawa, M.; Monguchi, Y.; Itoh, M.; Sajiki, H. Stainless Steel-Mediated Hydrogen Generation from Alkanes and Diethyl Ether and Its Application for Arene Reduction. *Org. Lett.* **2018,** *20,* 2892.

(58) Schumacher, C.; Crawford, D. E.; Ragu, Z. B.; Glaum, R.; James, S. L.; Bolm, C.; Hernández, J. G., Mechanochemical Dehydrocoupling of Dimethylamine Borane and Hydrogenation Reactions Using Wilkinson's Catalyst. *Chem. Commun.* **2018,** *54,* 8355.

(59) Portada, T.; Margetic, D.; Štrukil, V. Mechanochemical Catalytic Transfer Hydrogenation of Aromatic Nitro Derivatives. *Molecules* **2018,** *23,* 3163.

(60) Baláž, P.; Achimovičová, M.; Baláž, M.; Billik, P.; Cherkezova-Zheleva, Z.; Criado, J. M.; Delogu, F.; Dutková, E.; Gaffet, E.; Gotor, F. J. Hallmarks of mechanochemistry: from nanoparticles to technology. *Chem. Soc. Rev.* **2013,** *42,* 7571.

(61) Haley, R. A.; Mack, J.; Guan, H. 2-in-1: catalyst and reaction medium. *Inorg. Chem. Front.* **2017,** *4,* 52.

(62) Goodman, J.; Grushin, V. V.; Larichev, R. B.; Macgregor, S. A.; Marshall, W. J.; Roe, D. C. Fluxionality of [(Ph_3P) 3M (X)](M= Rh, Ir). The Red and Orange Forms of [$(Ph3P)_3$Ir (Cl)]. Which Phosphine Dissociates Faster from Wilkinson's Catalyst? *J. Am. Chem. Soc.* **2010,** *132,* 12013.

(63) Osborn, J. A.; Jardine, F.; Young, J. F.; Wilkinson, G. The preparation and properties of tris (triphenylphosphine) halogenorhodium (I) and some reactions thereof including catalytic

homogeneous hydrogenation of olefins and acetylenes and their derivatives. *J. Chem. Soc. A* **1966,** 1711.

(64) Golubkova, G.; Bazanova, I.; Gostikin, V.; Nischenkova, L.; Lomovsky, O. Mechanochemical promotion with molybdenum and catalytic activity of skeletal nickel catalysts in hydrogenation reactions. *React. Kinet. and Catal. Lett.* **1999,** *67,* 169.

(65) Trovarelli, A.; Matteazzi, P.; Dolcetti, G.; Lutman, A.; Miani, F. Nanophase iron carbides as catalysts for carbon dioxide hydrogenation. *Appl. Catal. A* **1993,** *95,* L9.

(66) Mulas, G.; Conti, L.; Scano, G.; Schiffini, L.; Cocco, G. Mechanically driven CO hydrogenation over NiZr amorphous catalysts. *Mater. Sci. Eng. A* **1994,** *181-182,* 1085.

(67) Alonso, F.; Osante, I.; Yus, M. Highly selective hydrogenation of multiple carbon–carbon bonds promoted by nickel(0) nanoparticles. *Tetrahedron* **2007,** *63,* 93.

(68) Nash, D. J.; Restrepo, D. T.; Parra, N. S.; Giesler, K. E.; Penabade, R. A.; Aminpour, M.; Le, D.; Li, Z.; Farha, O. K.; Harper, J. K.; Rahman, T. S.; Blair, R. G. Heterogeneous metal-free hydrogenation over defect-laden hexagonal boron nitride. *ACS Omega* **2016,** *1,* 1343.

(69) Zhang, P.; Wang, L.; Yang, S.; Schott, J. A.; Liu, X.; Mahurin, S. M.; Huang, C.; Zhang, Y.; Fulvio, P. F.; Chisholm, M. F. Solid-state synthesis of ordered mesoporous carbon catalysts via a mechanochemical assembly through coordination cross-linking. *Nat. Comm.* **2017,** *8,* 1.

(70) Toda, F.; Kiyoshige, K.; Yagi, M. $NaBH_4$ Reduction of Ketones in the Solid State. *Angew. Chem. Int. Ed. Engl.* **1989,** *28,* 320.

(71) Mack, J.; Fulmer, D.; Stofel, S.; Santos, N., The first solvent-free method for the reduction of esters. *Green Chem.* **2007,** *9,* 1041.

(72) Li, A. Y.; Segalla, A.; Li, C.-J.; Moores, A. Mechanochemical Metal-Free Transfer Hydrogenation of Carbonyls Using Polymethylhydrosiloxane as the Hydrogen Source. *ACS Sustainable Chem. Eng.* **2017,** *5,* 11752.

(73) Chacón-Huete, F.; Messina, C.; Chen, F.; Cuccia, L.; Ottenwaelder, X.; Forgione, P. Solvent-Free Mechanochemical Oxidation and Reduction of Biomass-Derived 5-Hydroxymethyl Furfural. *Green Chem.* **2018,** *20,* 5261.

(74) Yepez, A.; Hidalgo, J. M.; Pineda, A.; Černý, R.; Jíša, P.; Garcia, A.; Romero, A. A.; Luque, R., Mechanistic insights into the hydroconversion of cinnamaldehyde using mechanochemically-synthesized Pd/Al-SBA-15 catalysts. *Green Chem.* **2015,** *17,* 565.

(75) Al5-Naji, M.; Balu, A. M.; Roibu, A.; Goepel, M.; Einicke, W. D.; Luque, R.; Gläser, R. Mechanochemical preparation of advanced catalytically active bifunctional Pd-containing nanomaterials for aqueous phase hydrogenation. *Catal. Sci. Technol.* **2015,** *5,* 2085.

(76) Balaraman, E.; Gunanathan, C.; Zhang, J.; Shimon, L. J. W.; Milstein, D. Efficient hydrogenation of organic carbonates, carbamates and formates indicates alternative routes to methanol based on CO_2 and CO. *Nat. Chem.* **2011,** *3,* 609.

(77) Farina, V.; Gamba, N. S.; Gennari, F.; Garroni, S.; Torre, F.; Taras, A.; Enzo, S.; Mulas, G. O_2 Hydrogenation Induced by Mechanochemical Activation of Olivine with Water Under CO_2 Atmosphere. *Front. Energy Res.* **2019,** *7,* 107.

(78) Giammar, D. E.; Bruant, R. G.; Peters, C. A. Forsterite dissolution and magnesite precipitation at conditions relevant for deep saline aquifer storage and sequestration of carbon dioxide. *Chem. Geol.* **2005,** *217,* 257.

(79) Camille Jones, L.; Rosenbauer, R.; Goldsmith, J. I.; Oze, C. Carbonate control of H_2 and CH_4 production in serpentinization systems at elevated P-Ts. *Geophys. Res. Lett.* **2010,** *37,* L14306.

(80) Adams, C. J.; Kurawa, M. A.; Lusi, M.; Orpen, A. G. Solid state synthesis of coordination compounds from basic metal salts. *CrystEngComm* **2008,** *10,* 1790.

(81) Zhou, D.; Yu, M.; Fan, Y.; Wang, Z.; Dang, G.; Zhang, Q.; Xie, J. Sodium-induced solid-phase hydrogenation of carbon dioxide to formate by mechanochemistry. *Environ. Chem. Lett.* **2020,** *18,* 905.

(82) Chen, H.; Lin, W.; Zhang, Z.; Jie, K.; Mullins, D. R.; Sang, X.; Yang, S.-Z.; Jafta, C. J.; Bridges, C. A.; Hu, X.; Unocic, R. R.; Fu, J.; Zhang, P.; Dai, S. Mechanochemical Synthesis of High Entropy Oxide Materials under Ambient Conditions: Dispersion of Catalysts *via* Entropy Maximization. *ACS Mater. Lett.* **2019,** *1,* 83.

(83) Zhang, Z.; Gao, J.; Xia, J.-J.; Wang, G.-W. Solvent-free mechanochemical and one-pot reductive benzylizations of malononitrile and 4-methylaniline using Hantzsch 1,4-dihydropyridine as the reductant. Org. Biomol. Chem. **2005,** *3,* 1617.

(84) Martina, K.; Baricco, F.; Tagliapietra, S.; Moran, M. J.; Cravotto, G.; Cintas, P. Highly efficient nitrobenzene and alkyl/aryl azide reduction in stainless steel jars without catalyst addition. *New J. Chem.* **2018,** *42,* 18881.

(85) Dobrovolná, Z.; Červený, L. Ammonium formate decomposition using palladium catalyst. *Res. Chem. Intermed.* **2000,** *26,* 489.

(86) Menuel, S.; Leger, B.; Addad, A.; Monflier, E.; Hapiot, F. Cyclodextrins as Effective Additives in AuNP-Catalyzed Reduction of Nitrobenzene Derivatives in a Ball-Mill. *Green Chem.* **2016,** *18,* 5500.

(87) Gopiraman, M.; Saravanamoorthy, S.; Deng, D.; Ilangovan, A.; Kim, I. S.; Chung, I. M. Facile Mechanochemical Synthesis of Nickel/Graphene Oxide Nanocomposites with Unique and Tunable Morphology: Applications in Heterogeneous Catalysis and Supercapacitors. *Catalysts* **2019,** *9,* 486.

(88) Vellaichamy, B.; Prakash, P.; Thomas, J. Synthesis of AuNPs@RGO nanosheets for sustainable catalysis toward nitrophenols reduction. *Ultrason. Sonochem.* **2018,** *48,* 362.

(89) Zhang, Y.; Yuan, X.; Wang, Y.; Chen, Y. One-pot photochemical synthesis of graphene composites uniformly deposited with silver nanoparticles and their high catalytic activity towards the reduction of 2-nitroaniline. *J. Mater. Chem.* **2012,** *22,* 7245.

(90) Zhao, F.; Kong, W.; Hu, Z.; Liu, J.; Zhao, Y.; Zhang, B. Tuning the performance of Pt–Ni alloy/reduced graphene oxide catalysts for 4-nitrophenol reduction. *RSC Adv.* **2016,** *6,* 79028.

(91) am Ende, D. J.; Anderson, S. R.; Salan, J. S. Development and Scale-Up of Cocrystals Using Resonant Acoustic Mixing. *Org. Process Res. Dev.* **2014,** *18,* 331.

(92) Michalchuk, A. A.; Hope, K. S.; Kennedy, S. R.; Blanco, M. V.; Boldyreva, E. V.; Pulham, C. R. Ball-free mechanochemistry: *in situ* real-time monitoring of pharmaceutical co-crystal formation by resonant acoustic mixing. *ChemComm.* **2018,** *54,* 4033.

(93) Porta, R.; Benaglia, M.; Puglisi, A. Flow Chemistry: Recent Developments in the Synthesis of Pharmaceutical Products. *Org. Process Res. Dev.* **2015,** 20, 2.

(94) Vlachopoulos, J.; Strutt, D. Polymer processing. *Mater. Sci. Technol.* **2003,** *19,* 1161.

(95) Daurio, D.; Nagapudi, K.; Li, L.; Quan, P.; Nunez, F.-A. Application of twin screw extrusion to the manufacture of cocrystals: scale-up of AMG 517–sorbic acid cocrystal production. *Faraday Discuss.* **2014,** *170,* 235.

(96) Crawford, D. E.; Miskimmin, C. K. G.; Albadarin, A. B.; Walker, G.; James, S. L. Organic synthesis by Twin Screw Extrusion (TSE): Continuous, Scalable and Solvent-Free. *Green Chem.* **2017,** *19,* 1507.

(97) Crawford, D. E. Extrusion–back to the future: Using an established technique to reform automated chemical synthesis. *Beilstein J. Org. Chem.* **2017,** *13,* 65.

(98) Cao, Q.; Howard, J. L.; Crawford, D. E.; James, S. L.; Browne, D. L. Translating solid state organic synthesis from a mixer mill to a continuous twin screw extruder. *Green Chem.* **2018,** 20, 4443.

(99) Crawford, D. E.; Miskimmin, C. K.; Cahir, J.; James, S. Continuous multi-step synthesis by extrusion–telescoping solvent-free reactions for greater efficiency. *ChemComm.* **2017,** *53,* 13067.

(100) Yeboue, Y.; Gallard, B.; Le Moigne, N.; Jean, M.; Lamaty, F.; Martinez, J.; Métro, T.-X. Peptide Couplings by Reactive Extrusion: Solid-Tolerant and Free from Carcinogenic, Mutagenic and Reprotoxic Chemicals. *ACS Sustainable Chem. Eng.* **2018,** *6,* 16001.

(101) Crawford, D. E.; Wright, L.; James, S.; Abbott, A. Efficient continuous synthesis of high purity deep eutectic solvents by twin screw extrusion. *ChemComm.* **2016,** *52,* 4215.

(102) Karadeniz, B.; Howarth, A. J.; Stolar, T.; Islamoglu, T.; Dejanovic, I.; Tireli, M.; Wasson, M. C.; Moon, S.-Y.; Farha, O. K.; Friščić, T.; Užarević, K. Benign by design: green and scalable synthesis of zirconium UiO-metal–organic frameworks by water-assisted mechanochemistry. *ACS Sustainable Chem. Eng.* **2018,** *6,* 15841.

(103) Egleston, B. D.; Brand, M. C.; Greenwell, F.; Briggs, M. E.; James, S. L.; Cooper, A. I.; Crawford, D. E.; Greenaway, R. L. Continuous and scalable synthesis of a porous organic cage by twin screw extrusion (TSE). *Chem. Sci.* **2020,** *11,* 6582.

(104) Karak, S.; Kandambeth, S.; Biswal, B. P.; Sasmal, H. S.; Kumar, S.; Pachfule, P.; Banerjee, R. Constructing Ultraporous Covalent Organic Frameworks in Seconds via an Organic Terracotta Process. *J. Am. Chem. Soc.* **2017,** *139,* 1856.

(105) Crawford, D. E.; Porcheddu, A.; McCalmont, A. S.; Delogu, F.; James, S. L.; Colacino, E. Solvent-Free, Continuous Synthesis of Hydrazone-Based Active Pharmaceutical Ingredients by Twin-Screw Extrusion. *ACS Sustainable Chem. Eng.* **2020,** *8,* 12230.

(106) Chauhan, P.; Chimni, S. S. Mechanochemistry assisted asymmetric organocatalysis: A sustainable approach. *Beilstein J. Org. Chem.* **2012,** *8,* 2132.

(107) Krištofíková, D.; Mečiarová, M.; Rakovský, E.; Šebesta, R. Mechanochemically Activated Asymmetric Organocatalytic Domino Mannich Reaction-Fluorination. *ACS Sustainable Chem. Eng.* **2020,** *8,* 14417.